Grinding polycrystalline diamond using a diamond grinding wheel

Maryam Agahi
University of Wollongong

GRINDING POLYCRYSTALLINE DIAMOND USING A DIAMOND GRINDING WHEEL

A thesis submitted in partial fulfilment of the requirements for the award of the degree

Master of Engineering Research

from

University of Wollongong

by

Maryam Agahi, B. Sc.

School of Mechanical, Materials and Mechatronic Engineering

2006

CERTIFICATION

I, Maryam Agahi, declare that this thesis, submitted in partial fulfilment of the requirements for the award of Master of Engineering Research, in the Faculty of Engineering, University of Wollongong, is wholly my own work unless otherwise referenced or acknowledged. The document has not been submitted for qualifications at any other academic institution.

Maryam Agahi

July 13, 2006

TABLE OF CONTENTS

LIST OF TABLES

LIST OF FIGURES

GLOSSARY

C	Concentration
Conc.	Coolant concentration
CVD/PCVD Diamond	Chemical vapour deposited polycrystalline diamond
d_K	Grit diameter
d_S	Cup wheel diameter
DOS	Disc operating system
DSP	Digital signal processor
ECD	Electrochemical in-process controlled dressing
ECDM/ECAM/EEDM	Electro chemical discharge machining
EDG	Electrical discharge grinding
EDM	Electro discharge machining
ELID	Electrolytic in-process dressing
F_A	Contact force
F_d	Force in X direction
FFG	Form and finish grinding
F_N/Fn	Normal cutting force
F_R	Radial force
F_T/Ft	Tangential force
G-ratio/G	Grinding ratio
HPAWJ	High pressure abrasive water jet
HSS	High-speed steel

I/O	Input/output
Matlab	Matrix laboratory
MMC	Metal matrix composite
MRR/Q_W	Material removal rate
PcBN/PCBN	Polycrystalline cubic boron nitride
PCD	Polycrystalline diamond
RAM	Random access memory
R_P	Peak to mean line height
SEM	Scanning electron microscope/microscopy
SRG	Stock removal grinding
t_d	Sharpening cycle
TI	Texas Instrument
V_C/V_S	Peripheral speed
v_d/V_W	X-axis velocity/oscillation rate
VWW	Volumetric wheel wear during dressing
VWWR	Volumetric wheel wear rate during grinding
WC	Cemented tungsten carbide
WEDM	Wire electrical discharge machining
δ	Truing feed
α	Vertical angle between the work piece and the grinding wheel centre
μm	Micron
μ	Grinding coefficient

ABSTRACT

Application of ultrahard cutting tool materials is continuously expanding. One example of an ultrahard cutting tool material is polycrystalline diamond (PCD), which is widely used in tool making and machining. However, because of the high wear resistance of PCD it is characterised by low grindability and machinability. So, any mechanism used to machine PCD has to meet specific requirements. Grinding with a diamond grinding wheel is one of the economic ways to machine PCD compacts. This thesis considers the grinding of polycrystalline diamond using a conventional grinding machine and makes machining parameter recommendations to support the optimisation of PCD grinding.

The PCD grinding forces are mathematically analysed. These grinding forces are measured using a force sensor installed on a conventional grinding machine. The forces produced during grinding are investigated as a function of in-feed, contact zone, material removal rate (MRR) and oscillation rate. Wheel conditioning, another major aspect of PCD grinding, is studied and optimised in order to reduce the grinding forces, increase the cutting efficiency and achieve maximum removal rates and minimum wear ratios.

Grinding wheel wear is investigated as a recognized problem in PCD grinding. A series of experiments are conducted in which the material removal rate, the rate of wheel wear and the grinding forces are measured. The effects of in-feed, sharpening process and work piece hardness on the wheel wear are studied.

The edge quality of the PCD compacts is investigated as an important issue in tool making. Factors affecting PCD grinding quality include the in-feed, material removal rate, the condition of the diamond grinding wheel and the rigidity of the grinding machine. These are all studied to find their effect on edge quality.

The work presented in this thesis also shows that the capability of a conventional grinding machine designed for non-PCD is sufficient to grind PCD with acceptable quality.

ACKNOWLEDGMENTS

Most of all, I would like to thank my supervisor Professor Chris Cook for his kind support and priceless guidance throughout my research. The opportunity he gave me not only increased my knowledge but also allowed me to meet such wonderful and unique people at the university. His perpetual encouragement and invaluable advice are greatly appreciated.

I would like to give special thanks to Dr. Marta Fernandes, my "on-site" supervisor. Her endless ideas opened the closed doors and enlightened me about the problems I faced. Whenever I needed help she gave me the energy and motivation to finish what I had started. I would like to thank her for being such a wonderful friend even in her absence.

I would like to thank Mr. Jeff Moscrop, my co-supervisor for his priceless help. Jeff's friendly availability for the successful completion of this thesis is deeply acknowledged.

Many thanks to all general staff who helped me complete my research. Special thanks to Mr. Brian Webb for preparing my experimental setup and to Mr. Greg Tillman and Mr. Stuart Rodd who helped me use the various equipments. I would like to give special thanks to Dr. John Simpson for his valuable and helpful comments in solving problems with the grinding machine and also to Ms. Neda Zamani for helping me learn C programming. Thanks also to Ms. Catherine Todd for her comments in writing up my thesis and to Ms. Lorelle Pollard for her kindness and inspirational smile.

To my dear parents who always gave me the confidence and strength to work on my thesis. Their warm voices always gave me fresh energy and inspiration. It is due to their unconditional support that I have been able to reach my goal.

Last but not least, I would like to thank Mehrdad, my dear husband, for his love and never-ending support, for always being with me whenever I needed him and for having faith in me. I want to thank him for his encouragement when I was desperate or not focused. Without his patience I would not be able to finish this thesis.

CHAPTER 1 INTRODUCTION AND LITERATURE REVIEW

1.1. Background

According to ISO 3002, the grinding process is characterized by the kind of surface to be generated, the kinematics of the machining operation and the shape or profile of the grinding wheel [1].

Polycrystalline diamond (PCD) is one of the most interesting developments in the field of advanced cutting tool materials. With the growing use of cutting tools made from PCD for use on difficult-to-machine materials over the last 15 years, the development of machining processes of this material becomes essential. In today's competitive market, industries have the need for fast, lean, flexible and adaptable manufacturing processes in order to survive [2]. Grinding of polycrystalline diamond is a time consuming and costly task and any time and money savings in the grinding operation are very desirable.

With the expanding use of machining operations including CNC production equipment in order to improve productivity, increase tool life and to reduce downtime and costs, diamond is being considered as one of the most economical choices of cutting tools. The cost of a diamond tool is approximately 40 times the equivalent carbide tool but will last approximately 150 times longer [3]. The most significant advantage of using diamond tools is the enormous reduction in machine downtime. Furthermore, diamond not only remains sharp for a longer time but also results in more satisfactory quality of the cutting edge.

A conventional grinding machine was used in this thesis to grind Polycrystalline diamond. Because the hardness of PCD generates high machining forces during grinding, PCD blanks are often ground using specific machines with high dynamic and static stability. Consequently, to grind PCD tools, conventional grinding machines designed for non-PCD uses may need to be modified. The grinding mechanisms designed specifically for PCD grinding are often costly and require specially trained operators. However, conventional machines are more likely to have problems in areas

such as the rigidity of the system, material removal efficiency, grinding wheel wear, edge quality.

The grinding process can be monitored by measurement of the grinding forces and the amount of material removed. One of the motivations for measuring the grinding forces and amount of removed material is to obtain more valuable information about the PCD grinding process and the relation between grinding parameters. Measuring grinding forces also helps to study the reliability of the grinding machine during grinding PCD.

PCD blanks are usually ground using diamond grinding wheels. The grinding wheels must be trued occasionally to remove the irregularities of the wheel profile generated by the previous grinding operations. Due to the great hardness of PCD, the grinding wheel wears out extremely quickly. Therefore, the wheel surface must be opened and resharpened again for further grinding operations. Considering these details, the PCD grinding process is noticeably longer than grinding cemented carbide and in fact the wheel dullness is one of the limitations of PCD grinding resulting in a time consuming machining process.

Several authors recommend that constant force be used in PCD grinding [4-9] and in some research PCD is ground using only constant force [10-16]. Nevertheless, most conventional machining operations are carried out using constant feed rate and in many publications [17-24] PCD compacts are also ground using constant feed. Since a conventional grinding machine was used in this thesis all the experiments were carried out using constant feed. However, many of the conclusions are applicable to constant force and constant feed grinding.

PCD blanks can also be machined by other techniques such as electro discharge machining (EDM) [12, 18, 24-26] which is the most popular PCD cutting technology [27], wire electrical discharge machining (WEDM) [28-30], electrical discharge grinding (EDG) [11, 31, 32], laser cutting method [10, 33, 34] and high pressure abrasive water jet (HPAWJ) [27]. The two latter technologies have not been used extensively because of the higher cost and higher machining technology [27]. Undoubtedly, each technique has its own advantages and disadvantages. However, the simple nature of conventional

grinding encourages much of the industry to use this method as a convenient process for machining PCD. The research done by Tso and Liu [9, 24] confirms that grinding is the most successful way to make high quality diamond tools with the proper working parameters.

In this thesis, the possibility of grinding PCD using a conventional grinding machine is examined. The research also exploits previous work performed by Simpson [35] to develop force estimation and control schemes. The aim of the investigations presented here is to indicate the relationships between the machining parameters and the quantitative grinding results and thereby supply the basis for optimization of PCD grinding.

In this chapter a literature review of work relevant to this thesis and a review of other research work in the area of PCD grinding is given. In particular, key aspects of the grinding process investigated in this research are described in the following sections. In Section 1.2 the general information about polycrystalline diamond and its application is given. The properties of polycrystalline diamond compared to other cutting tool materials are discussed in Section 1.2.1.

The detailed mechanism of grinding including the wear mechanism and specifications of a PCD grinding machine are given in Section 1.3. Section 1.3.1 reviews the mechanism of material removal and wear modes in PCD grinding. In particular the relationship between grinding forces and the grinding process are discussed. Section 1.3.2 describes the diamond grinding wheels and their characteristics in PCD grinding.

The wheel conditioning processes including truing and dressing procedures are discussed in Section 1.4. The conventional truing and dressing methods are described in Section 1.4 and also some unconventional truing and dressing methods are given. Section 1.5 reviews the PCD machining methods other than conventional grinding. In Section 1.6 the specific PCD grinding machines in the market are mentioned. The grinding wheel wear and the effect of truing and dressing on the wheel life are discussed in Section 1.7. The edge quality is reviewed in Section 1.8 as an important issue in PCD tool grinding. The objectives and significance of this research are given in Section 1.9 and the thesis chapters are outlined in Section 1.10.

1.2. Polycrystalline Diamond

Following the introduction of synthetic diamond grit in 1950s [36], polycrystalline diamond was first developed in 1970s [19, 36, 37]. Until the late 1980s, the only commercial diamond products available for manufacture of edge defined cutting tools were the synthetic diamond grit and polycrystalline diamond [36]. PCD consists of compacted sintered diamond and cobalt randomly distributed with approximately 0.5 or 0.7mm thickness supported on a carbide substrate serving as a damper [9]. When a single grain breaks, the surrounding grains prevent the further growth of fractures through the material and this makes PCD an extremely hard, strong and tough material [4-6]. Depending on the grain size of the starting material, the resultant compact is about 85% diamond, with the balance cobalt [38]. PCD is an isotropic material without preferential cutting planes [4-6].

PCD compacts are produced under a specific high-pressure (about 6GPa [30]) and high-temperature (approx. $1500^{\circ}C$ [30]) process. The combination of abrasion resistance of diamond and carbide's strength "produces a cutting tool material that achieves a tremendous increase in machining performance" [21]. On account of high wear resistance of PCD and its durability (10-20 times longer than tungsten carbide [9]), the demand for PCD in tool making has increased since its introduction to the market in the 1970s.

PCD cutting tools can be found with different grades according to the size of the diamond crystals used in producing PCD blanks.

PCD was first used for turning and milling operations [12]. PCD cutting tools are used in machining nonferrous metals (such as aluminium, copper, magnesium and their alloys [3, 10, 39], brass, bronze, zinc and sintered tungsten carbide [38, 39]) and non-metallic materials (such as, wood based materials, ceramics and polymers). "The presence of iron (in ferrous materials), cobalt or nickel in work piece alloys causes a thermo-chemical reaction with PCD" [10]. This reaction causes the diamond to wear rapidly and as a result, makes PCD unsuitable for machining these materials [10, 36].

PCD grinding technology is used in various industries such as automotive industry (for machining pistons, engine blocks, brake cylinders and transmission cases) [30], aerospace industry (for machining engine components) [30], manufacturing industry (for producing aluminium mirrors [36], machining hyper-eutectic aluminium-silicon alloys [10, 19, 37, 38], machining glass-reinforced plastic [3-6, 10, 12, 19, 21, 29, 37, 38] and metal matrix composites (MMCs) [36]), polymer and woodworking industry (for machining chipboards [4-6, 10, 37], particle boards [12, 30], fibreboards and composite materials [19, 30]), jewellery industry (for flycutting and engraving) [30] and textile industry (for machining water jet cutting nozzles) [30]. PCD can even be used in dressing of corundum wheels as a substitute for mined diamond dressing [40].

As Cassidy [19] states, the PCD cutting tools fabrication includes three or four processing steps; wire EDM machining of PCD blanks (to be discussed later) to achieve the desired shape, mounting by means of brazing the PCD insert onto a carbide shank and finally grinding the edges of PCD inserts. Figure 1.2.1 illustrates a typical PCD work piece.

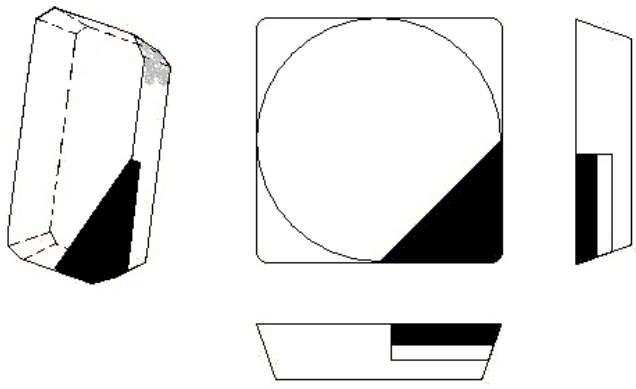

Figure 1.2.1 PCD work piece

1.2.1. Properties of PCD

A layer of PCD has about the same hardness as diamond monocrystals. Due to the diamond's superior hardness, wear resistance and low coefficient of friction, high quality and efficient production can be attained [9]. The physical characteristics of PCD make it a good competitor with cemented carbides and ceramic cutting materials. The properties of PCD among different cutting tool materials with respect to their

wear resistance and fracture toughness are shown in Figure 1.2.2. Wear resistance and fracture toughness are the two indicators of tool life and resistance against cutting forces, respectively. As shown in Figure 1.2.2, an ideal material that has a long tool life and withstands high cutting forces occupies the top right hand corner of the graph. It is not possible to have both properties at the same time since as one of them increases the other one decreases. For example, high-speed steel wears quickly but withstands high cutting forces while ceramics "tend not to be very tough" [36].

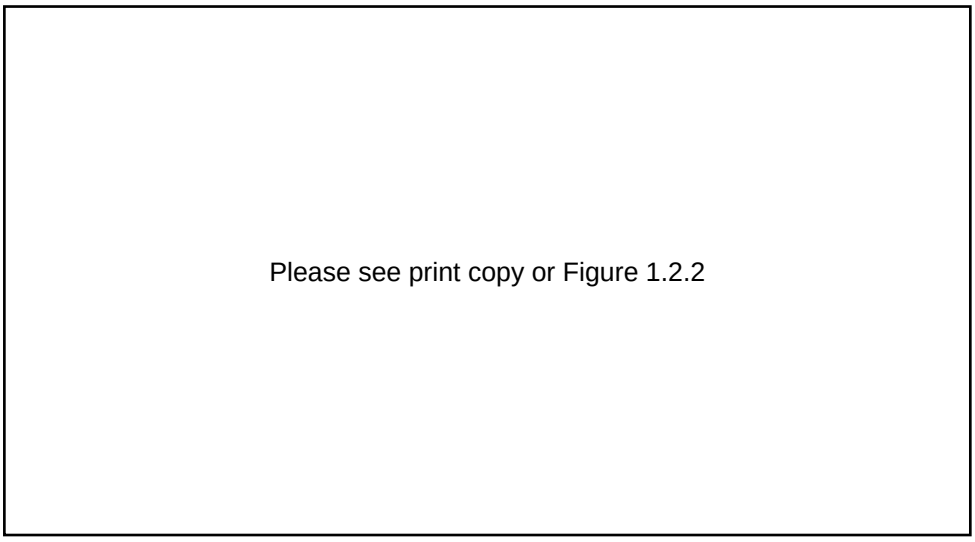

Figure 1.2.2 Properties of cutting tool materials [36]

The cutting tool materials abbreviations used in Figure 1.2.2 stand for polycrystalline diamond PCD, chemical vapour deposited (low pressure) polycrystalline diamond shown as CVD diamond or PCVD diamond, polycrystalline cubic boron nitride PcBN, cemented tungsten carbide WC and high-speed steel HSS. CVD diamond includes two types of products. One is a polycrystalline diamond coated by chemical vapour deposition, referred to as "thin film" and the other one is brazeable and often referred to as "thick film" [36]. PcBN, the other ultra-hard polycrystalline tool material, was introduced to the market in the late 1970s soon after production of PCD [36, 38]. It is superior to PCD because of its ability for machining hard ferrous materials. PCD or PCBN tools can be reground between two and six times [41]. In fact, according to Oderbolz without regrinding, PCD and PCBN tools are in most applications not cost effective [41].

According to Figure 1.2.2, PCD lies almost in the middle of the graph. At temperatures below $700^{\circ}C$, PCD tends to be wear-resistant while over this value the wear-resistance reduces, significantly. The reason is the presence of cobalt, which results in conversion of diamond back to graphite at lower temperature [36]. However, it is unrealistic to approach this temperature either in tool fabrication or in its usage [36]. The high wear resistance of PCD tends to result in high wear of the equipment made to machine it. PCD is also tough enough for relatively high impact operations such as milling and other interrupted cutting operations [36].

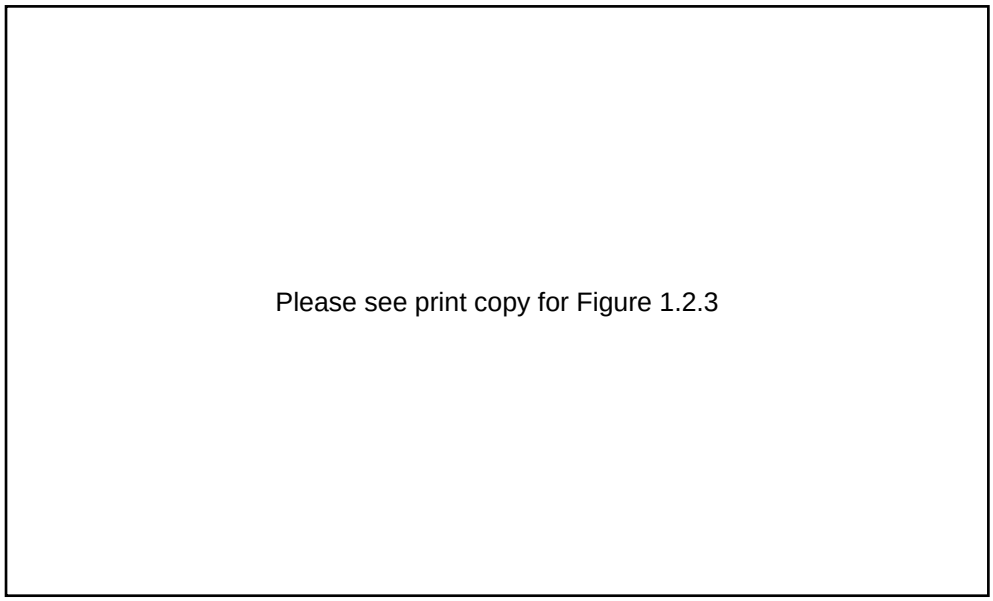

Figure 1.2.3 Thermal conductivity of cutting tool materials
[36]

Figure 1.2.3 shows the other important property of cutting tool materials. Thermal conductivity affects the "machining efficiency" and "tool stability". A thermal conductive tool has a longer life since the heat produced during machining can be transferred from the tool tip into the tool body. As shown in Figure 1.2.3, diamond products possess a satisfactory thermal conductivity compared to the other tool materials. However, the purity, structure and orientation of the diamond alter its thermal conductivity [36]. PCD has the lowest thermal conductivity among the diamond tool materials due to its intrinsic structure and, in the case of synthesised PCD, the presence of solvent/catalyst metal [36].

Figure 1.2.4 shows the fabrication and performance properties of some cutting tool materials. Among the existing cutting tools, PCD possesses satisfactory properties except in the case of corrosion resistance.

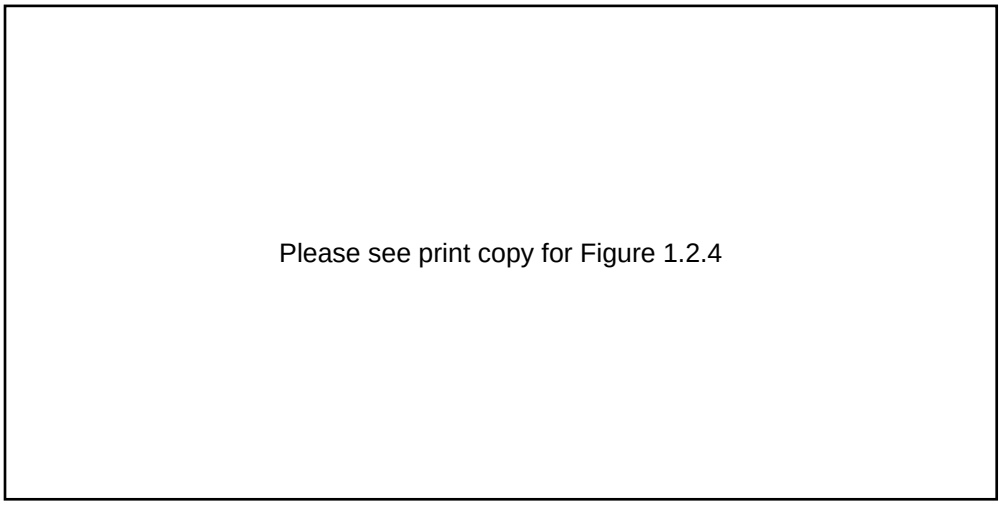

Figure 1.2.4 Tool fabrication and performance properties
[36]

1.3. Grinding Process and Wear Mechanisms

According to Shaw [42] "grinding is performed by refractory abrasive particles of relatively uncontrolled geometry, producing many small chips at very high speed". The grinding process can be divided into these categories; stock removal grinding (SRG) and form and finish grinding (FFG) [42]. In SRG the amount of material removed is the important objective other than the surface quality. While, in FFG the surface finish and quality is a major concern. In this thesis, the basic knowledge and fundamentals of metal grinding are also used but adapted for the grinding of PCD compacts.

The grinding machine used in grinding of PCD has to meet specific requirements [4-8, 11, 14, 17, 20-22, 41, 43]. To achieve an efficient grinding process and higher material removal, the requirements can be listed as below:

- High rigidity of the grinding machine i.e. dynamic and static stability
- High power drive
- High accuracy of wheel spindle

- Centring device with high precision
- High performance grinding wheel

Instead of using an expensive grinding machine specifically designed for PCD-uses, which meets all the above requirements the capability of a conventional grinding machine has been studied in the research presented in this thesis.

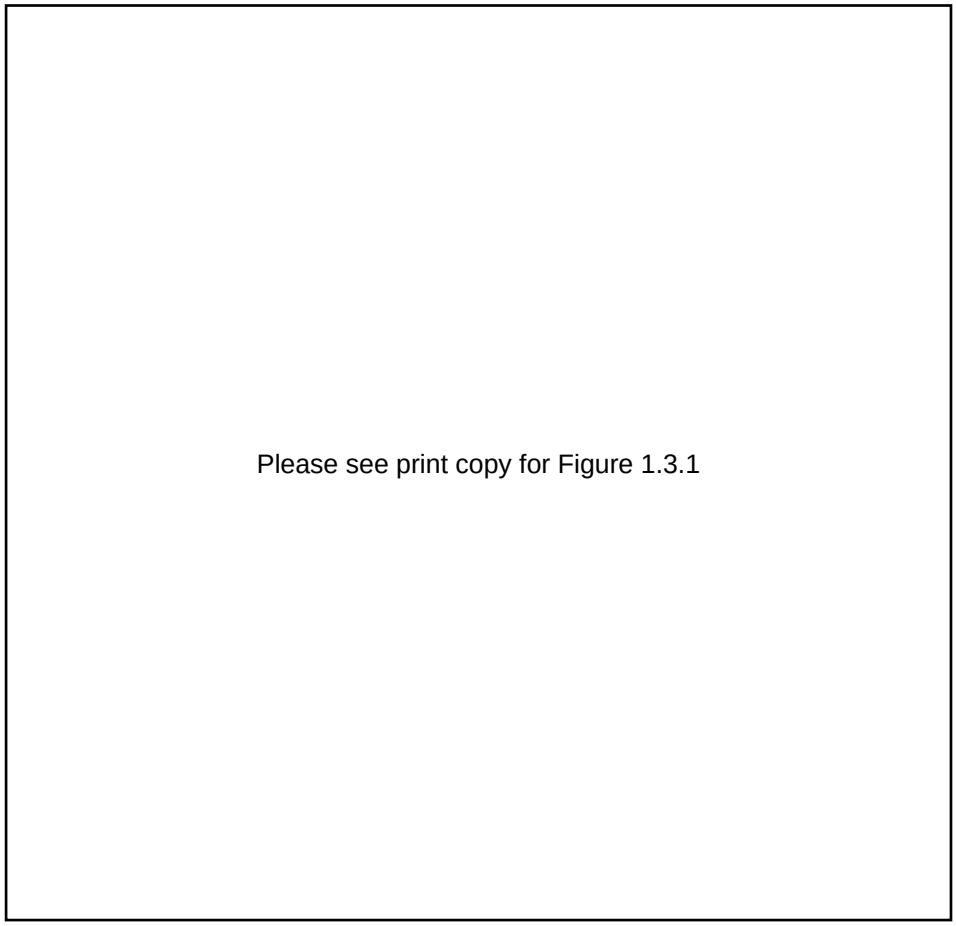

Figure 1.3.1 Structural relationship between input and output values in PCD grinding [8, 15, 16]

The grinding process is affected by the variables shown in Figure 1.3.1. These provide information on the grinding results and efficiency of process control. More details are discussed in [8, 15, 16].

The grinding process can be monitored by online measurement of the grinding forces and/or drive power. Figure 1.3.2 shows the cutting force components and the

kinematics involved in the grinding process. During grinding, the wheel is pressed against the work piece with a contact force F_A [5, 6, 8]. Due to the hardness of PCD compacts and the diamond grits of grinding wheels [9], which are in contact with each other during grinding, it is often recommended to grind PCD using a constant contact force instead of constant feed [4-9]. When the wheel blunts if the in-feed rate is too high, macro cracks occur on the friction partners. Furthermore, improper selection of grinding parameters may lead to excessive temperature resulting in degradation of diamond quality [9, 23]. Grinding with constant load tends to prevent these situations from occurring. However, careful choice of in-feed can also help to prevent these from occurring. Strategies for optimising the in-feed are presented in this thesis.

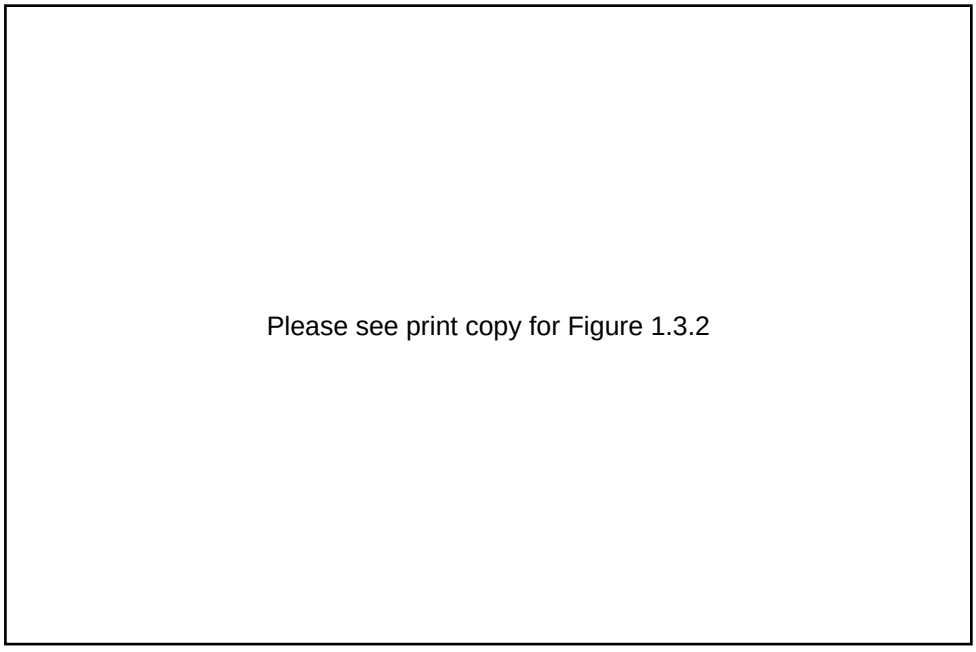

Figure 1.3.2 Kinematics and forces in grinding PCD [4-6]

The adjustable contact force F_A is responsible for the normal cutting force component F_N [5, 6, 8]. To avoid uneven wear of the grinding wheel during grinding, the grinding wheel or the work piece oscillates. This movement generates the third component with variable direction and magnitude [4-6, 8]. If the direction of oscillation is aligned with the radius of the wheel, the third component will be named the radial force F_R. The rotation of the grinding wheel at a peripheral speed V_C results in the tangential force component F_T [4-6, 8].

During grinding, if the contact load goes over a certain value the in-feed will stop until the load is decreased to the limiting value. If the contact force does not decrease in a certain time, it means the diamond wheel is blunt and needs to be regenerated. In other words, with a constant contact force, when the wheel is clogged to a certain degree, the material removal stops and the friction partners (grinding wheel and work piece) keep sliding against each other with constant normal force F_N [4-6]. Now, if in this case, constant feed is used the PCD work piece will remove the diamond layer resulting in short wheel life and high grinding costs [4-6]. So, monitoring the contact force helps to control the grinding process and to achieve effective PCD grinding [9].

The disadvantage of specific PCD grinding systems is their high cost in comparison with a conventional grinding machine. On the other hand, a conventional grinding machine is most likely to grind with constant feed rather than constant force. Nevertheless, a conventional grinding machine can be a suitable choice as long as the PCD grinding results are adequate.

The grinding profitability [8] and efficiency [9] can be evaluated by material removal rate (MRR or Q_W) and the G-ratio. The former indicates how much PCD volume is removed per unit of time and as a result provides information on the grinding time. The G-ratio is the ratio of the volumetric material removed from the work piece to the volumetric material removed from the grinding wheel. In PCD grinding the absolute material removal rate and G-ratio are very low.

The normal force F_N, has a significant effect on MRR and G-ratio of the grinding wheel [4-6]. The normal and tangential grinding forces not only depend on the state of sharpness of the wheel but also on the size of the grinding contact surface and the feed rate, and therefore do not represent an absolute value for the sharpness of the abrasive layer [44]. The ratio of the tangential force to the normal force is called the grinding coefficient μ. If the relationship between F_N and F_T is established then the dependencies of the size of the grinding contact zone and of the feed rate become apparent. So, as Kramer [44] claims, the ratio of the grinding forces will be a "control value by which the grinding wheel can be kept in an optimum state of sharpness".

In the research presented in this thesis PCD grinding is optimized among working parameters such as the in-feed, oscillation rate, truing and dressing parameters in order to achieve higher material removal rate and lower volumetric wheel wear. Furthermore, the edge quality of the PCD work piece is studied considering in-feed, material removal rate, grinding wheel type and grinding method.

1.3.1. Material Removal Mechanisms

In conventional grinding the cutting edges of the abrasive particles penetrate the work piece on a very flat path [8]. As the angle between the work piece surface and the cutting edge contour is very small due to the cutting edge rounding, initially no chip is formed. "The material is only displaced sideways, forms mounds and flows under the cutting edge" [8]. After this phase of elastic deformation and plastic flow, only if the cutting edge has penetrated deep enough into the work piece, the actual chip formation begins [8]. The number of grains in contact with the wheel will comprise the ultimate material removal. Based on the physical condition of the grinding wheel, relative movement between the friction partners and the type of intermediate medium, the wear types are categorized [8]. Examples of these wear types can be rolling wear, vibration wear, sliding wear and scoring wear (as illustrated in Figure 1.3.3). The energy and material interactions between the individual elements of a wear system are called wear mechanisms. The most important wear mechanisms are adhesion, abrasion, tribochemical reaction and surface fracture [8].

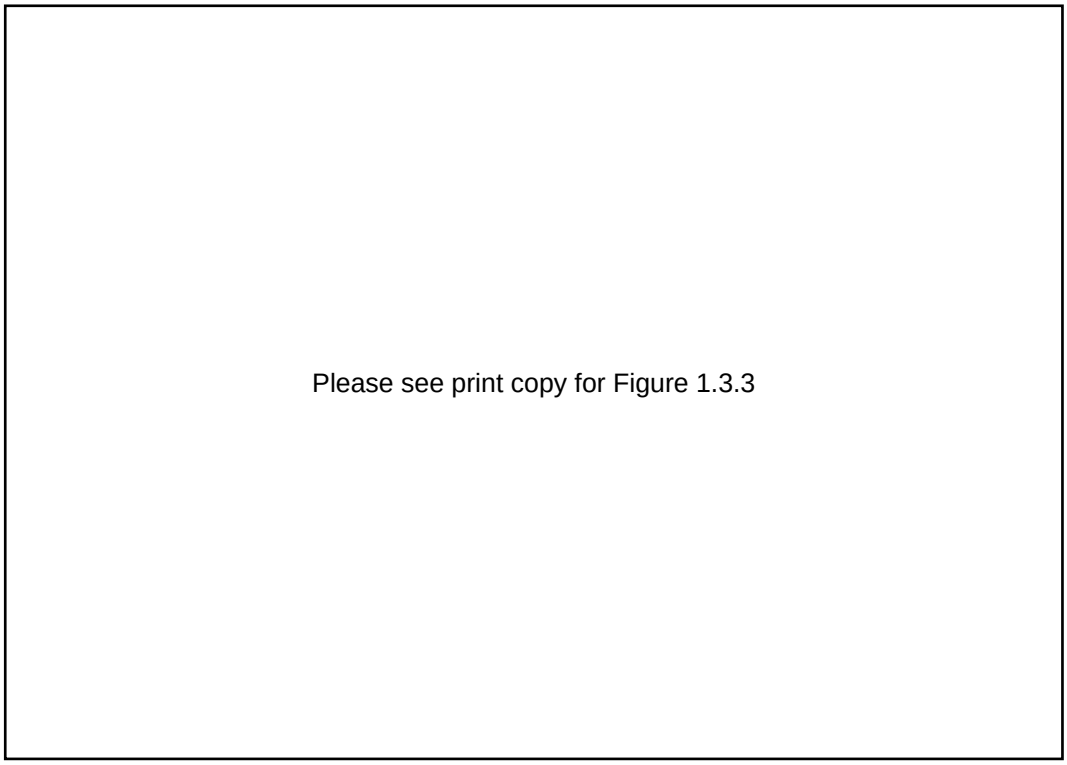

Figure 1.3.3 Schematic representation of selected types of wear [8]

In the case of PCD, the wear modes can be classified as shown in Figure 1.3.4.

It can be assumed that in PCD grinding, in the case of scoring wear and sliding wear, the material is removed under constant contact force [8]. Based on Kenter's [8] research, removal by scoring wear is not applicable for PCD grades with greater toughness. This type of wear is characterised by penetration of the diamond grit into the PCD surface. When the wheel wears out, the wheel surface becomes flat and the contact areas between the friction partners increase. In this phase the removal by scoring wear changes into the removal by sliding wear. Sliding wear is characterised by the "translatory relative movement of smooth surfaces, which are in frictional contact". Following that, abrasion, tribochemical reaction and surface fracture come into consideration [8].

Under the repeated friction contact, the stressed material surface is deformed excessively and the cracks form, which will result in the removal of small particles. The crack distribution and the surface roughness of blank face indicate the effects of grinding diamond tools [9].

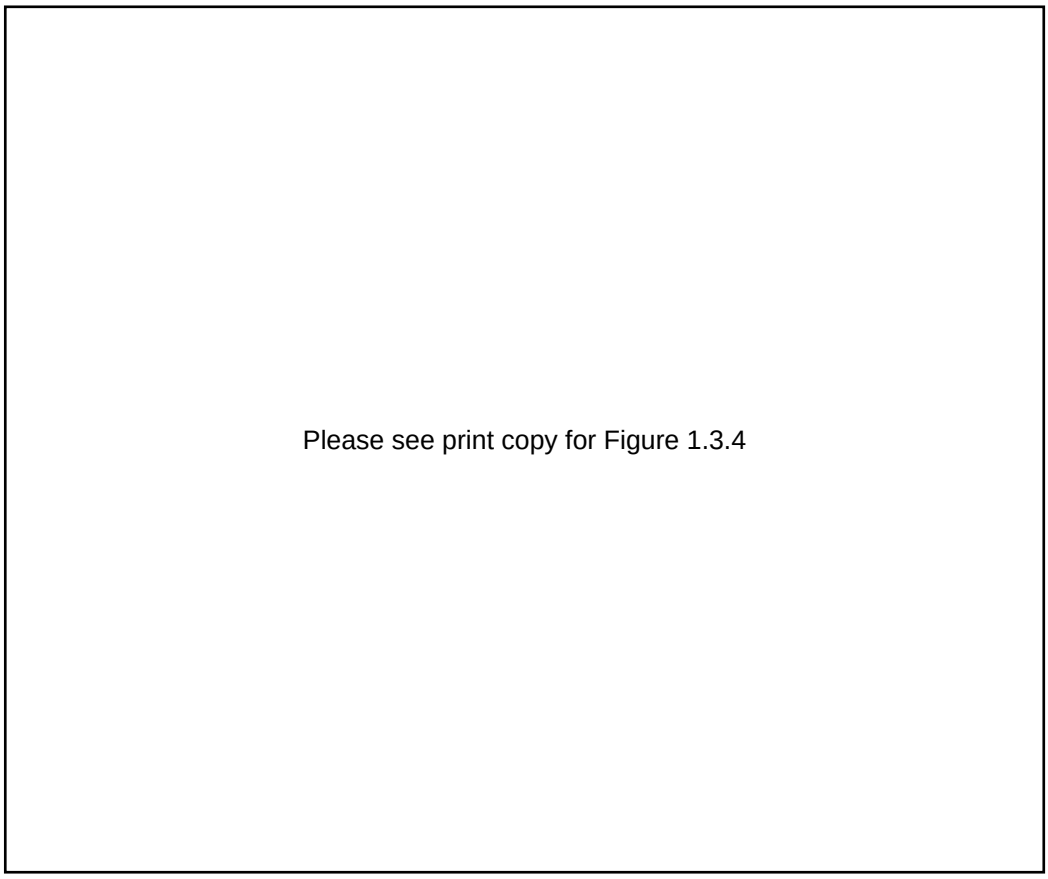

Figure 1.3.4 Wear modes in PCD grinding, adapted from [4]

In the presence of coolant, the friction condition between the abrasive layer of the wheel and work piece is mixed friction. The real contact area between the wheel and the work piece depends on the "roughness of the friction partners, the contact force and the sliding speed" [8].

Werner and Kenter [4-6] studied the relation of normal force with MRR and G-ratio under constant contact force. They found that in rough grinding as the normal force increases more material will be removed from the PCD work piece and a removal rate of 0.4-0.5mm^3/min is obtainable, whereas fine grinding yields a removal rate of 0.05mm^3/min (Figure 1.3.5). They also realized that at increasing normal force the grinding ratio decreases, slightly (Figure 1.3.6).

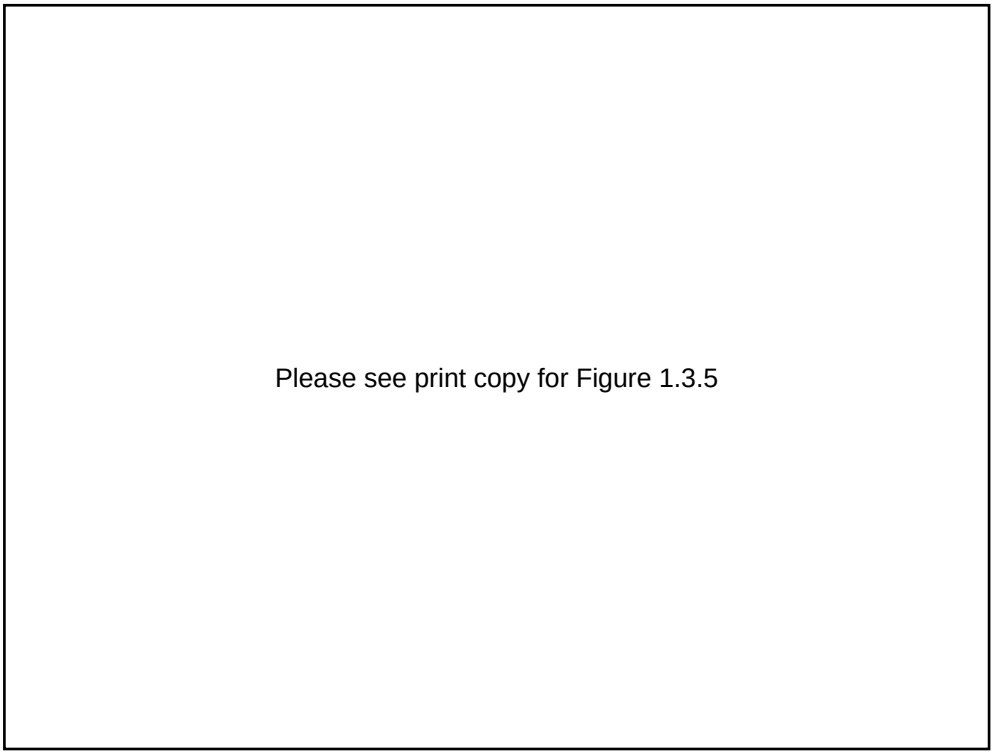

Figure 1.3.5 Relationship between material removal rate and normal force in PCD grinding using constant contact force, adapted from [4]

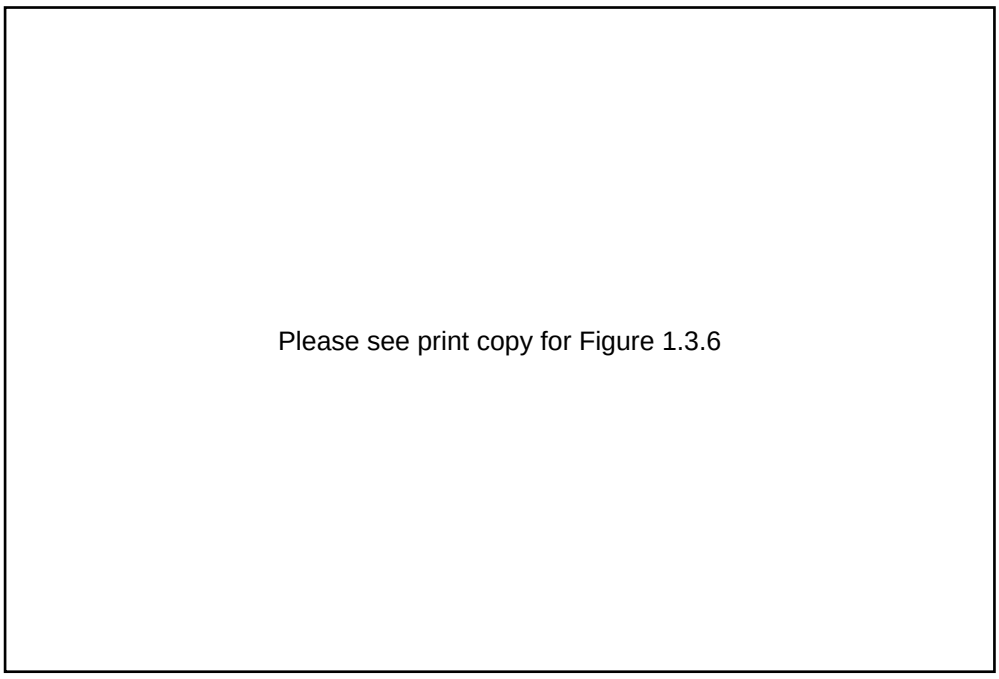

Figure 1.3.6 Relationship between G-ratio and normal force in PCD grinding using constant contact force, adapted from [4]

Kenter [8] has studied the effect of cooling and cleaning of the wheel/work piece contact zone on the operating results and explained the material removal mechanism as a basis for optimisation of PCD tool grinding. His research was carried out under constant contact force and can be summarised in Figure 1.3.7. The normal force F_N depends primarily on the contact force F_A [8]. It is also clear how these input variables affect the tangential force F_T. In all the experiments Kenter [8] conducted, Q_W and G-ratio had the same trend as F_T. In other words, higher friction between the work piece and the grinding wheel will result in higher material removal. Low wheel speeds, high contact forces, large grinding wheel diameters with high diamond concentration and the use of coolants with the least possible lubricating effect help to achieve higher tangential force or in other words higher material removal rate [8]. However, the limit of the rigidity of the machine limits the increase in contact force which leads to lower MRR and G-ratio [8].

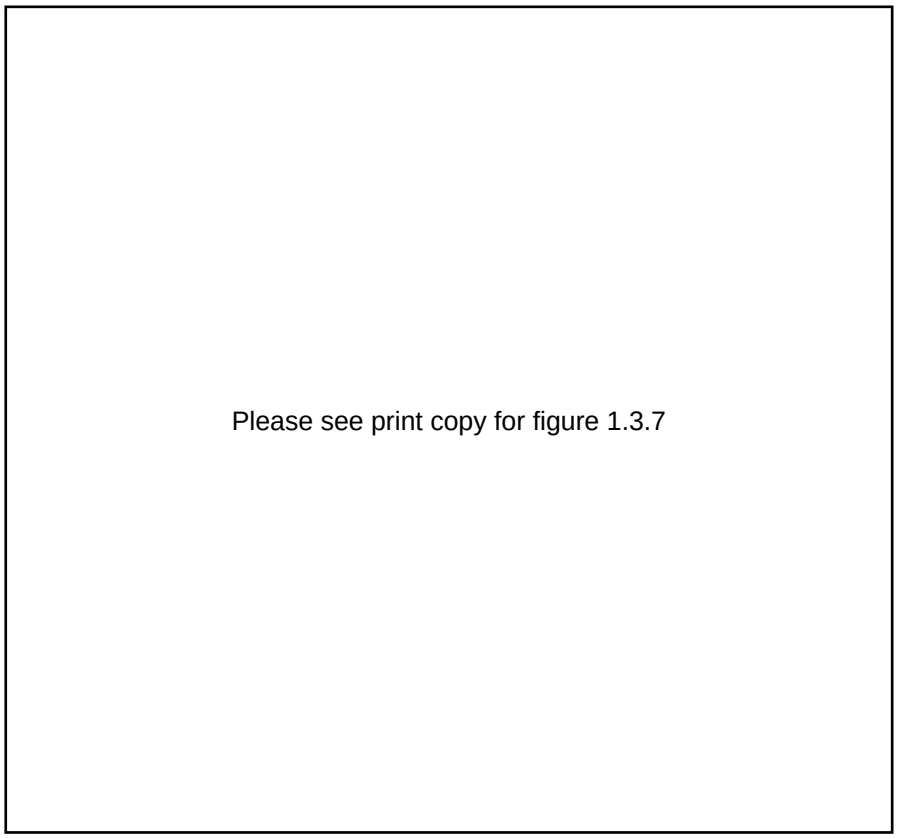

Figure 1.3.7 Qualitative relationships between grinding parameters [8]

Werner and Kenter [5, 6] also carried out numbers of experiments using metal bond diamond cup wheels of varying grain size in grinding of different types of PCD in terms of their grindability. They found that with fine-grained PCD (SYNDITE 002 grade) the highest cutting performance and MRR are achieved.

Studying the effect of PCD type on the PCD grinding parameters is beyond the scope of this research. In this thesis a conventional grinding machine and a fine diamond grinding wheel are used in order to investigate the behaviour of the grinding forces considering in-feed, MRR, material type, contact area, condition of the grinding wheel surface, oscillation rate and wheel wear.

1.3.2. Grinding Wheels

A grinding wheel is considered "a cutting tool with infinite cutting points" [45]. A grinding wheel consists of abrasive particles, bond bridges and pores [42]. The bond holds the abrasive particles together and the pores provide enough space for chips and fluid. Depending on the grain or grit size graded from coarse to fine, or the mesh size, which corresponds to the space between the grains, the cutting action varies. Due to the PCD hardness only diamond wheels with grain size D46 or finer are used in grinding of PCD [4-6]. For a certain operation the bond type depends on the "wheel and work speeds, area of wheel in contact with the work, vibration in wheel spindle or work, shape and weight of work and many other like variables" [45]. A common choice of grinding wheel in conventional grinding of PCD is a diamond cup wheel. There are several types of bonding materials used in grinding wheels. Superabrasive grinding wheels are used with resin, metal and vitreous bonding materials. Liu and Tso [9] have done research on wheels with different specifications used in grinding diamond tools. Their research investigates bond type and wheel structure (including the grit size and mesh size). The grinding process can be characterized according to the diamond grinding wheels used in the grinding process.

Resin Bond

In this case, the grinding process is characterised by low grit retention forces, low degree of grit protrusion and the abrasive grains being deeply embedded in the bond [44]. High contact forces and temperatures in the contact zone will cause an

interrupted self-sharpening effect [44]. Because of the resin softness, a resin bond wheel makes the most severe deformation of the PCD tips so that they become a convex curve rather than a plane surface [9]. Fewest edge cracks can be observed using a resin bond wheel and the most prone to cracks is the metal bond wheel [9]. It takes more time to grind PCD with a resin bond wheel (double the grinding time of metal bond) [9].

Metal Bond

With a metal bond diamond wheel the lowest gap between cracks in cutting edge is achieved [9]. In other words, using suitable grinding parameters, the metal bond wheels will produce a superior finish and edge quality [27]. The metal bond wheel produces the best surface roughness followed by the vitrified bond wheel. However, the worst edge cracks belong to metal bond wheels [9]. In fact, metal bond wheels create the most severe damage on the PCD edge. Metal and vitrified bonds have higher capacity to hold the diamond grits during grinding. As a result, their G-ratios are about 20 times higher than that of the resin bond. Because of the higher bonding strength of metal compared with vitrified bond, a metal bond wheel needs longer grinding time [9] and it has to be dressed more regularly [7].

Vitrified Bond

Vitrified bond wheels have a higher grit protrusion and a better self-sharpening effect. The biggest advantage of using these wheels is the reduced temperature in the contact zone due to the open-pored characteristics of the bond [7]. Considering the characteristics about resin and metal bond wheels, Liu and Tso [9] found that vitrified bond diamond wheels are the most suitable wheels for grinding PCD.

The grindability of PCD grade, the requirements on the tool edge quality and the profitability indicate the specifications of the grinding wheel [8].

Werner and Kenter [4, 8] investigated the influence of the grinding wheel diameter on the grinding process and the macroscopic wear. It was found that a larger grinding wheel provides higher MRR and G-ratio [8]. Moreover, a small wheel has to be trued

more often than the large one. In other words, because the large wheel wears more evenly, dressing the wheel without truing can be sufficient for the respective grinding process [4].

Although there are publications [46-50] dedicated to monitoring grinding wheel conditions prior and after grinding, in the research presented in this thesis the PCD grinding parameters are controlled in order to achieve a higher MRR and lower rates of wheel wear with satisfactory edge quality.

In the research presented in this thesis both metal and vitrified bond diamond grinding wheels are used. The majority of the experiments are carried out using a metal bond cup wheel though it is expected that the general conclusions drawn from the research will remain similar irrespective of the bond. Detailed information about the optimal diamond wheels for grinding diamond tools is discussed in [9, 13, 16, 21, 22, 24, 51].

1.4. Truing and Dressing

The grinding wheel needs to be prepared before and after the grinding process by truing and dressing. Due to the microscopic and macroscopic wear occurring at the grinding wheel surface (including the bond and the diamond grains) the original wheel contour changes to a concave or convex shape. To avoid this geometric error the grinding wheel needs to be trued. Truing removes the material from the surface of the wheel so that the grinding wheel face will "run true" [45] at grinding speed. In contrast, dressing removes the dull abrasive grains from the glazed cutting face so that new sharp grain edges are formed.

In a conventional truing method, a silicon carbide wheel and brake-type truing device can be used, while for dressing, a medium hardness aluminium oxide dressing stick is recommended. To optimize the wheel flatness and eliminate the risk of over dressing the wheel or chipping tools, the size of the particles of the dressing stick should be the same as the mesh of the grinding wheel [7]. The abrasive and the bond type of the grinding wheel are the most important criteria for deciding the type of truing and dressing to use [17].

Cutting efficiency is an important feature of a grinding wheel, which is often described as wheel sharpness [52]. According to Chen [52], a sharp grinding wheel should provide high material removal rate, low grinding force and low energy consumption, small residual stock and high size accuracy, low grinding temperature, and good surface integrity. Usually, after a grinding time of less than 30s, the grinding wheel wears out and its abrasive surface becomes glazed and material removal stops. In this phase, if constant normal force is used, work piece and grinding wheel rub against each other at a constant contact force. So, dressing of the grinding wheel becomes necessary. In grinding PCD, the main purpose of dressing is to remove the bond in order to free new diamond grains and create enough space between the grains for cutting fluid and chips [4-6].

As Shaw [42] has stated, in stock removal grinding (SRG), due to the high stock removal the grinding wheel wears more quickly and so dressing the wheel surface periodically is not necessary. In the case of form and finish grinding (FFG), to provide a sharp cutting edge having a sharp wheel becomes essential. So, the grinding wheel needs to be dressed periodically. Figure 1.4.1 illustrates the process of conventional truing and dressing.

Shaw [42] has also stated that some of the reasons for redressing include,

- Excessive forces or power
- Poor surface integrity
- Inadequate dimensional accuracy due to the excessive temperature or wear
- Instability, leading to waviness

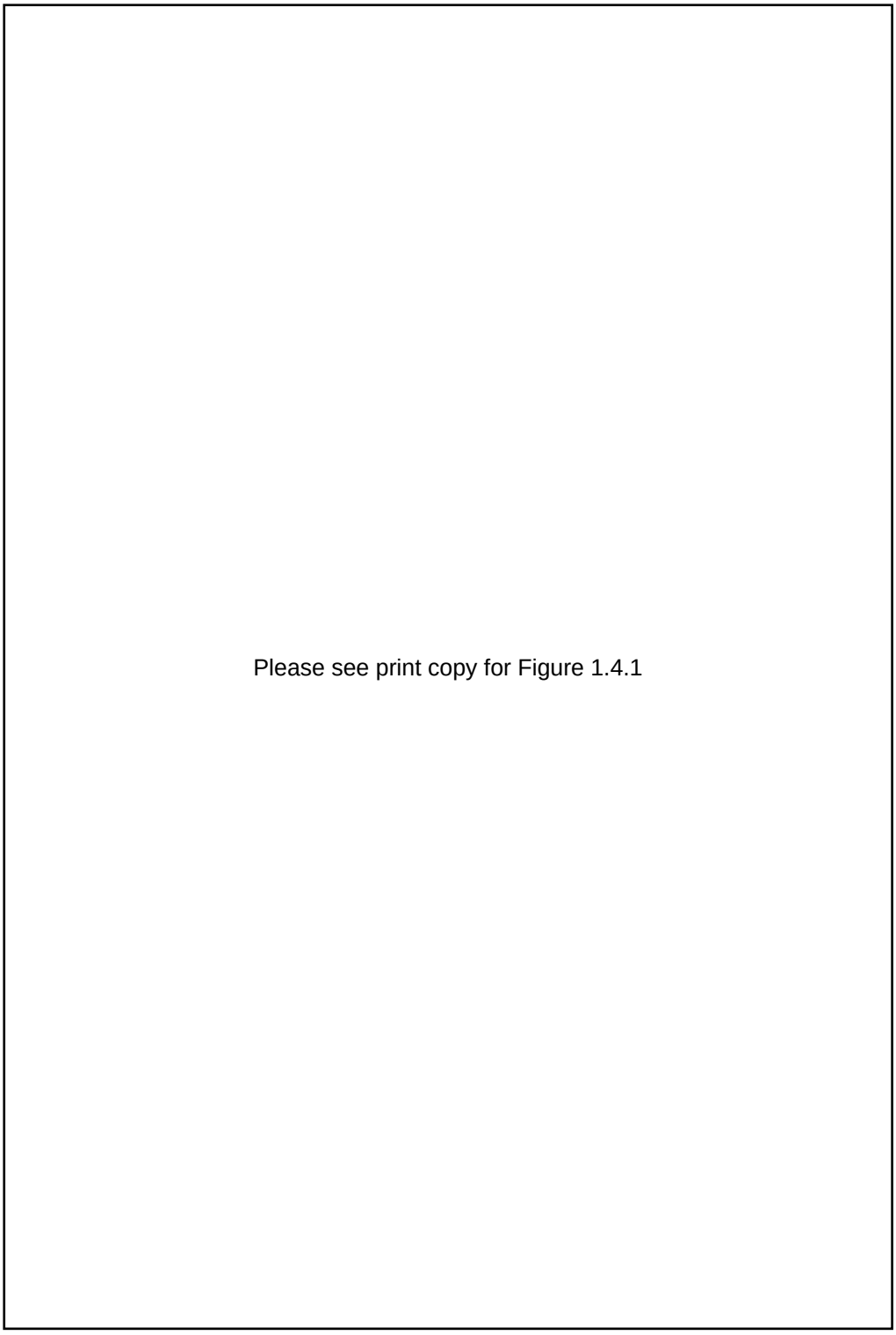

Figure 1.4.1 Conventional truing and dressing process [53]

Before truing or dressing the machine has to be run long enough to attain normal temperature in the bearings. Otherwise, the wheel may not be trued properly with the spindle [45].

Usually, the grinding wheel needs to be dressed after less than 30s grinding [4-6, 8]. There are different surface parameters to measure and characterise the topography of the grinding wheel surface. The peak to mean line height R_p is one of those parameters suitable for describing the space for chips due to bond wear. R_p gives the best information about the dressed condition [4-6].

It is important to use a suitable dressing procedure. If an inappropriate dressing procedure is adapted, too many diamond grains will break out of the bond without having removed the work piece material [4-6]. The dressing intervals should also be selected such that a better grinding performance and reasonable wheel wear are achieved [47]. Hence, dressing is an important aspect of PCD grinding and is included in the research in this thesis.

1.4.1. Unconventional Truing and Dressing Methods

Other than the silicon carbide wheel and brake-type truing device, some other unconventional preparation methods of grinding wheels can be used. These techniques were not used in this thesis but for relevance are briefly discussed here. They include:

- **EDM** (electrical discharge machining) is a non-contact method, which can be used as a truing and dressing method [54, 55]. In EDM dressing no special dressing equipment is required. The dressing can be conducted on grinding machines and the power source of conventional EDM machines can be chosen. Dressing with this method is easily changed to in-process dressing. The wheel is dressed directly on the spindle of the grinding machine, so there is no assembling error. The EDM dressing can even be used to true the grinding wheels. [54]

- **ECM** (electro chemical machining) can be used for dressing the wheel. It is based on the anodic dissolution of the layer and hence results in higher grain protrusion [56].

- **ECDM** (electro chemical discharge machining) also known as ECAM or EEDM is a hybrid technology of EDM and ECM, which is used for truing and dressing of metal bond diamond wheels in one step. EDM shapes the grinding wheel and ECM dresses it [56].

- **ECD** (electrochemical in-process controlled dressing) **grinding** is a method with electrochemical in-process controlled sharpening which has been reported to improve the G-ratio by 5 times when compared with conventional grinding as well as reducing costs and increasing productivity [44, 57, 58]. It is based on the electrochemical dissolving of the metal bond system. Due to the voltage applied between the grinding wheel and the electrode, in the presence of the coolant a current flows, which breaks down the metal bond system into the ions and converts them into hydroxides and oxides. The grinding wheel bond is dissolved and set back behind the tips of the grains, causing an optimum grit protrusion to be established or abrasive grains that have become blunt to be released from the bond. The sharpening speed is proportional to the speed at which the metal bond is dissolved. [44, 57]

- **ELID** (electrolytic in-process dressing) **grinding** is an effective method to dress the grinding wheel during grinding. It is based on the electrolytic in-process dressing of the grinding wheel during grinding. When the grinding wheel is subject to loading and glazing, the wheel is dressed automatically using electrolysis [47].

1.5. Other Methods of Machining PCD Blanks

Although the most suitable process for manufacturing good quality diamond tools is grinding [9], machining PCD is not limited to grinding. Machining methods for PCD blanks include:

- **EDM** (electro discharge machining) [12, 18, 24-26] is the most popular PCD cutting technology [27]. Although the diamond is not electrically conductive, the presence of cobalt in PCD as solvent/catalyst provides enough conductivity for EDM process [29]. In EDM, the material is removed by

means of the erosive effect of electrical sparks between two electrodes. The actual cutting tool is a precise electrical spark, which occurs typically 1000000 times per second. Each individual spark removes metal by creating a miniature molten pool generated by intense heat present at the tip of the spark. The Electrical Discharge Machining is a thermal-mechanical process: thermal heat from the spark and imploding of the gas bubble [31]. It is claimed that the surface integrity in grinding is better than that in EDM [24]. It is said that EDM damages up to 0.05mm depth on the surface, so, grinding can be combined with EDM to remove this damaged area [29].

- **WEDM** (wire electrical discharge machining) [28-30] uses a wire of 0.05 to 0.025mm as a tool electrode and the dielectric (deionized water) is injected into the gap. The advantages of WEDM are the low cost of the wire and the non-contact nature of the process [30].

- **EDG** (electrical discharge grinding) [11, 31, 32] uses an electrically conductive wheel to erode the material from the work piece. The wheel, which is usually made of a low grade graphite, is very porous and easy to machine. A steel tool can be used to form the required profile into the wheel, and the wheel will erode that profile into any conductive material [31].

- **Laser cutting method** [10, 33, 34] can be used for PCD fabrication. This method has the ability to start the cutting of the large diameter PCD discs anywhere on the discs, which reduces the wastage and the cutting operation takes less time [33].

- **HPAWJ** (high pressure abrasive water jet) is one of the new methods used to machine PCD [27].

Laser cutting method and HPAWJ have not been used extensively because of the higher cost and higher machining technology [27]. Undoubtedly, each technique has its own advantages and disadvantages. However, conventional grinding is relatively

simpler to implement and this encourages the industry to use this method as a convenient process for machining PCD compacts.

The reported research in this thesis does not include unconventional truing/dressing methods and PCD machining operations other than grinding using a diamond grinding wheel. However, the information about the other methods mentioned above provides a general view for users interested in PCD machining and shows the simplicity of using a conventional grinding machine and diamond grinding wheels.

1.6. Available Machines

The grinding machines in the market have been either developed particularly for grinding PCD or modified for PCD grinding uses. The available grinding machines include Ewag RS 10 [13, 14] developed in early eighties, Agathon 250-PA-CNC machine [43] in mid eighties and Ewag RS 12 [11] in the nineties. Modern PCD grinding machines include Dia-Profile-CNC, M-1050-Automatic (PCD automatic grinding machine), PCD 300 with tool head all three developed by LACH, M-4040-CNC (PCD universal grinding machine), SR-9000-CNC (PCD grinding machine for top grinding), Profil-CUT-8000-CNC (an EDM wire erosion machine by LACH), WCD 55 HELLIX, RS-09 for PCD precision grinding, RS-15, COBORN RG6FE, COBORN RG6 CNC grinding machine and RG 5A PCD grinding machine [39]. These publications [11, 13, 14, 39, 43] present detailed information in order to compare the specifications of a particular PCD grinding machine with an ordinary grinding machine designed for non-PCD uses. Each of these machines has its own facilities and advantages.

1.7. Wheel Life

Due to the high wheel wear rates detecting wheel wear is particularly important in PCD grinding. In FFG, depending on how often the wheel needs to be dressed the wheel life changes [42]. In SRG, the wheel life is measured based on the grinding ratio (G = "volume ground away/volume of wheel consumed" [42]). Due to the hardness of PCD and high wear resistance, more material is removed from the grinding wheel than from the PCD work piece when grinding PCD. Depending on the machining operation, the volume of the grinding wheel wear is generally 50 to 200 times the

volumetric material removed from the work piece. In other words, it is usually found that the G-ratio is less than 1 (approx. 0.005 to 0.02 or even less). So, one of the major concerns in PCD grinding is how to minimize the macroscopic and microscopic wheel wear.

The wheel wear includes wear flats on abrasive particles, attritious wear, microchipping and loss of entire grits due to bond fracture [42]. The wear of individual abrasive particles involves rubbing without chip formation, which emphasises attritious wear, and chip formation, which gives greater emphasise to microchipping [42].

For a PCD grinding system it is important to determine when to true and/or dress the diamond grinding wheel. The truing and dressing operations affect the wheel wear and the wheel wear affects the grinding process and wheel life to a large extent. So, research has been conducted and reported in this thesis covering these aspects of PCD grinding.

1.8. Edge Quality

The quality of PCD cutting edge is an important indicator of a successful PCD grinding operation. The small range of in-feed (a few microns) in PCD grinding makes the process of studying the quality of the contact zone difficult. The material removal mechanism can be monitored on the basis of tribological relationships and scanning electron microscopes (SEM) [8]. The chief quality features are the geometrical accuracy and evenness or serration of the ground PCD cutting edge [8]. Typically the edge quality is examined using a microscope with 10-50x [8, 15, 16, 21, 41, 59] magnification and if no chipping is visible the quality is acceptable. The edge quality of PCD insert has a critical effect in the performance and life of the tool and as a result the overall cost of the PCD tool and so the cost of the cutting operation are both affected [19].

Many authors [8, 9, 11, 13, 15, 16, 19, 24] state that the diamond grit size on the wheel affects the ultimate edge quality. In fact, smaller cutting edge serration is achieved with finer grit, but in a longer grinding time. On the other hand, a coarser wheel removes more material from the PCD in a shorter time. So, to have a better edge quality it is suggested that the MRR and G-ratio are set to a lower value. According to Kenter [8,

15] the PCD grade also affects the edge quality. The finer initial grain size results in smaller serrations.

Cassidy [20] has examined the input variables such as the grinding wheel speed, in-feed rate and oscillation frequency on the resulting edge quality of PCD tools.

Kenter [8, 15] also claims that "shorter wheel sharpening times with low sharpening pressures at the end of the grinding process, and longer spark-out times" improve the edge quality.

To avoid unsatisfactory cutting edges in all PCD grinding operations measures of the grinding parameters, which improve the edge quality are necessary.

1.9. Thesis Objectives

From the literature review above it has been shown that there are considerable advantages in using PCD cutting tools. Many researchers have worked on different aspects of PCD grinding and its applications. However, there are still unknowns about the process of grinding PCD that need further investigation. The majority of the research presented in this thesis covers detailed information about the grinding forces, range of in-feed, material removal rate (MRR), truing and dressing processes, wheel wear and the edge quality using a conventional grinding machine designed for non-PCD uses.

As discussed in the literature there has been much research on several aspects of PCD and the related machining operations including:

- PCD applications,
- PCD grinding methods,
- Specific PCD grinding machines in the market,
- Grinding force analysis,
- Material removal analysis,

- Optimization of the diamond grinding wheels including the bond type and grit size,
- Grindability of different kinds of PCD compacts,
- Truing procedure of diamond grinding wheels,
- Dressing procedure of diamond grinding wheels,
- Wheel condition monitoring, including the study of grinding wheel wear,
- PCD grinding optimization,
- Influence of temperature in PCD grinding,
- Optimization of the PCD grinding process,

From the literature review it is concluded that due to the high number of variables affecting the PCD grinding process, optimization is usually dependent on the particular conditions used for testing, and therefore for each new material or application new studies are necessary. Regardless of all the studies undertaken in the literature review, there are a few aspects that still need to be addressed.

From the literature review it was shown that due to the special characteristics of PCD, grinding machines are modified or a specific grinding system is designed in order to meet the PCD grinding requirements. There is not much literature considering the PCD grinding capability of a conventional grinding machine designed for non-PCD uses. So, one of the objectives of this thesis is to investigate grinding of PCD using a conventional grinding machine.

As discussed in the literature it is recommended to grind PCD using a constant contact force. However, because of the limitations of a conventional grinding machine it is most likely that such a machine will use a constant feed. So, another aspect of this research takes into consideration the optimization of the grinding parameters using a constant in-feed.

There are considerable advantages in measuring the grinding forces and the removed material from the work piece and the grinding wheel. The related objectives are to quantify the relation of grinding forces, in-feed, material removal rate, grinding wheel wear, truing, dressing, spindle speed, oscillation rate, grinding operation and edge quality. None of the available publications has studied the variation of all of these parameters using constant feed.

Some other researchers have controlled a few grinding parameters, but often have ignored other PCD grinding issues. So, another aspect of the work controls and monitors as many parameters as possible in order to achieve a satisfactory material removal rate, wheel wear and edge quality.

Due to the very high rates of wheel wear, frequent dressing is one of the most important issues in grinding PCD as discussed in the literature. However, there is not much literature discussing research on the truing and dressing procedures regarding the PCD grinding application in particular. So, another major area of work addressed in this thesis is to optimize the dressing process in PCD grinding. A dressing model that accounts for wheel wear, productivity and cutting efficiency is therefore necessary.

The purpose of this research is to examine the parameters used during the grinding of PCD work pieces as a superabrasive and to determine an optimum setting in order to achieve a satisfactory quality of the PCD cutting edge, maximum productivity and minimum rate of wheel wear. This research emphasizes the approach for optimising the grinding process using polycrystalline diamond (PCD) abrasive. One novel aspect of this research is to study the capability of a conventional grinding machine designed for non-PCD uses. Outcomes of this thesis will include analysing and evaluating the PCD grinding process using a conventional grinding machine, and then developing and expanding the method or the results to other PCD grinding applications.

Detailed analysis of cost is beyond the scope of this thesis. However, many of the topics in these investigations will provide useful information to users wishing to make their tradeoffs.

1.10. Thesis Outline

The experimental equipment used in this thesis is described in Chapter 2 . Two experimental rigs were used in the experimental work. The first was a 3-axis surface grinding machine and is referred to as the "grinding machine" in the rest of the chapters except in Chapter 6 where it is referred to as "Machine 1". Two axes of the grinding machine were automated. The grinding machine was equipped with a 3-axis force sensor and a truing setup. The ordinary surface grinding wheel designed for metal uses was replaced with a diamond cup wheel. The second test rig was a very rigid 2-axis machine with variable spindle speeds used for manual tool machining operations and will be referred to as "Machine 2". No force sensor was installed on Machine 2. The mathematical description of the grinding forces developed in this chapter is used in the grinding force analyses of Chapter 3 , Chapter 4 and Chapter 5 .

The forces produced during grinding are investigated in Chapter 3 . The grinding parameters are optimized in Chapter 3 taking into account the grinding forces. The relation between the maximum grinding forces and several process variables including in-feed, contact zone, material removal rate MRR and the oscillation rate are developed in Chapter 3 . The obtained results are used in the subsequent chapters.

Chapter 4 studies the effect of the abrasive layer condition of the grinding wheel on the PCD grinding results. In this chapter the grinding wheel is prepared in different ways. Then the truing/dressing influences are investigated with respect to the grinding forces. The obtained results reflect the importance of truing and dressing procedures. Several aspects of dressing operation are taken into consideration including when and for how long the wheel needs to be dressed. The dressing process is compared for two types of material. In Chapter 4 the dressing process is optimized considering some of the process parameters.

Chapter 5 is dedicated to the wheel wear study. The grinding wheel wear is considered as a recognized problem and limitation in the grinding of PCD compacts. The behaviour of the grinding wheel as it wears out is considered in Chapter 5 . The grinding parameters are optimised in order to achieve the minimum material removed from the grinding wheel. The relation between the in-feed and the rate of material

removed from the grinding wheel is studied regarding the material removal rate. The dressing method and its effect are investigated in particular. Chapter 5 compares and quantifies the volumetric wheel wear rate (VWWR) for two types of material (PCD and cemented carbide) having different hardness.

The quality of the PCD cutting edges is investigated in Chapter 6 . An optical microscope was used in order to analyse the ground cutting edge of the PCD compact. The grinding parameters discussed and optimized in the three previous chapters are optimized considering the edge quality of the PCD work piece. Two machining operations and two different diamond grinding wheels discussed in Chapter 2 are tested in Chapter 6 and their related results are analysed.

The conclusions of the work developed in this thesis are given and discussed in Chapter 7 . The PCD grinding optimization results are intended to maximize the material removal rate and edge quality and minimize the rate of material removed from the grinding wheel while satisfying the system constraints including grinding forces, in-feed, wheel wear, dressing process. The advantages and possible applications of such a grinding system are pointed out as well as the limitations of the current work. Suggestions for future work studies are also presented in Chapter 7 .

CHAPTER 2 EXPERIMENTAL SETUP

2.1. Introduction

A conventional grinding machine was used in this research for the experiments undertaken in Chapters 3-6. However, this research does not focus on grinding alone but also includes the dressing and truing of the grinding wheel. The details of experimental equipment used in this thesis are described in this chapter.

A digital signal processor (DSP) controls the grinding machine. The DSP output voltage, which is also the servo drive input voltage, is considered a motor torque value multiplied by a scaling factor. "The DSP gives a flexible and easy to program system that allows a variety of control and signal processing strategies to be implemented" [35]. The grinding machine uses AC servomotors in current control mode and the output voltage of the DSP is a torque command input to the servomotor.

In Section 2.2 the grinding machine system is discussed. The details of the modifications made to the grinding machine and the physical arrangement of the grinding machine are described. The PCD samples and the grinding wheels used are illustrated and detailed. The grinding wheel preparation methods including truing and dressing are explained and configured in Subsections 2.2.2 and 2.2.3, respectively. The material removal measurements from the work piece and the grinding wheel are described in Subsection 2.2.4. Data acquisition and control procedures are discussed in Section 2.3. a flow chart of the software process is also shown in that section. Following that, the grinding forces are described in Section 2.4. Finally, the experimental arrangement is summarised in Section 2.5.

2.2. Grinding Machine

The grinding machine used in this thesis was originally a manual surface-grinding machine with three axes. The spindle motor has nameplate ratings; 1.1kW rated power, 380Volts rated voltage, 2.5Amps rated current and 2840rpm rated speed. Two of the axes of the grinding machine were automated by modifying the system with AC servo drives and retrofitting the motors. To measure the grinding forces produced during

grinding, force sensors were also installed. The grinding machine had an air extraction and coolant circulation system. So, the grinding condition was wet. The grinding machine was also equipped with a truing device mounted on the main table. Figure 2.2.1 shows a photo of the grinding machine.

Figure 2.2.1 Grinding machine setup

The three axes of the grinding machine are denoted as X, Y and Z. The X-axis moves the main table where the work piece is mounted on. The Y-axis moves the same table in a plane at 90 degrees to the X-axis motion. The Y-axis is the only axis that is moved manually. The Z-axis is used to lower the grinding wheel into an appropriate position to the work piece and the truing wheel. The grinding wheel spindle is attached on the Z-axis. Directions of motion of these 3 axes are perpendicular to each other. Figure 2.2.2 shows the axes orientation of the grinding machine.

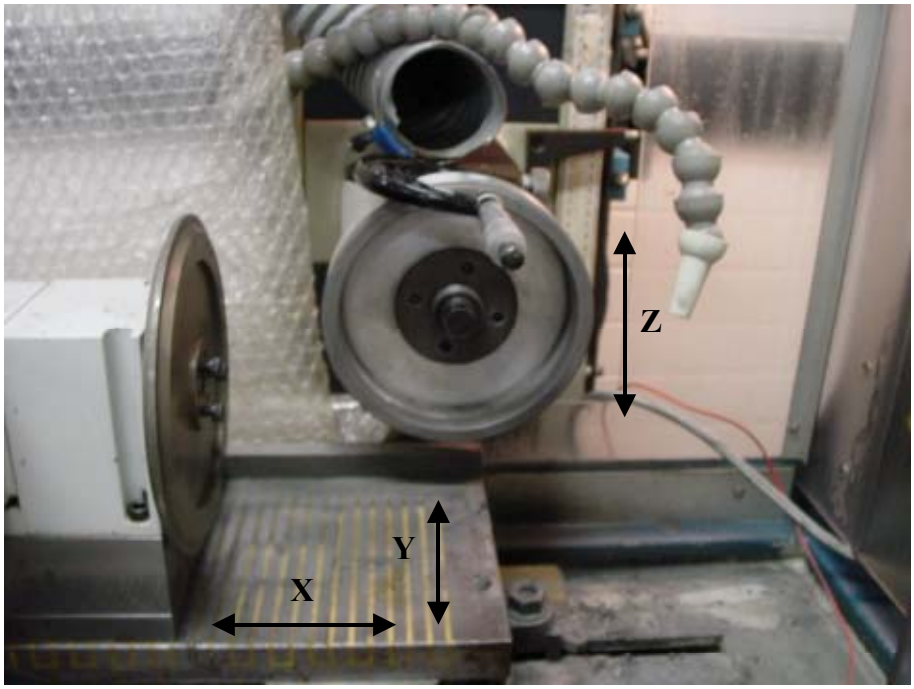

Figure 2.2.2 Axes orientation of the grinding machine

The grinding machine has been previously used for plunge grinding where the grinding wheel and the work piece motion has been in the same plane. In other words, in plunge grinding the X-axis moves but the Y-axis does not. However, in this research the grinding machine was used for face grinding because of different grinding conditions including the grinding wheel type and work piece material. Usually the grinding wheels used in grinding PCD are different types of cup wheels. Thus, the two grinding wheels used in this thesis were both cup wheels. The Y-axis was used to give in-feed and at the end of each experiment it was rewound. The original accuracy of the Y-axis was ± 20 microns, and to increase the accuracy of the Y-axis in order to give smaller in-feeds, a dial indicator with ± 10 microns accuracy was positioned under the Y-axis rail using a magnetic holder, so the in-feed could be adjusted according to the dial indicator (Figure 2.2.3). The X-axis provides oscillations to avoid uneven wear of the grinding wheel.

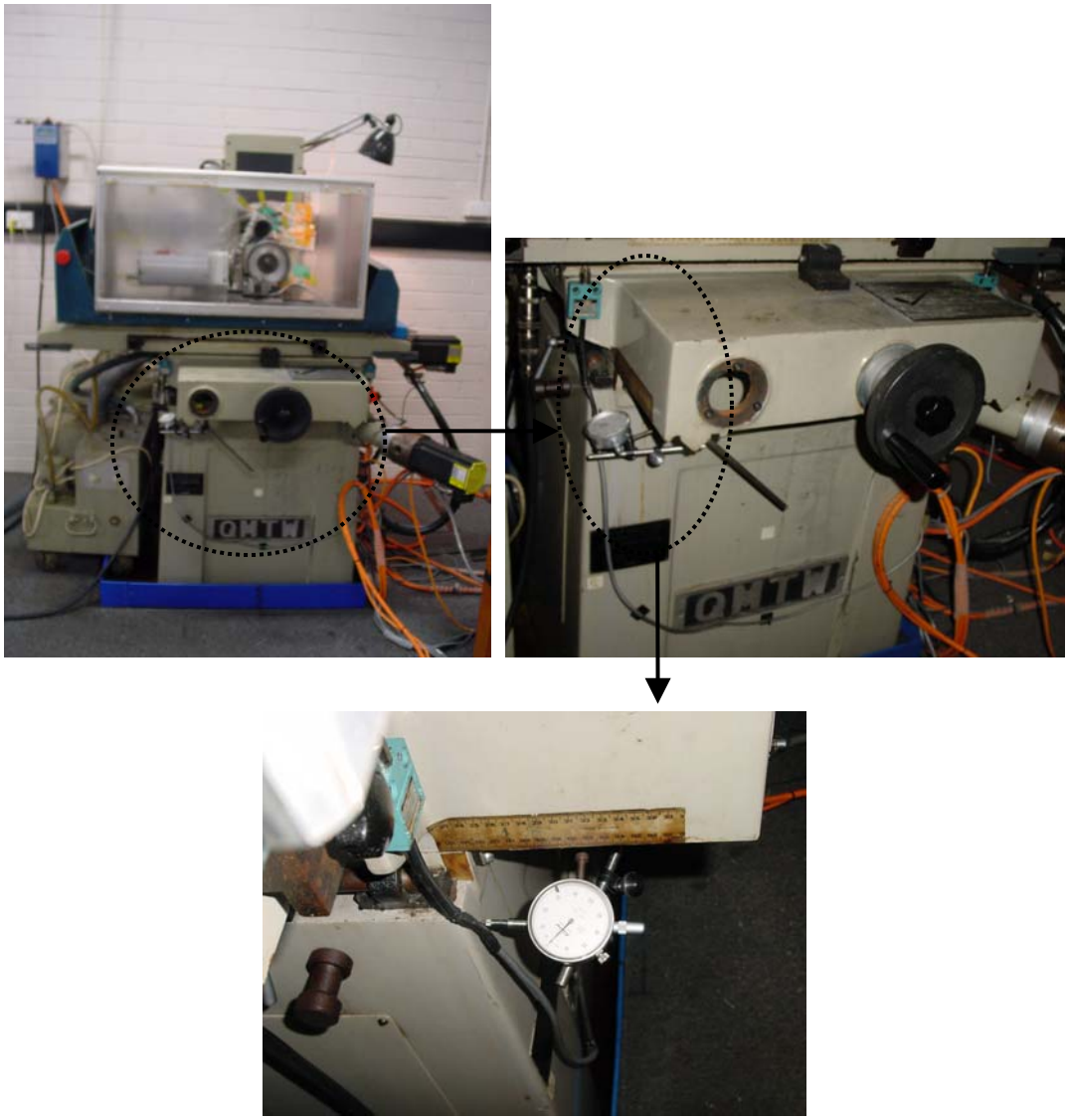

Figure 2.2.3 Giving in-feed in Y-direction using a dial indicator

The in-feed was calibrated using a piece of paper. Firstly, a paper was held between the grinding wheel and the work piece. Then, the Y-axis was wound until the work piece and the wheel held the paper and the indicator was set to zero. Figure 2.2.4 shows the configurations of the machine for grinding.

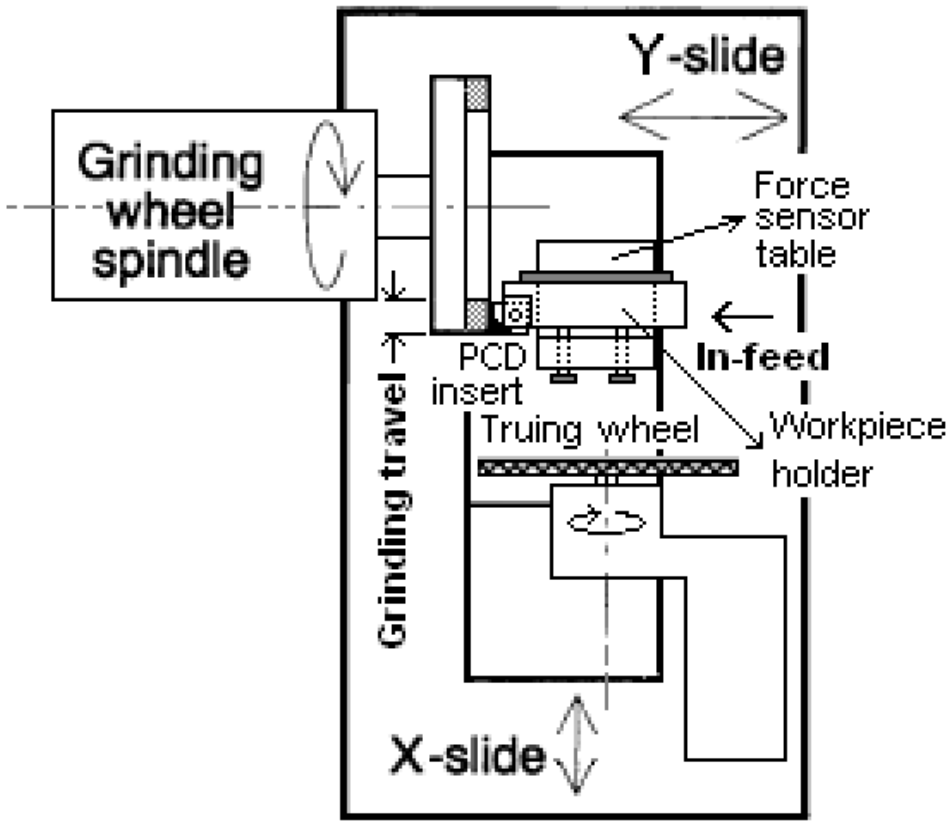

Figure 2.2.4 Top view of the grinding system

The X-axis mechanism of the original machine was replaced with a linear ball screw. The screw arrangements of the other 2 axes were not changed.

The servomotors on X and Z-axes are identical permanent magnet brushless servomotors. Resolvers installed on the motor shafts record the position data to be used in the control loop.

To measure the grinding forces produced during the grinding process, a three-axis piezoelectric force sensor was also installed between the work piece and the mounting table. Each axis of the force sensor allows the measuring of the forces applied to the work piece in X, Y and Z directions, which can be combined as tangential and normal forces. The force sensor has a zeroing button on the DSP board to ensure that all force readings were set to zero before grinding started.

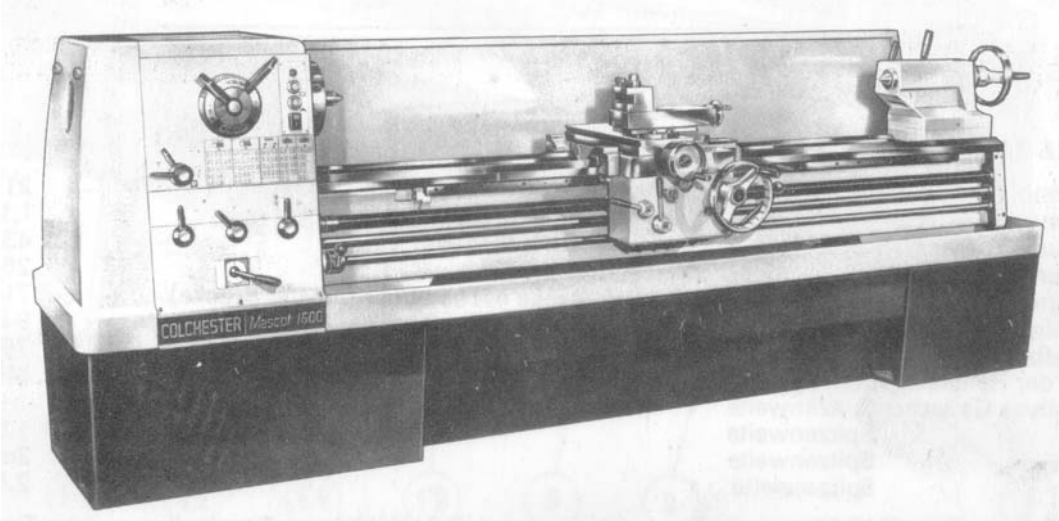

Figure 2.2.5 The second grinding machine used to grind PCD

Another machine shown in Figure 2.2.5 was also used in this research to grind PCD. The results of the experiments using this machine are presented in Chapter 6 where it is referred to as Machine 2. This machine is model MASCOT 1600 80-gap, which is a very rigid 2-axis lathe with minor fittings added to allow grinding. This machine weighs 2430kg and has a motor power of 9.3kW. It has variable spindle speeds in the range of 20-1600rpm and a different system of holding the work piece during grinding. The significant differences between the 2 grinding machines are due to the different axes, stiffness, power rating, spindle speeds and work piece holder. Figure 2.2.6 shows the minor fittings of the second grinding machine.

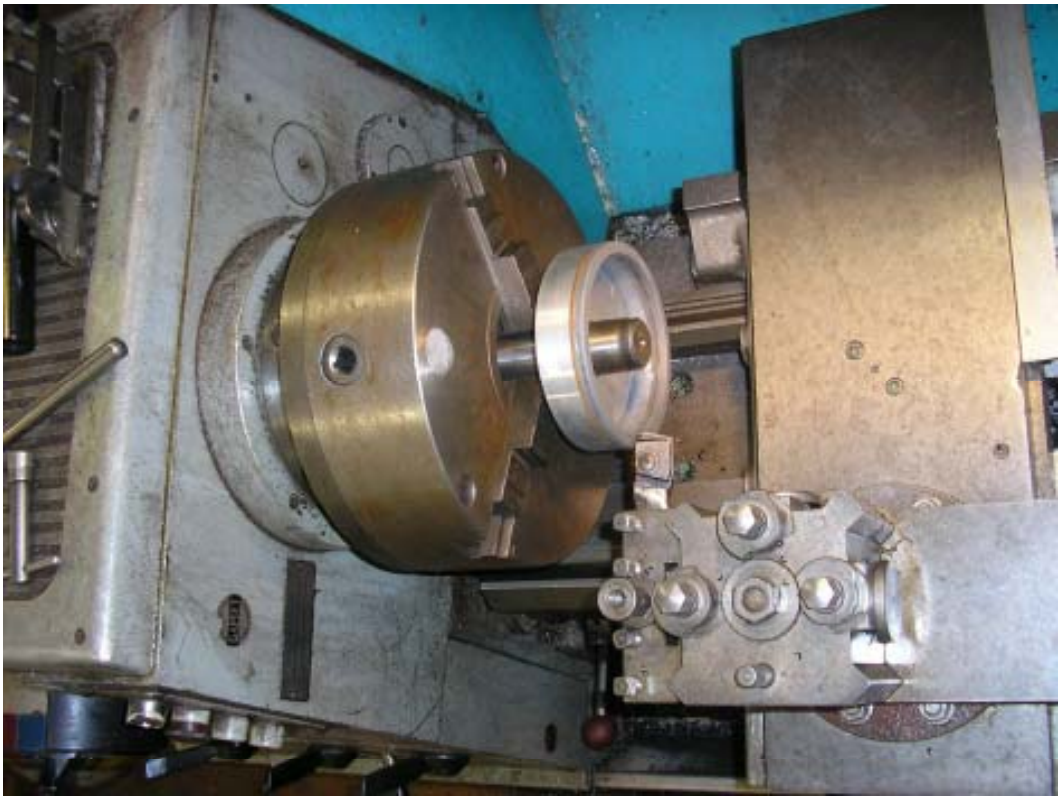

Figure 2.2.6 Top view of the second grinding machine setup

2.2.1. PCD Samples and Grinding Wheels

Figure 2.2.7 and Figure 2.2.8 show the PCD blanks and the grinding wheels used in this research. The grinding wheels were both supplied by Cape Diamond Products Ltd. The model of the metal bond wheel was C0324001-D22/36 and the vitrified bond was VIT Q10822-D16 3004/2 8.0.

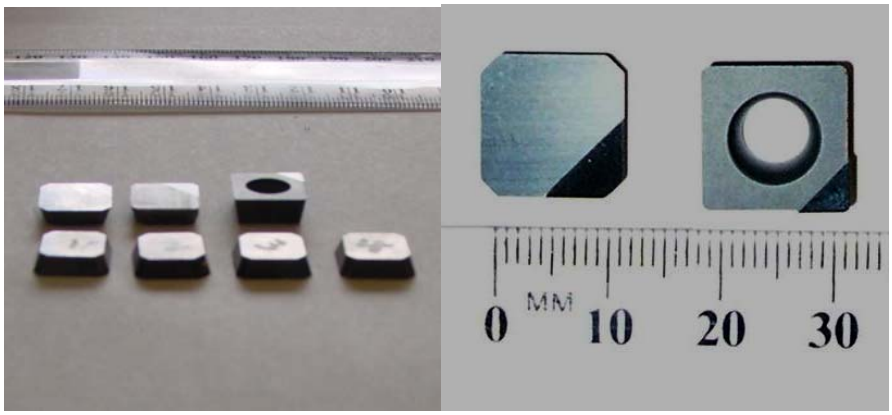

Figure 2.2.7 PCD samples

Most of the experiments were conducted using the wheel with metal bond cup wheel. The other wheel was mainly used to study the edge quality. The first wheel is a fine metal bond grinding wheel and the second wheel is a coarser vitrified one. They were both 150mm in diameter. The first one had 10mm rim width and the second one 20mm. Figure 2.2.8 shows the two diamond grinding wheels used in this thesis.

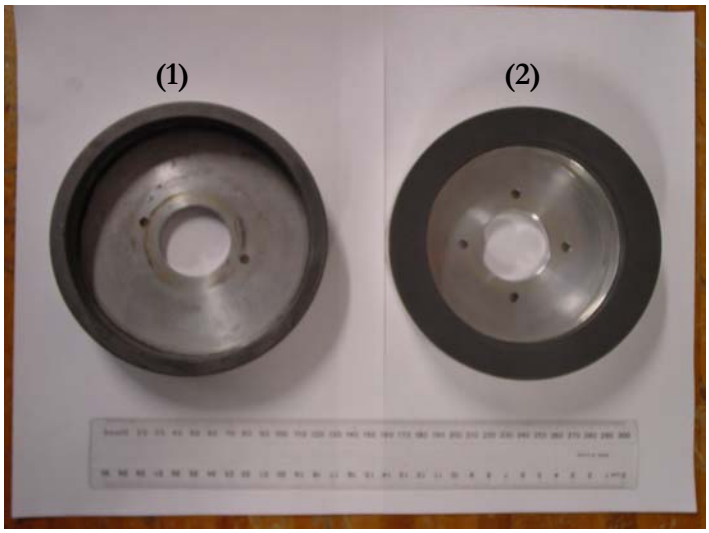

Figure 2.2.8 Grinding wheels (1) Metal bond (2) Vitrified bond

2.2.2. Truing

As discussed in Chapter 1 , the grinding wheel needs to be trued frequently to maintain the wheel topography. The grinding wheel attached to the Z-axis is lowered to a certain point and the truing wheel is positioned perpendicular to the grinding wheel as shown

in the top photograph of Figure 2.2.9. The truing occurs in the X-direction and depending on the rim width of the truing wheel and the grinding wheel, the truing wheel oscillates until the whole rim is trued and the desired contour is achieved. In order to have an even abrasive surface, enough of the grinding wheel has to be removed.

The spindle speed of the truing wheel was 3000rpm and it was 150mm in diameter (the same size as the grinding wheel). Figure 2.2.9 shows a photograph of the truing device beside the grinding wheel.

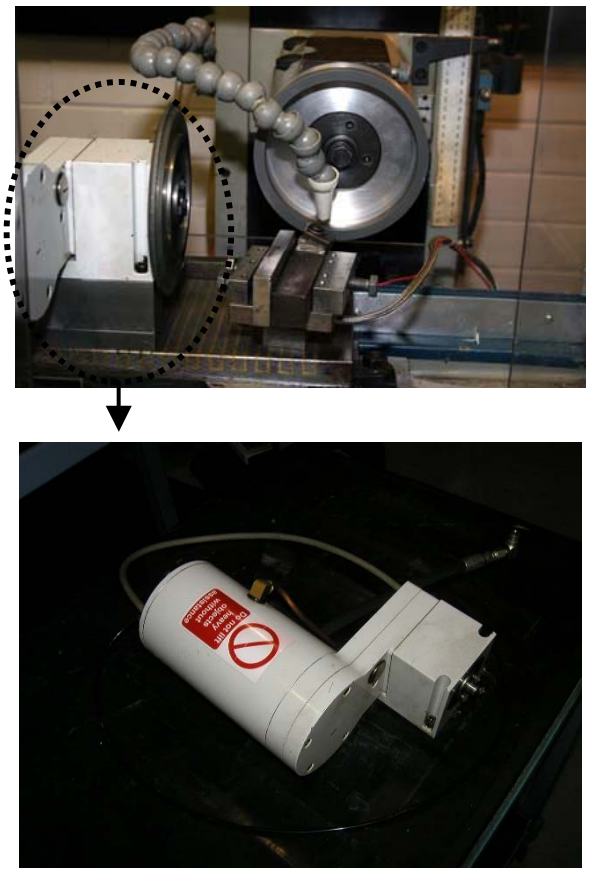

Figure 2.2.9 Truing device

Figure 2.2.10 shows how the truing wheel oscillates at v_d and removes material from the grinding wheel. The truing travel and the direction of in-feed are both pointed out in Figure 2.2.10. The truing in-feed is given in the same direction as grinding in-feed. To avoid uneven wear of the truing wheel during truing, the truing wheel was frequently taken out and screwed to the other side.

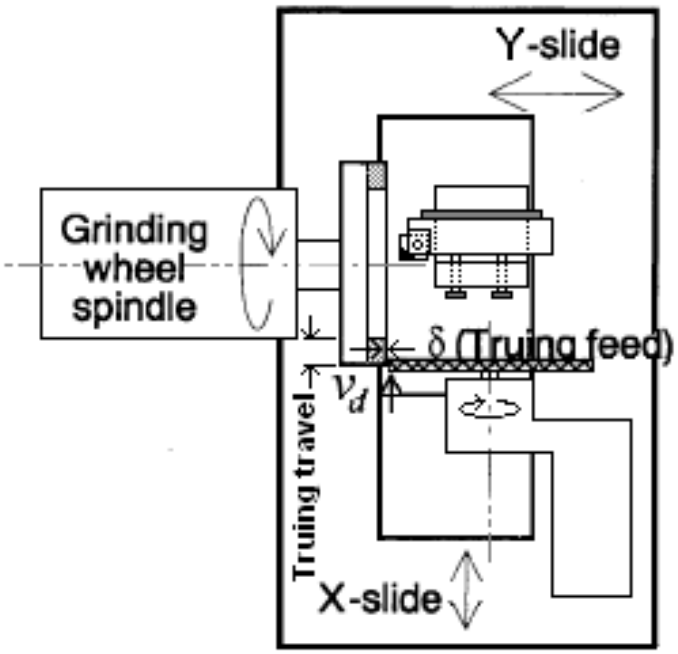

Figure 2.2.10 Truing configuration

2.2.3. Dressing

In order to achieve an effective cutting process the grinding wheel needs to be dressed regularly. Different dressing methods can be used to open the grinding wheel surface. In the experiments conducted in this research an aluminium oxide dressing stick was used (Figure 2.2.11). It is very important to dress the grinding wheel with a wet stick and the stick was kept wet in the coolant tank. It was pressed against the wheel as the wheel was rotating. The pressure has to be sufficient to melt the stick and open the grinding surface.

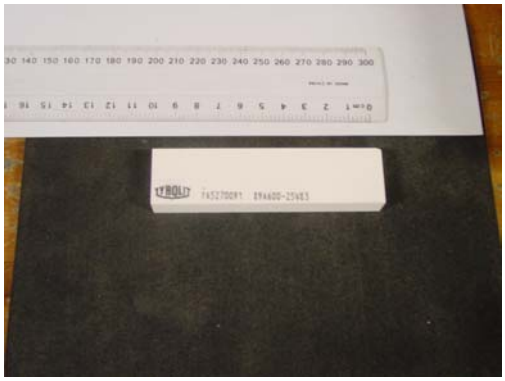

Figure 2.2.11 Aluminium oxide dressing stick

The dressing configuration is illustrated in Figure 2.2.12. The dressing in-feed should be given in a way that the entire grinding surface is covered. After dressing the grinding wheel is sharp and no longer glazed, which can be verified by touching the surface and by visual inspection.

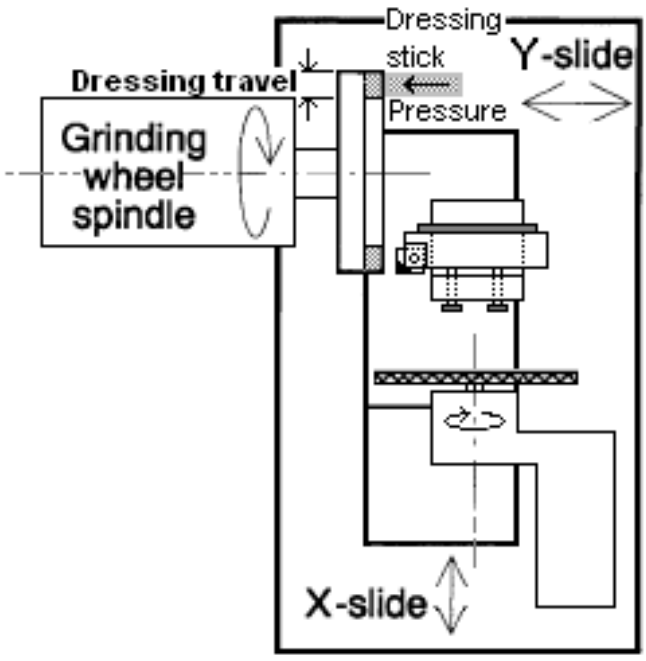

Figure 2.2.12 Dressing configuration

2.2.4. Micrometer

To measure the amount of material removed from the grinding wheel and the work piece, three micrometres were used (Figure 2.2.13 and Figure 2.2.14).

Figure 2.2.13 Manual micrometres

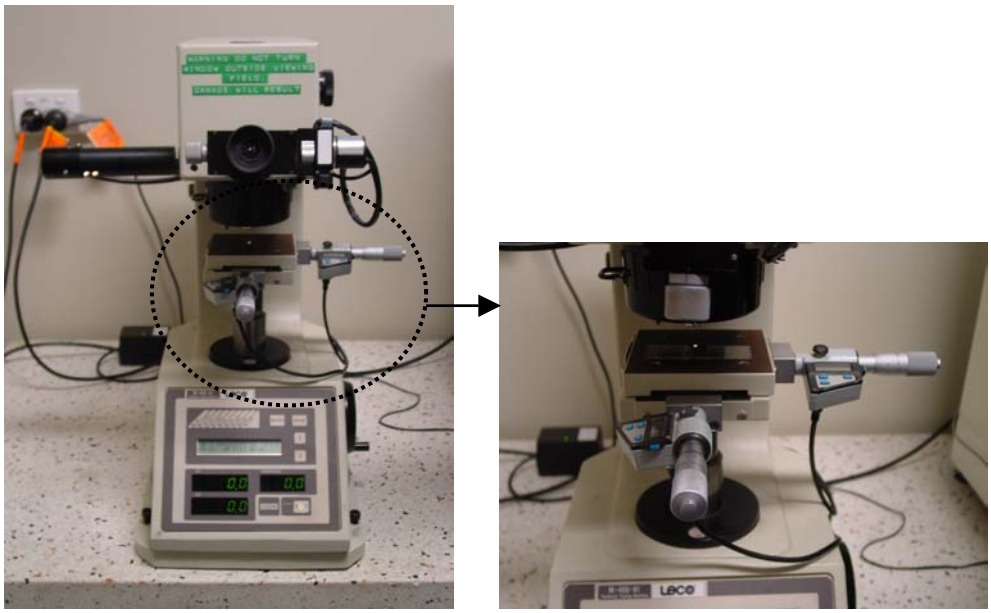

Figure 2.2.14 Optical microscope and the electronic micrometre

The depth of the material removed from the work piece was measured using a manual micrometre with ± 1 or ± 2 microns accuracy (shown in Figure 2.2.15). To measure the actual depth of removed material from the wok piece, a more precise measurement was undertaken. For error measurement an electronic micrometer connected to an optical microscope was used.

Figure 2.2.15 Material removal measurements

Table 2.1 shows the percentage error in the related measurements. To arrange this table, 5 samples were measured. Obviously the error is not significant and means that the manual measurements were reliable.

Table 2.1 Measurement error using the micrometre

Manual Micrometer (mm)	**Electronic Micrometer (mm)**	**Error %**
12.6095	12.6035	0.048
12.6445	12.6475	0.024
12.651	12.6505	0.0040
12.6565	12.6625	0.047
12.2035	12.1945	0.074

The depth of removed material from the grinding wheel was also measured using another micrometer within 5 microns accuracy (shown in Figure 2.2.15). The reason for using the micrometer with larger jaw (as shown in Figure 2.2.13) was that the micrometre with smaller jaw did not fit the grinding wheel width. The wheel width was measured twice at 4 different points of the wheel and the average was taken.

2.3. Data Collection and Control Procedure

The grinding machine DSP system was fitted with a 32-channel digital input/output board PC/32DIO using an additional digital I/O board. Texas Instrument (TI)

manufactures the DSP chip. All the DSP programs are written in C and are compiled using the TI C compiler. The compiler is discussed in detail in [35, 60].

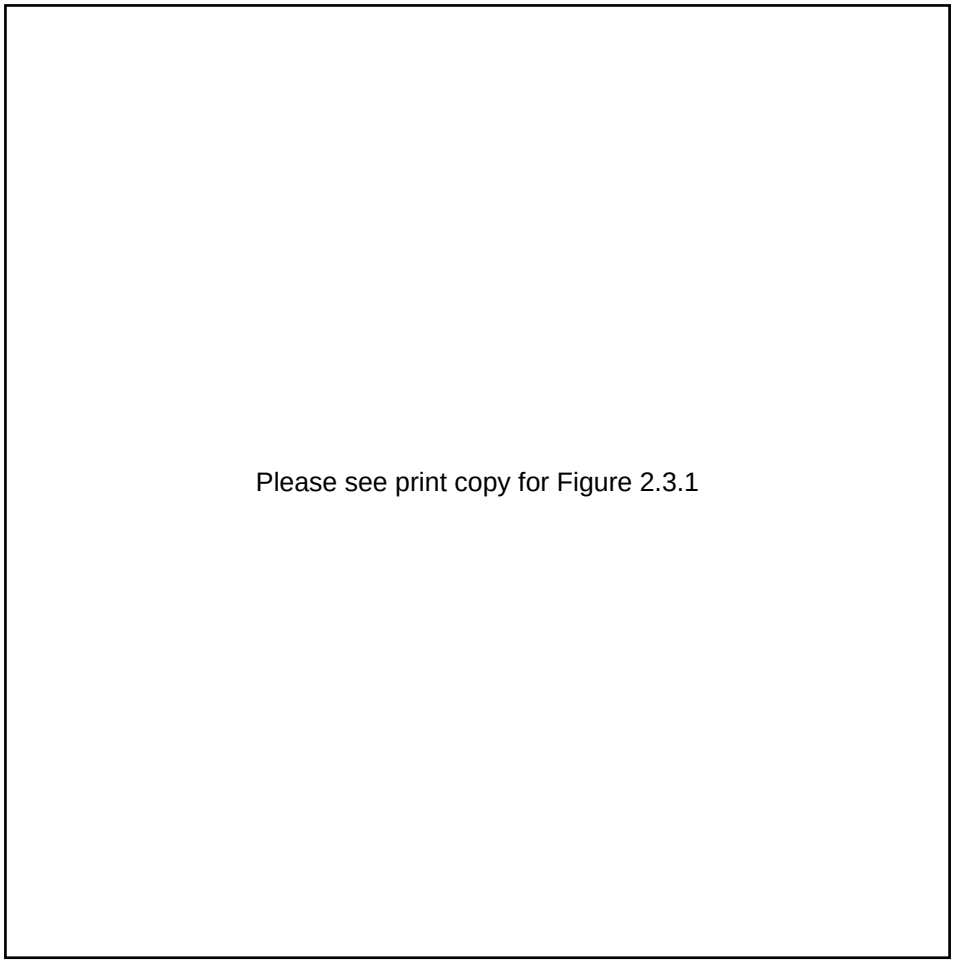

Figure 2.3.1 DSP soft ware flow chart [35]

The TI C compiler takes the C code as an ASCII file, compiles it and produces an executable file with a .out extension. The executable files can be run from the MPCView program (a C source debugger) or from the dataxfer.exe program [35]. Once the C codes are compiled the programs can be run from the Windows98 DOS prompt. The program resets the DSP, downloads and runs DSP code and transfers data to and from the Dual Port RAM. The executable program dataxfer.exe downloads DSP Code, reads the input data file input.txt and transfers to DSP and saves the output data received from DSP in another text file data.txt. This output data file is then analysed using Matlab® (**mat**rix **lab**oratory). Matlab® is a data-manipulation software package that allows data to be analysed and visualized using existing functions and

user-designed programs. A DOS program can be easily run from the Matlab® environment. Using a Matlab m-file the dataxfer.exe is run and "once the DSP program has finished controlling a process (eg a machining operation) the recorded data is then processed and displayed in Matlab" [35]. The software process flow chart is shown in Figure 2.3.1.

A detailed description of position data and calibration procedure is given in [35].

2.4. Mathematical Description of the Grinding Forces

As previously discussed, there are three forces applied to the work piece during grinding; normal force F_N, tangential force F_T and the third force produced due to the oscillating motion named here as F_d. The forces read by force sensors are in three directions other than the directions of F_N, F_T and F_d. The forces read by force sensors are called F_X, F_Y and F_Z. Figure 2.4.1 shows the forces acting on the PCD work piece during grinding. The revolving grinding wheel produces a force tangential to the wheel circumference. Depending on the position of grinding wheel in contact with the work piece the direction of F_T changes.

Normally, F_N and F_T are of interest in the grinding process. In fact, the third force F_d is too small (a few Newtons) to be analysed appropriately. As a result, in this research the discussions are mainly around F_T and specially F_N. According to Figure 2.4.1 F_N is in the Y direction. In other words, the Y-axis of the force sensor is aligned with F_N. Thus, F_Y does not need to be changed. But, since F_T has 2 components on X and Z-axes, F_Z needs to be written in terms of F_T. To analyse the results of grinding experiments F_Y and F_Z are written as below,

$$\begin{cases} F_Z = F_T \sin\alpha \\ F_Y = F_N \end{cases} \tag{2.1}$$

So,

$$\begin{cases} F_T = \dfrac{F_Z}{\sin\alpha} \\ F_N = F_Y \end{cases} \tag{2.2}$$

As shown in Figure 2.4.1, α is an indicator of work piece location with respect to the grinding wheel circumference. A Matlab code was written to compute the tangential and normal forces based on the force sensor data.

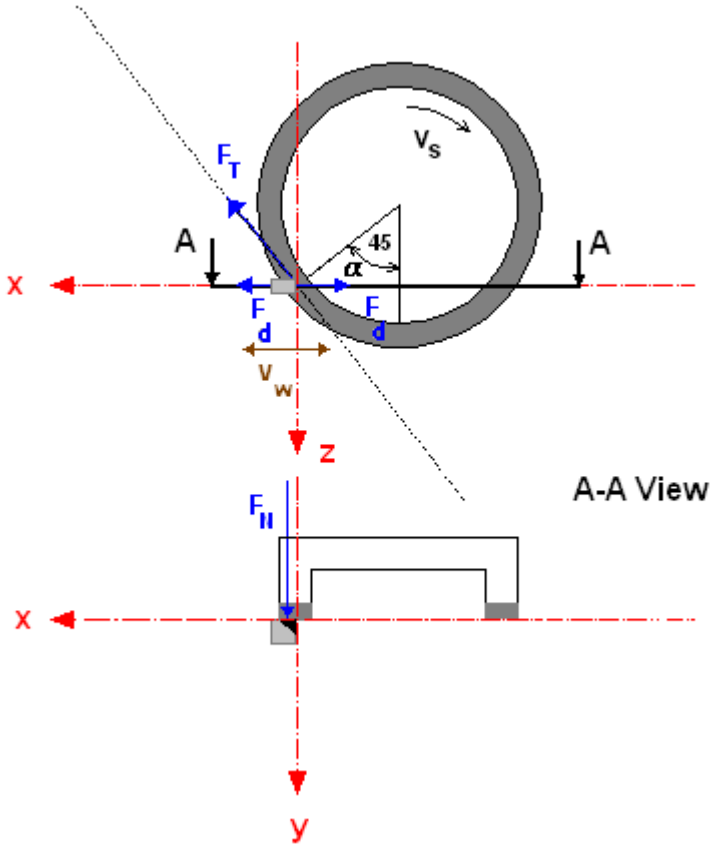

Figure 2.4.1 Kinematics and forces in grinding of Polycrystalline Diamond

2.5. Conclusions

The details of experimental equipment used in this thesis were described in this chapter. The routines were similar to the industrial applications normally used. The main parts of the electrical and mechanical circuits were explained. Different equipment including the PCD sample, grinding wheel and analysing tools were

introduced in this chapter. Truing and dressing conditions were also studied. Then it was shown how the data is collected and analysed.

To transfer the force sensor results to the desired and practical forces, the grinding forces were analysed and mathematically described. It was explained that the 3 grinding forces F_N, F_T and F_d acting on the work piece could be written in the form of F_X, F_Y and F_Z of the force sensors.

CHAPTER 3 GRINDING AND FORCE ANALYSIS

3.1. Introduction

As discussed in Chapter 1 the forces produced during grinding contain useful information about the grinding process. This information gives a better understanding of the whole process. The importance of these forces was well described in the literature review of Chapter 1 and the details of experimental setup used in this research were explained in Chapter 2 . In the following experiments described in this chapter, a diamond grinding wheel was used to grind PCD and cemented carbide. The aim of grinding cemented carbide in addition to PCD was to compare the results of PCD grinding with typical grinding of cemented carbides. The grinding forces generated during grinding will be analysed based on the data obtained using the force sensor and the mathematical description of the grinding forces as explained in Section 2.4. The relation between the grinding forces and in-feed, material type, material removal rate and oscillation rate will also be studied in this chapter.

The experiments undertaken in this chapter are explained in Section 3.2. A description of the relation between in-feed and grinding forces is given in Section 3.3. In Section 3.4 different contact zones have been ground and the results are compared. Useful information about the grinding process is available by studying the volumetric material removed from the work piece. In Section 3.5 the material removal rate has been measured for different in-feeds and different contact zones. To show the effect of oscillation rate in the grinding process a number of experiments have been undertaken in Section 0. Finally, Section 0 summarizes the results of the experiments presented in this chapter.

3.2. Description of Experiments

The experimental setup used in this research was described in Chapter 2 . The details of each procedure and where they were used were also explained. To improve reliability, each experiment in this chapter was repeated many times with specific settings. The work piece was ground using a constant oscillation rate and in-feed at

each run, except in one experiment where the in-feed was varied during the experiment. The settings used in the following experiments are listed in Table 3.1.

Table 3.1 Experimental settings

In-feed [μm]	Oscillation Rate [mm/s]
10	6
20	6
30	6
40	6
50	6
100	6
20	3
40	3
20	10
40	10

The range of in-feeds was selected based on the physical characteristics of the grinding machine. The oscillation rate or the X-axis velocity can be varied up to 100mm/s. However, to avoid burning the work piece surface and the grinding wheel, due to the PCD hardness, it is conservative to work under 10mm/s. The first 5 rows of Table 3.1 have also been repeated for the cemented carbide side of the work piece.

In Section 3.3, to study the relation between the grinding forces and in-feed the following experiments were undertaken.

1. The grinding wheel was trued once at the commencement of the experiment in accordance with commonly used industrial practice. The grinding wheel was

trued for less than 2 minutes while the truing wheel was oscillating at 5mm/s. Due to the lack of accuracy in the available grinding machine it is impossible to use small truing in-feeds (about 2 microns) as recommended. Therefore, the truing in-feed used was 5 microns. The in-feed was given 2-3 times during truing wheel oscillation to make sure the desired grinding wheel topography is achieved. The details of truing procedure were discussed in Section 2.2.2.

2. The grinding wheel was dressed using a wet dressing stick before each experiment for about 25 seconds.

3. Then, just one in-feed as specified in Table 3.1, was given at each run.

4. The traverse speed was kept constant in each experiment.

5. Steps 2-4 were repeated but with the in-feed increased in steps of 10 μm up to a maximum of 50 μm .

6. The results of these experiments are plotted together as shown in Figure 3.3.1 to Figure 3.3.2 and Figure 3.3.3 to Figure 3.3.5.

In those experiments where the work piece was moving along the X-axis, to use the whole surface of the grinding wheel, the work piece has travelled about 20% of the total contact area off the grinding wheel at each side. Note that the work piece was always in contact with the grinding wheel.

To find out the best way of giving in-feed which affects the forces produced during grinding, experiments related to Figure 3.3.6 and Figure 3.3.7 are conducted. In these experiments the routine is the same as before except that the in-feeds were changed during grinding.

Figure 3.4.1 is the result of grinding the work piece without moving it in the X direction i.e. grinding on one spot. In these experiments different parts of the work piece including cemented carbide part, PCD part and the section consisting of both PCD and cemented carbide have been tested.

The experiment as done in Figure 3.3.1 was repeated on the cemented carbide section of the work piece to obtain the graphs in Figure 3.4.2 and Figure 3.4.3.

The graphs shown in Figure 3.5.1 and Figure 3.5.2 are the results of the same experiments considered in Figure 3.3.1 and Figure 3.4.2 including the material removal measurement after each experiment. In the experiments of section 3.5 a micrometer was used to measure the depth of material removed in order to find out the volumetric material removed from the work piece.

To obtain the graphs in Figure 3.6.1 the velocity was varied but kept constant at each run. A certain in-feed of 20 μm was selected for each set of 3 experiments while remaining constant for each test. The same set of experiments was repeated for another in-feed of 40 μm . In other words, each point in these 2 figures corresponds to the maximum grinding force in each experiment.

3.3. Grinding Forces and In-feed

As shown in Section 2.4 the force sensor data provides information to model the grinding process and measure the normal and tangential forces. However, since both forces show the same trend mostly, only the normal force will be discussed here, except for the grinding coefficient calculations related to Figure 3.3.4, Figure 3.3.5, Figure 3.4.4 and Figure 3.4.6 and in case of comparing the behaviours of maximum forces against in-feed related to Figure 3.3.3 and Figure 3.4.3.

Figure 3.3.1 shows the normal force produced during grinding of polycrystalline diamond. Each section presents a separate experiment completed in 15-20s. According to this figure as the work piece moves along the X-axis the normal force changes. For a better understanding, a magnified part of the first section of Figure 3.3.1 is illustrated in Figure 3.3.2. The point of Figure 3.3.2 is that the normal force fluctuations are shown with respect to the position of work piece in contact with the grinding wheel. Initially, the normal force is zero because there is no contact between the work piece and the grinding wheel. But, as the in-feed commences the normal force rises. Then, as a part of material is removed the force drops (the first 4 circles in Figure 3.3.2). However, because the in-feed has not yet completed, it goes up again up to the

maximum point P_1 almost equal to 8.5N corresponding to the maximum in-feed and maximum contact area. Then, as the work piece moves further, the right side of the PCD blank (cemented carbide part) loses contact with the wheel and the normal force decreases to V_1. Then, as the contact area increases the normal force increases up to P_2 and later falls as the left side of the PCD blank (PCD part) loses contact with the wheel.

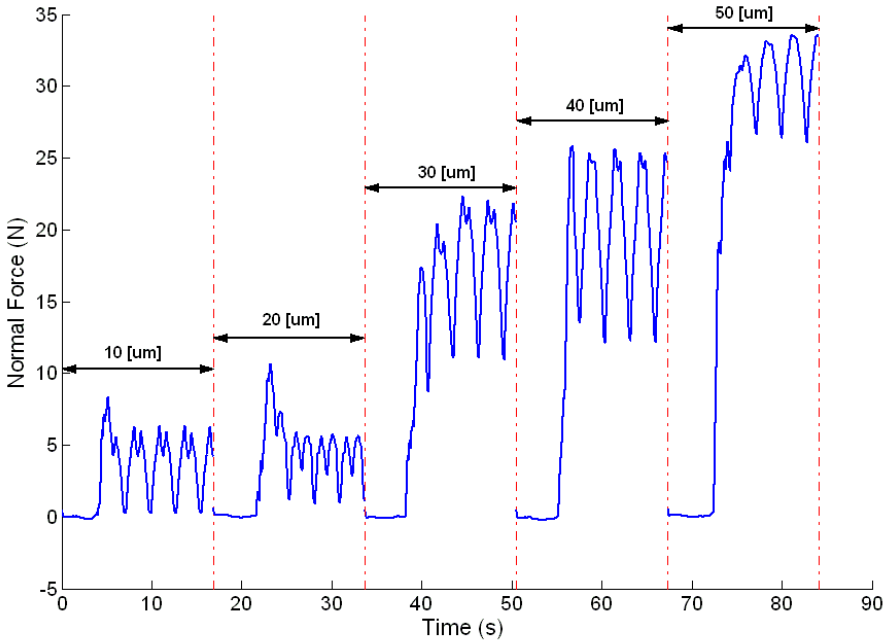

Figure 3.3.1 Normal force vs. time for different in-feeds

In Figure 3.3.3, P_3 and P_4 show the normal forces at the same position of the work piece with respect to the grinding wheel but with different directions of work piece movement and that is why they are slightly different. The normal force of valley point V_1 is higher than that of V_2 for 3 reasons. First and the least significant reason is because of the same reason explained for P_3 and P_4 i.e. different directions of work piece movement. The second one is as a result of having less contact at one end compared to the other end. In other words, the grinding surface of the work piece cannot be perfectly positioned parallel to the grinding wheel surface. The third reason is due to the different types of material in contact with the wheel. In other words, at V_1 PCD section is mostly in contact with the wheel while at V_2 the cemented carbide

section is. So, due to the PCD hardness V_1 has a bigger value than the minimum value at V_2.

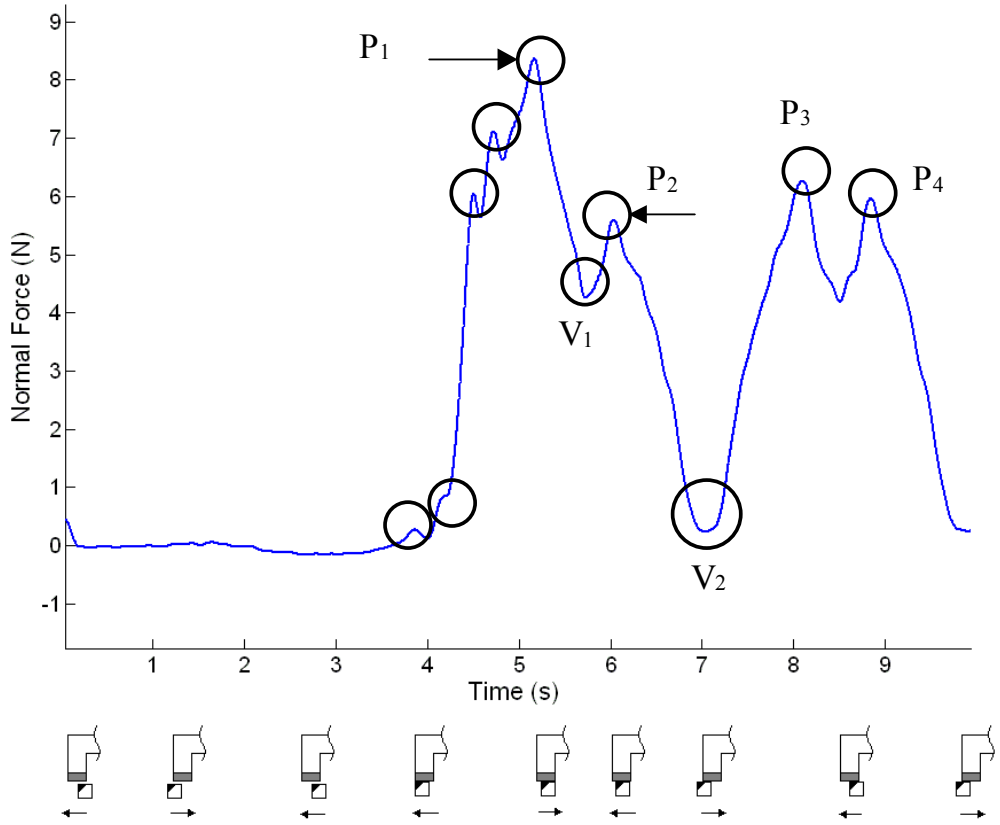

Figure 3.3.2 Magnified normal force vs. time with respect to the contact position

Returning to Figure 3.3.1 one can see that the last peaks of each section have not changed noticeably. This shows that in PCD grinding when the grinding wheel becomes blunt to a certain degree, the grinding wheel and work piece keep sliding against each other with constant normal force F_N. If constant contact force was used the same result would be obtained as discussed in [4-6]. The difference in these experiments is that here one single in-feed is given at each run. In other words the work piece is not being fed continuously until the end of the experiment.

The results of Figure 3.3.1 are unlike grinding of cemented carbide where for the same range of in-feeds, as soon as the in-feed commences most or all the material is removed and the forces drop significantly.

In the third 30 µm in-feed and fifth 50 µm in-feed sections of Figure 3.3.1, the first peaks are lower than the rest since the magnitude of the first peaks depends on where the in-feed commenced i.e. whether in the middle of travel where there is full contact or at the ends where the contact area was not as much as in the middle. This shows the relation between the force and the contact area. In fact, the greater the contact area the higher the normal force will be.

Because of the high cost of grinding wheels, it is important to consider that giving in-feeds higher than 20 µm , especially 50 µm , makes the wheel become blunt sooner. That is why in the last section of Figure 3.3.1 every peak is higher than the previous peak.

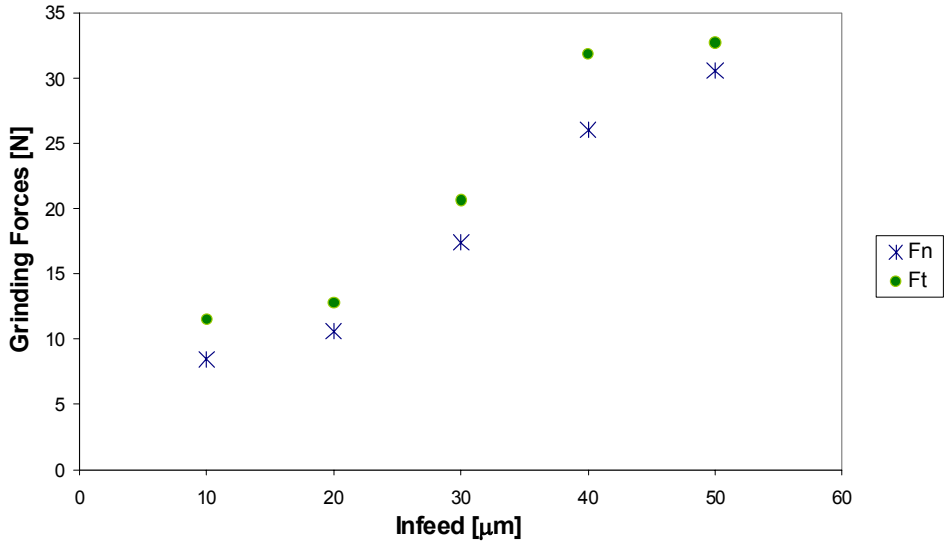

Figure 3.3.3 Maximum tangential force and the corresponding normal force against in-feed

Figure 3.3.3 is drawn based on Figure 3.3.1 and the corresponding figure related to tangential force. Figure 3.3.3 shows the maximum applied force for a certain amount of in-feed. According to Figure 3.3.3,

1. The behaviours of F_T and F_N are roughly similar.

2. The range of F_T is higher than F_N.

3. As expected, when the in-feed increases the grinding forces increase.

4. The relation between force and in-feed is not proportional.

5. With contact area between 11.5-12.5mm^2, the grinding forces vary in the range of 5-35N for in-feeds between 10 and 20 microns.

In Figure 3.3.4, the grinding forces in Figure 3.3.3 are plotted against each other. According to Figure 3.3.4, for a range of 10-50 μm in-feed and using a sharp wheel, the relation between F_T and F_N is approximately proportional. This experimental procedure can be extended to other cases to find the relation between F_T and F_N.

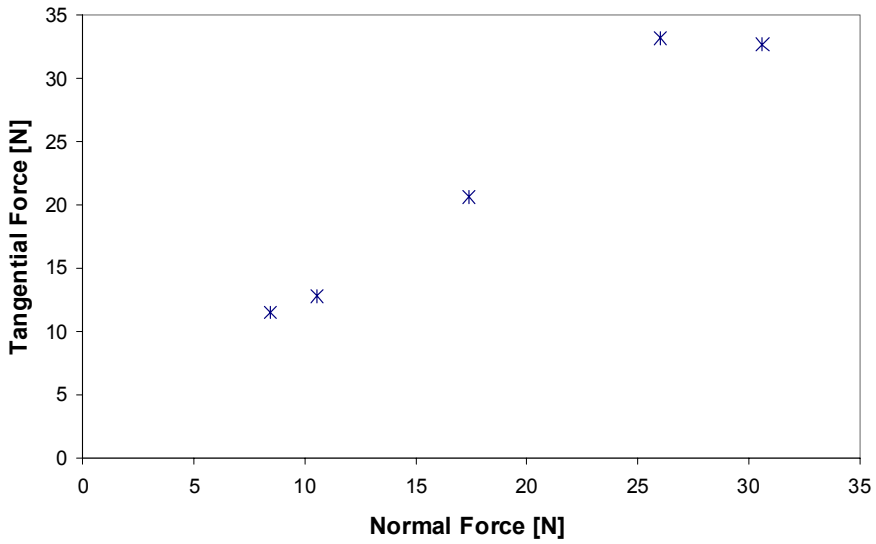

Figure 3.3.4 Maximum tangential force against maximum normal force

As discussed in Section 1.3 the grinding coefficient is a specific value, which depends on the state of sharpness of the grinding wheel. Figure 3.3.5 illustrates the relation between the grinding coefficient (μ) and in-feed. It can be seen that as the in-feed increases this coefficient decreases gradually and based on Figure 3.3.3 F_T and F_N increase. Combining these 2 facts, as the in-feed increases F_T does not increase as much as F_N does. Considering Figure 3.3.5 and Kramer's research [44] high grinding coefficient (μ) values mean high tangential forces and low normal forces, which are "the effects of a sharp wheel topography".

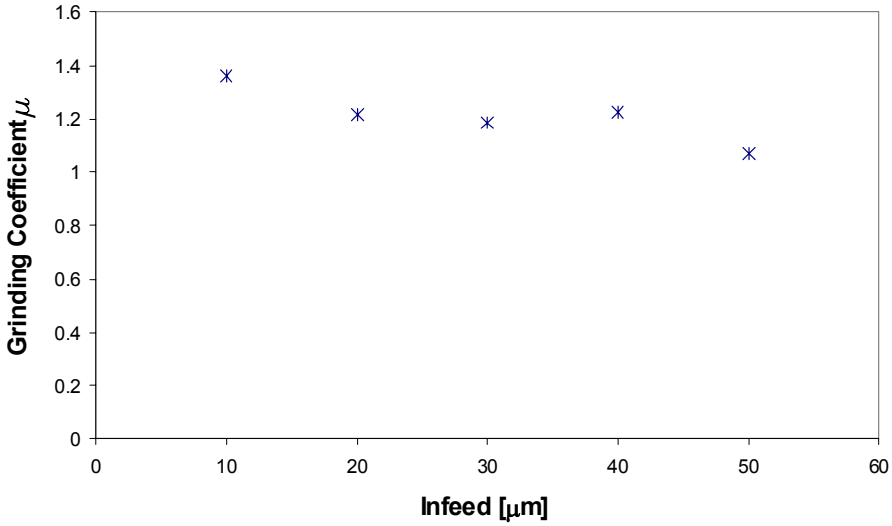

Figure 3.3.5 Ratio of the maximum tangential to the corresponding normal force against in-feed

The behaviour of the grinding coefficient will be discussed in detail in Section 4.3.

As described in Section 3.2 to optimize in-feeding new experiments were conducted. In this series of experiments the in-feed was given in steps during grinding. Figure 3.3.6 shows the results of these experiments.

Undoubtedly, the grinding forces depend to a large extent on the position where the in-feed was commenced. The contact position indicates the contact area and the material type. The contact position will be discussed in detail in Section 3.4. According to Figure 3.3.6, in each section, depending on the contact position, every new in-feed (with higher or even lower value than the previous in-feed) generates a force bigger than that of the previous in-feed. This shows that in PCD grinding the desired material cannot be removed all at once.

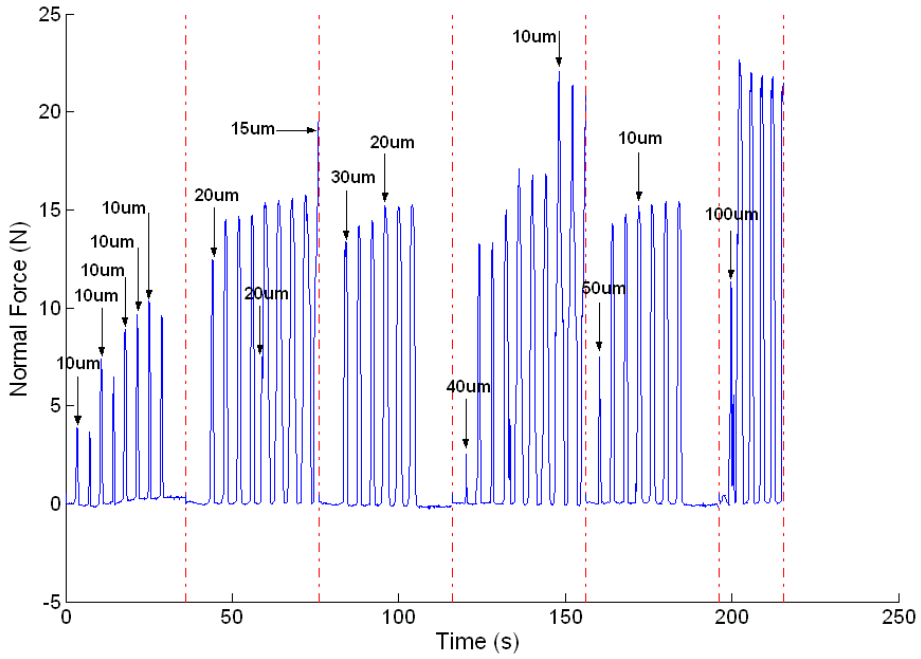

Figure 3.3.6 Normal force vs. time for number of in-feeds given in each experiment

Figure 3.3.7 shows the peaks of normal force drawn from Figure 3.3.6. In the lowest curve of Figure 3.3.7, the F_N of the nth in-feed i.e. P_1 is not the same as the F_N of the sum of those in-feeds at once or in other forms of summations. For example in Figure 3.3.7 P_1 has the lowest F_N compared to the other curves. In other words,

$$(F_N)_{5\times10\mu m} \neq (F_N)_{2\times20+10\mu m} \neq (F_N)_{30+20\mu m} \neq (F_N)_{40+10\mu m} \neq (F_N)_{50\mu m} \quad (3.1)$$

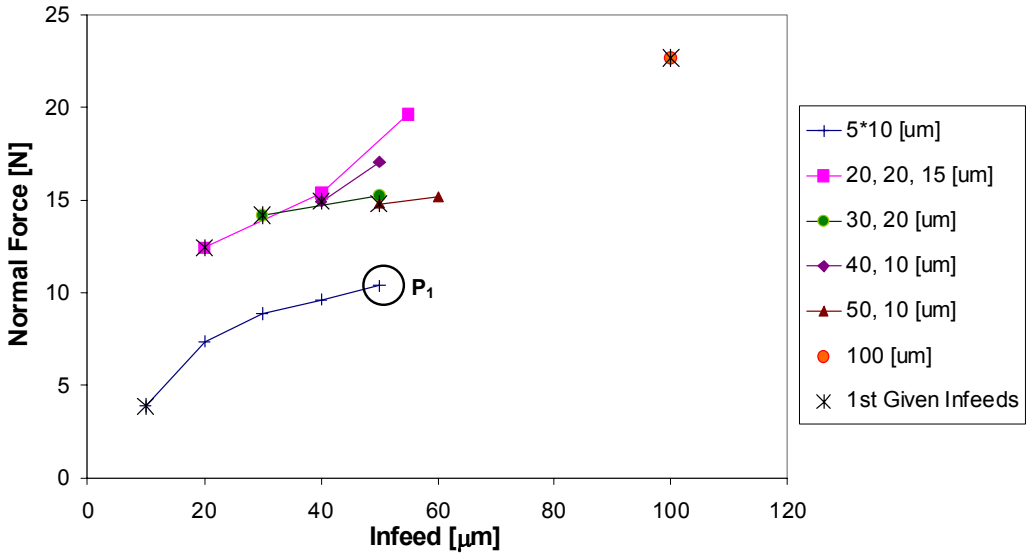

Figure 3.3.7 Peaks of normal force vs. in-feed selected from Figure 3.3.6

Suggestions about optimising in-feed strategies are discussed in Chapter 5 .

3.4. Grinding Forces and the Work Piece Position

Experiments used in this section have been explained in Section 3.2. Figure 3.4.1 shows how the normal force changes over time. The same in-feed was used in the experiments of Figure 3.4.1. This is in order to investigate the effect of different contact positions on the grinding forces. According to Figure 3.4.1;

1. The greater the contact area the higher the grinding forces,

2. With the same contact area, when the PCD part of the work piece is in contact with the grinding wheel the forces produced during grinding are higher than the forces in grinding cemented carbide. This shows how hard PCD is.

3. When the cemented carbide is being ground, as soon as the in-feed commences the normal force drops dramatically. It is evident how quickly the grinding wheel becomes blunt in PCD grinding. Since in grinding cemented carbide the force drops in less than a second and besides the difference between the maximum and minimum force values is greater for cemented carbide.

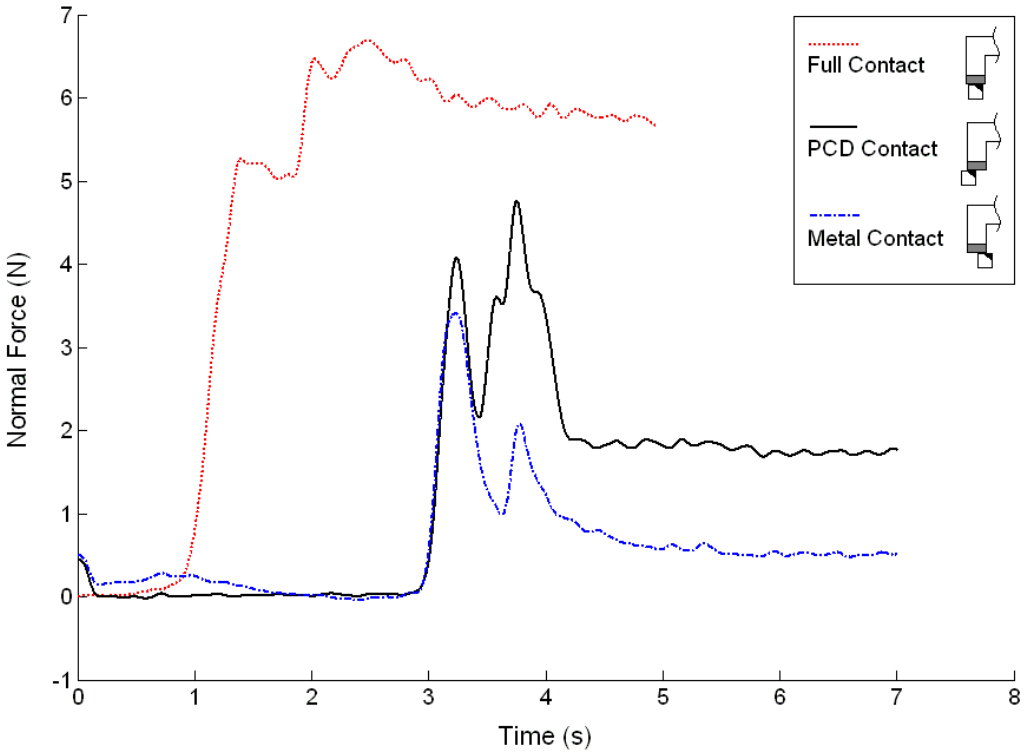

Figure 3.4.1 Normal force vs. time, without moving the work piece, for different contact positions and 15 µm in-feed

The analysis of grinding cemented carbide gives a better understanding about the PCD grinding process. Figure 3.4.2 shows the changes of F_N over time in grinding cemented carbide. In this figure the results of 5 experiments with same settings but different in-feeds are plotted. Clearly there is one peak in each section is completely noticeable. This shows how fast the material is removed from the cemented carbide in contrast to PCD grinding.

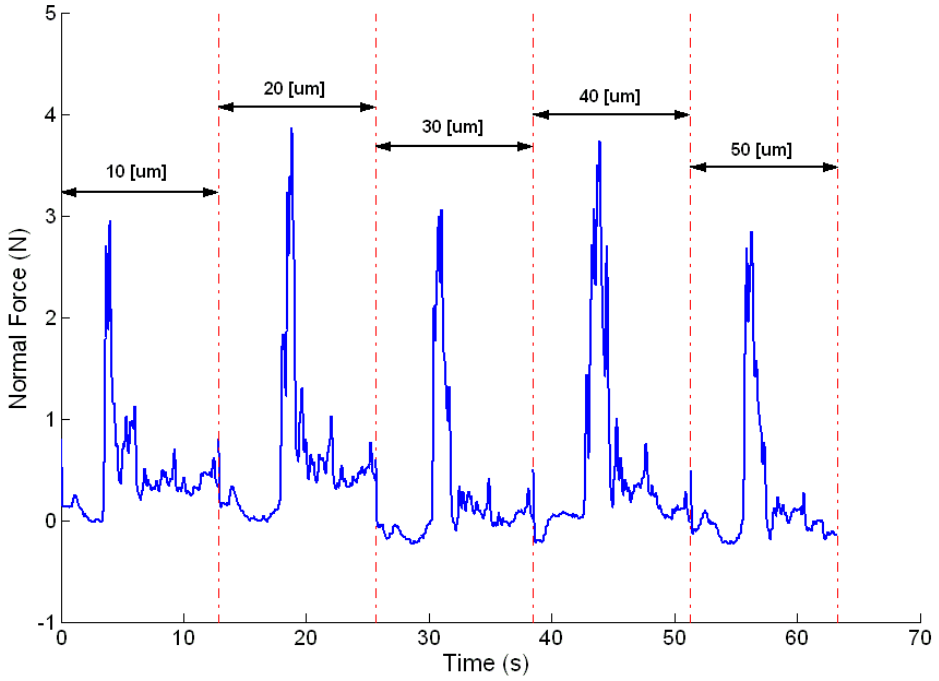

Figure 3.4.2 Normal force vs. time for different in-feeds in grinding cemented carbide

Figure 3.4.3 illustrates the maximum F_N and F_T (obtained from Figure 3.4.2) versus in-feed.

Although there is no doubt that the higher in-feed means higher grinding forces due to the high grindability of cemented carbide no significant relationship between the forces and in-feed emerges from this analysis. Moreover, according to Figure 3.4.3 it also can be seen that the tangential force is greater than the normal force in spite of the published data [61]. This happened for 2 reasons. Firstly, in grinding cemented carbide as soon as the in-feed commences most of the material is removed, and secondly the limitations of the available grinding machine make it difficult to give the desired in-feed in one step. In fact, it is possible that the range of in-feed used was not wide enough to show a difference, and that the variation of the grinding forces was so small that the force sensor would not pick it up. So, in this case, it was difficult to observe the increasing trend of the normal force as in-feed was increased. However, the cutting force F_T still has the expected trend.

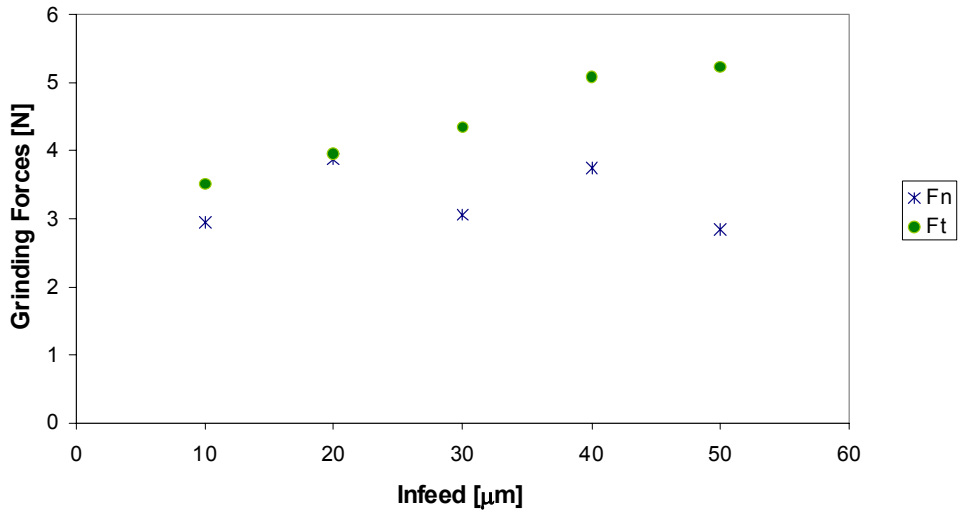

Figure 3.4.3 Maximum grinding forces against in-feed
in grinding cemented carbide

Figure 3.4.4 shows the tangential force against the normal force comparing cemented carbide and PCD. According to this graph the grinding forces are considerably lower and closer to each other for grinding cemented carbide whereas in PCD grinding these forces occupy a higher and wider range. For instance F_T varies about 5N for cemented carbide but for PCD grinding F_T lies in the range of 12-34N, i.e. 2-7 times more. A similar explanation explains variations in F_N.

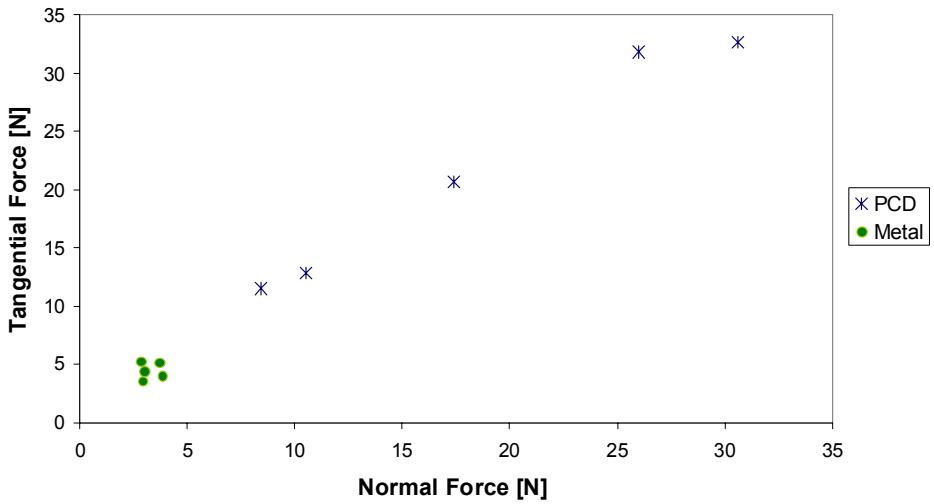

Figure 3.4.4 Maximum tangential force against the maximum normal force for different contact zones

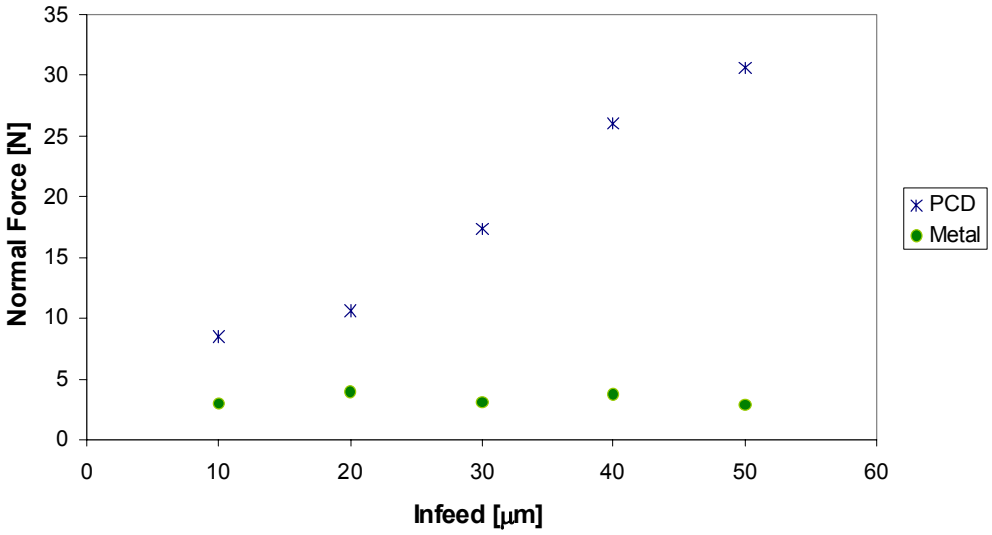

Figure 3.4.5 Maximum normal force against in-feed for different contact zones

In Figure 3.4.5 the normal force produced during cemented carbide and PCD grinding are compared in an additional way. This figure is a combination of Figure 3.3.1 and Figure 3.4.2. It shows a separate comparison of F_N and in-feed variations for PCD and cemented carbide in one plot. Considering Figure 3.4.5, it can be seen that once again, in grinding PCD as the in-feed increases a higher force is produced whereas no trend

like that is found in grinding cemented carbide. In fact, in grinding cemented carbide, the range of 10-50 μm in-feed is a low range to produce forces as high as forces in PCD grinding and that is why F_N of cemented carbide has not changed much in this figure. More details can be found through the explanations of Figure 3.3.1 and Figure 3.4.2.

Figure 3.4.6 shows the relation between the grinding coefficient μ and in-feed for cemented carbide and PCD. From Figure 3.4.6 it can be concluded that in grinding of cemented carbide for a range of 10-50 μm , as in-feed increases μ increases gradually. So, despite PCD grinding, as in-feed increases the rate of increase in F_T is higher than the rate of increase in F_N. It is also clear that μ fluctuates in the range of 1-1.8 showing that F_T is greater than F_N.

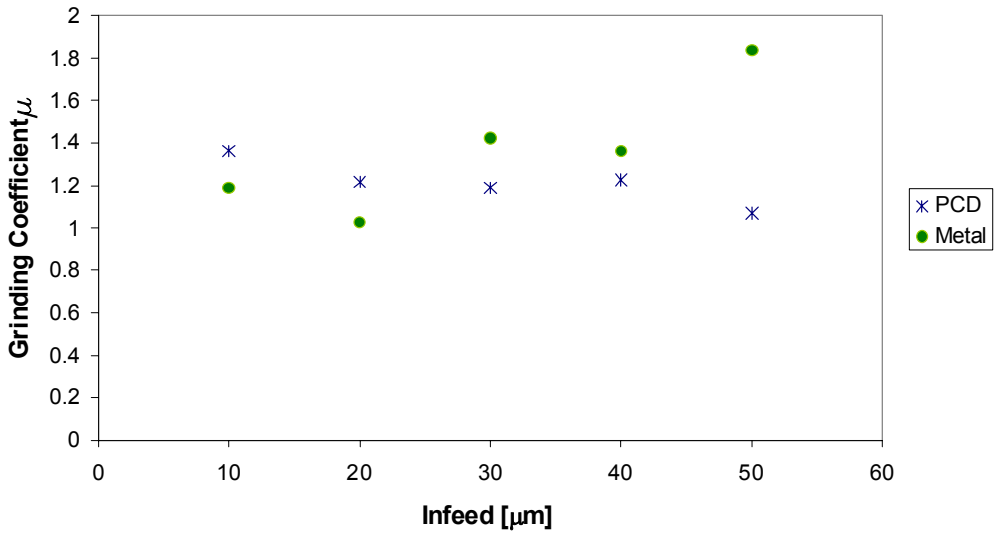

Figure 3.4.6 Ratio of the maximum tangential force to the maximum normal force against in-feed for different contact zones

3.5. Material Removal Rate

In the previous sections the effect of in-feed and contact zone on changing the grinding forces were discussed. The volumetric material removed from the work piece during grinding time is also an important characteristic to quantify. As explained in Section 1.3.1 material removal rate (MRR) indicates how much material is removed

from the work piece in a certain time. Note that the maximum area in contact with the wheel was about 10mm^2.

Figure 3.5.1 illustrates the relation between the material removal rate and in-feed for cemented carbide and PCD. According to Figure 3.5.1 and considering different vertical scales used for MRR it is concluded that:

1. MRR in cemented carbide grinding is higher than MRR in PCD grinding. For a range of 10-50 µm in-feed, MRR of cemented carbide was between 0.017-0.097mm^3/s. While, for PCD this was reduced to 0.0027-0.0055mm^3/s.

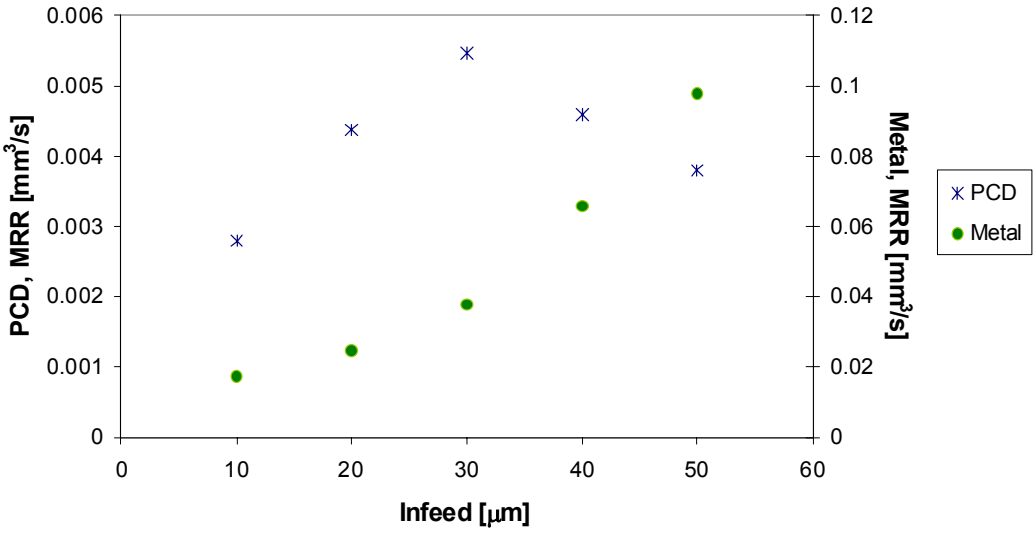

Figure 3.5.1 Relationship between material removal rate and in-feed for different contact zones

2. As the in-feed increases, MRR of cemented carbide increases almost proportionally. In this case, at 50 µm in-feed MRR is 5 times greater than MRR at 10 µm . The point is that in-feeds in this range do not make the wheel dull. Whereas, for PCD, up to 30 µm in-feed, as the in-feed increases MRR increases to its maximum value 0.0055mm^3/s. But, for in-feeds over 30 µm , MRR keeps decreasing.

This can be because of 2 possible causes. The first one is the low stiffness of the system so that the work piece is not held sufficiently rigid to resist backlash. However, graphs of Figure 3.3.3 and Figure 3.5.2 disprove this theory. As discussed previously, according to the former figure, higher force means higher in-feed. So, in the later one, the maximum F_N (at P_5) corresponds to highest in-feed i.e. $50\,\mu m$. Although MRR at P_5 is low the higher force at P_5 shows that the machine is not flexing.

The second possible cause is because of the grinding time. In-feeds more than $30\,\mu m$ make the grinding wheel blunt. So, to remove the same amount of material from PCD more time is required. Consequently, with these settings it is advised to use in-feeds not more than $30\text{-}40\,\mu m$.

3. In the cemented carbide grinding experiment, grinding was started with a small contact area. But, within 5 experiments the final MRR has reached up to 26 times higher than the corresponding MRR of PCD. In fact, in grinding cemented carbide the desired in-feed is equal to the actual depth of removed material or in other words, as soon as the in-feed is given all the material is removed. While in PCD grinding the grinding wheel can become blunt before all the desired material is removed.

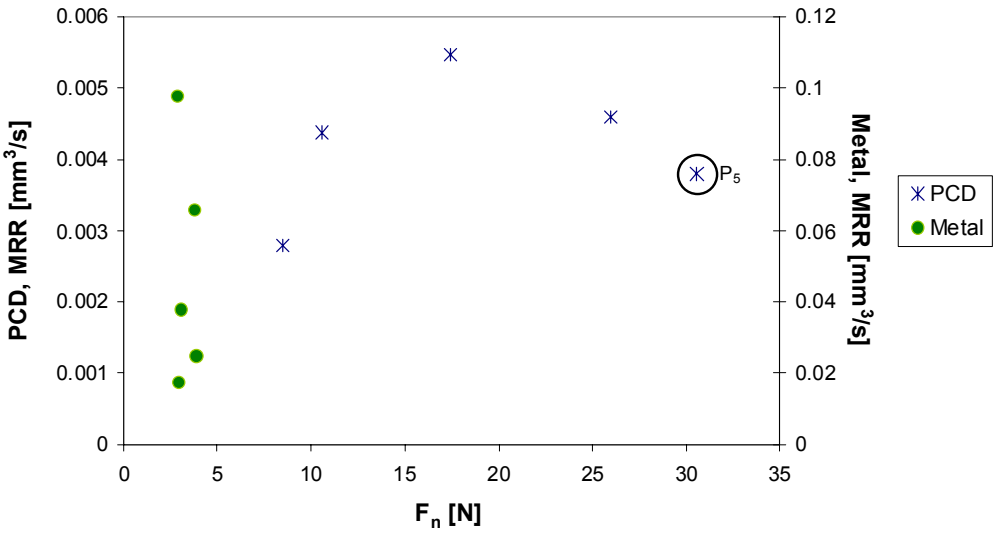

Figure 3.5.2 Relationship between material removal rate and normal force for different contact zones

Figure 3.5.2 shows the material removal rate (MRR) against the normal force, for cemented carbide and PCD. The additional conclusion drawn from Figure 3.5.2 is that in grinding of cemented carbide a small force removes a range of 0.017-0.097mm^3/s material from the work piece. While, in PCD grinding to remove 1/6-1/17 of the mentioned value i.e. a range of 0.0027-0.0055mm^3/s material, forces about 2-6 times greater than in cemented carbide grinding are required.

3.6. Grinding Forces and the Oscillation Rate

To use all the abrasive layer of the grinding wheel and avoid wearing out the grinding wheel unevenly, the grinding wheel or the work piece oscillate. In most applications the grinding wheel oscillates. But, in the conventional grinding machine used in this research, the work piece moves parallel to the grinding wheel face.

In this section the relationship between the velocity of the work piece (oscillation rate) and the grinding forces is explored. As mentioned in Section 3.2, the velocities selected in these experiments are less than or equal to 10mm/s.

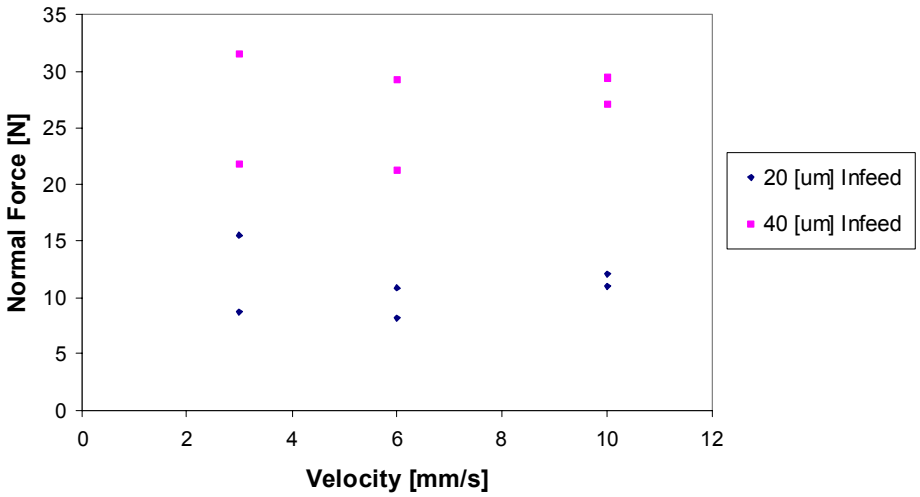

Figure 3.6.1 Relationship between the normal force and oscillation rate for 2 different in-feeds

Figure 3.6.1 shows the relation between the normal force and work piece velocity for 2 specific in-feeds 20 and 40 μm . According to Tso and Liu [24] with lower oscillation rate a finer PCD surface can be obtained. However, no trend or consistent relation emerges from the graph in Figure 3.6.1. It is possible that the range of velocities used was not wide enough to show a difference, and that the variation of the normal force was so small that the force sensor would not pick it up.

3.7. Conclusions

In this chapter, the relation between the grinding parameters and the forces produced during grinding was studied. Different experiments with different settings were conducted to find how the grinding forces are affected by the in-feed, contact zone, material removal rate and oscillation rate.

The experimental results of this chapter provide valuable information about the range of forces produced during grinding. The obtained results allowed the following conclusions to be drawn for this research:

- There is a proportional relationship between the in-feed and grinding forces for the range of 10-50 μm in-feed in this research. A similar procedure can be

used for other settings and similar grinding operations to approximate the grinding forces for a range of in-feed.

- In PCD grinding when the grinding wheel becomes blunt the normal force F_N becomes constant.

- When the diamond grinding wheel is too blunt to grind PCD, it can be still sharp enough to grind cemented carbide.

- The higher forces produced during grinding PCD indicate how hard PCD is, in comparison with grinding cemented carbide.

- In-feeds over 30 μm wear out the grinding wheel quickly.

- F_N and F_T showed the same trends for the grinding conditions of this research.

- In PCD grinding, as the in-feed increases F_T does not increase as much as F_N does.

- To remove the desired amount of material and avoid the high grinding forces produced during grinding it is suggested to divide the in-feed into smaller steps instead of a single high in-feed.

- In the settings used, the grinding forces in PCD grinding were up to 2-6 times greater than the forces produced in grinding cemented carbide.

- Up to a certain in-feed, as the in-feed increases MRR increases as well. But, after that the value of MRR decreases. Although more material has been removed it has taken more time to remove that much material from the work piece.

- Because the grinding wheel wears so quickly it needs to be dressed before each experiment.

- Different oscillations less than 10mm/s produce forces in the same range. In fact, these oscillations do not affect the grinding forces significantly.

There are also useful published data about grinding forces [4-6, 8, 11, 13-16, 22, 41, 44, 57], in-feed [19, 20, 22] and material removal rate [4-6, 8, 9, 11, 13-16, 22, 41] as discussed in the literature. However, due to the different contexts such as different grinding methods, grinding operations using constant feed or constant load, and different grinding parameters some results of these published materials were not compared to a part of the results of this chapter.

The conclusions of this chapter give basic information about PCD grinding in order to help improve the process of grinding.

CHAPTER 4 TRUING, DRESSING AND GRINDING

4.1. Introduction

Different parameters affect the grinding process and, as discussed in Chapter 1 , one of the most important ones is the condition of the grinding wheel surface. In this chapter, a study of how different factors in preparing the grinding wheel can enhance the cutting efficiency of the wheel is carried out. The aim of the related experiments is to show what the forces produced during grinding look like when a sharp wheel is used in comparison with a worn wheel. In the previous chapter the grinding forces generated during grinding process were analysed for different in-feeds and contact zones. This general information about grinding will be a guide or reference to evaluate the results of grinding in this chapter. In fact, it will be shown for a certain in-feed how the grinding forces vary by using a diamond grinding wheel prepared differently in each experiment to grind a PCD work piece.

Ultimately, the aim of this chapter is to show how important the dressing process is and to determine when and for how long the grinding wheel needs to be resharpened.

In Section 4.2 the details of experiments conducted in this chapter are explained. In Section 4.3, the changes in the grinding forces using differently prepared wheels are studied. In the following section (Section 4.4), methods for determining when it is time to dress the wheel are found combined with how effectively a blunt grinding wheel grinds. Following that, the effect of dressing duration on the material removal rate and the grinding forces is investigated. Section 4.5 gives the conclusions.

4.2. Description of Experiments

The experimental setup used in this research was described in Chapter 2 . Several experiments with different settings were conducted in this chapter in order to analyse the effect of the grinding wheel on the grinding process. At each run, the work piece was ground with constant oscillation (except in Figure 4.3.1 where there was no oscillation) and one single in-feed.

In Figure 4.3.1, the work piece was ground using a blunt wheel on 3 different contact zones. In fact, the wok piece position was kept constant when it was being ground. The given in-feed was 15 μm per experiment.

The experimental data plotted in Figure 4.3.2 to Figure 4.3.4 is based on the same sets of experiments. Firstly, an un-trued and un-dressed wheel was used. The work piece oscillation was 6mm/s and the in-feed ranged from 10 to 120 μm . The in-feed was given when the wheel was spinning and the work piece was oscillating. The same procedure was repeated using a trued but un-dressed wheel. The grinding wheel was trued before each single experiment with a truing wheel. The grinding wheel was trued for less than 2 minutes while the truing wheel was oscillating at 5mm/s in accordance with commonly used industrial practices. Normally, the in-feed given during truing is a few microns because the reason for truing is "to remove wheel profile irregularities produced by previous grinding operations" [41]. However, due to lack of accuracy in the available grinding machine it is impossible to follow this routine. Therefore, the truing in-feed was 5 μm as discussed in Section 3.2. The in-feed was given 2-3 times during truing wheel oscillation to make sure the desired grinding wheel topography was achieved. Finally, the same sequence of experiments as in the previous 2 was repeated using a dressed and trued wheel. The grinding wheel was trued occasionally (as in typical industrial applications) but not before every single experiment. After truing the wheel, it was dressed using a wet dressing stick for about 25s prior to each test. To be conservative, the duration of each grinding test was about 30s. The dressing in-feed was given continuously and manually during the grinding wheel rotation. The range of grinding in-feed was 10-60 μm and an additional in-feed of 100 μm for the last test.

To compare the effect of truing and dressing conditions on the subsequent grinding process the results of these 3 sets of experiments were drawn together.

In Figure 4.4.1 and Figure 4.4.2 the aim is to show the behaviour of a blunt wheel. So, the experiment was started with a trued and dressed wheel. The grinding wheel was trued (with the same settings as before) and dressed (for about 25s) just once for the first experiment. In other words, looking at Figure 4.4.1, the grinding wheel was not trued or dressed in sections after the first section. The 20 μm single in-feed was kept

constant per experiment and it was given during oscillation (6mm/s). To find the MRR, the depth of removed material was measured after each experiment using a micrometer.

The next set of experiments is based on different dressing durations. Considering Figure 4.4.3 and Figure 4.4.4, in the first section the grinding wheel is dressed for 10s, while in the last section it is dressed for a longer period (50s). The work piece oscillation was 6mm/s and each experiment lasted less than 20s. The routines are as below.

1. Firstly, the grinding was trued using the same settings as usual.
2. The grinding wheel was dressed for 10s.
3. 10 μm in-feed was given.
4. MRR was measured with a micrometre.
5. The wheel was dressed for 20s.
6. Steps 3-4 were repeated.
7. The wheel was dressed for 30s.
8. Steps 3-4 were repeated.
9. The wheel was dressed for 40s.
10. Steps 3-4 were repeated.
11. The wheel was dressed for 50s.
12. Steps 3-4 were repeated.
13. Steps 2-12 were repeated. But, this time with 20 μm in-feed.

The results of these experiments are studied in the next sections in order to show how the truing and dressing parameters influence the grinding process.

4.3. Truing, Dressing and the Grinding Forces

Figure 4.3.1 shows the normal force against time for 3 different contact zones. The grinding wheel used in this experiment was not dressed. It is clear that when the in-feed is being given F_N increases to its maximum value. Now, if the material in contact is just cemented carbide, F_N drops noticeably. Otherwise, no significant change in the F_N value can be observed. Comparing this graph with Figure 3.4.1, one can easily notice how high the forces in Figure 4.3.1 are. In fact, the grinding forces produced using a blunt wheel can be greater by up to 4 times. Apparently, a blunt diamond grinding wheel can still be sharp enough to grind cemented carbide. However, the forces will be lower and the grinding time shorter, if the wheel used is dressed. Here, the maximum F_N in full contact is under 25N while for cemented carbide contact it reduces to about 12.5N.

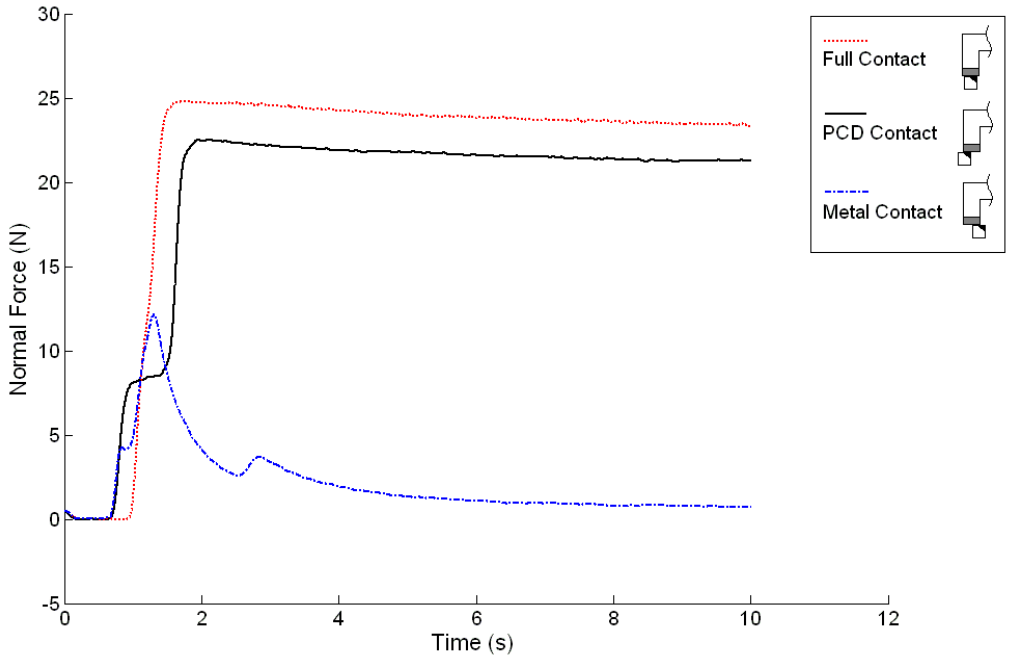

Figure 4.3.1 Normal force vs. time, using a blunt wheel, without moving the work piece, for different contact positions and 15 μm in-feed

To sum up, with a blunt wheel, when the PCD is in contact with the grinding wheel, forces remain constant. While, with a sharp wheel, after the in-feed is given the forces drop to a certain value and then remain constant.

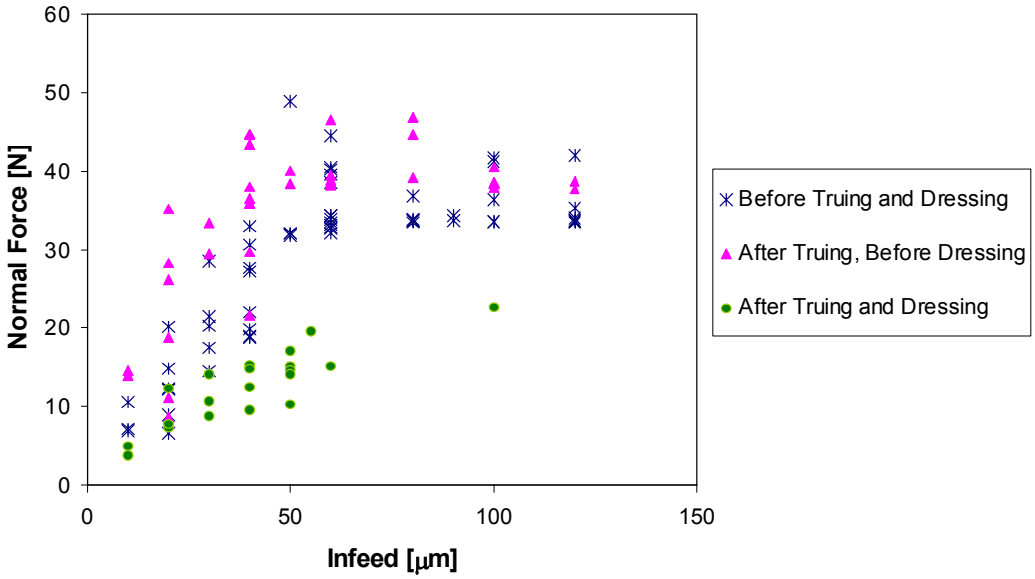

Figure 4.3.2 Maximum normal force against in-feed, for different grinding wheel conditions

Figure 4.3.2 illustrates the normal force against in-feed for 3 differently prepared grinding wheel cases. Due to unavoidable inaccuracies in giving in-feed, a wide range of F_N can be seen for some in-feeds. Evidently, a grinding wheel that is just trued generates the highest forces while, as expected, a trued and dressed wheel produces the minimum forces. It is true that the grinding surface of a trued wheel behaves uniformly. But, the truing itself does not sharpen the wheel and it has the tendency to wear out the grinding wheel and make the grinding results worse. The higher normal forces in Figure 4.3.2 verify that. Interestingly, after truing, the wheel dullness can be observed because of the glazed surface and can be detected by touching the surface of the wheel. Considering the first 2 series in Figure 4.3.2, as the in-feed increases, up to a value around $50\,\mu m$, the grinding forces increase as well while, for in-feeds over $50\,\mu m$ no significant increase in the value of forces can be detected. The decreasing trend of F_N for in-feeds over $50\,\mu m$ shows that one of the reasons can be because of not holding the work piece tight enough in its position, which leads to backlash. Actually, if the wheel is blunt and more in-feed is given, then because of the wheel

dullness not only the material will not be removed but also high resistance and reaction of the system will push back the work piece until less material becomes in contact with the wheel. To conclude, it is suggested that PCD work pieces should be ground using in-feeds less than 50 μm .

In the third series of Figure 4.3.2 i.e. after truing and dressing, as the in-feed increases the grinding forces increase gradually. No in-feed between 60 and 120 μm was tested since the selected range provides enough information. With a sharp wheel less force is required to remove the same amount of material. The sharpness of the wheel reduces the high resistance of the system against the material removal mechanism and that is why the trend is gradual. The forces produced during grinding are approximately one third of the forces in the other 2 series.

Note that while the forces increase sharply in the first 2 series, the trend in the third series is gradual.

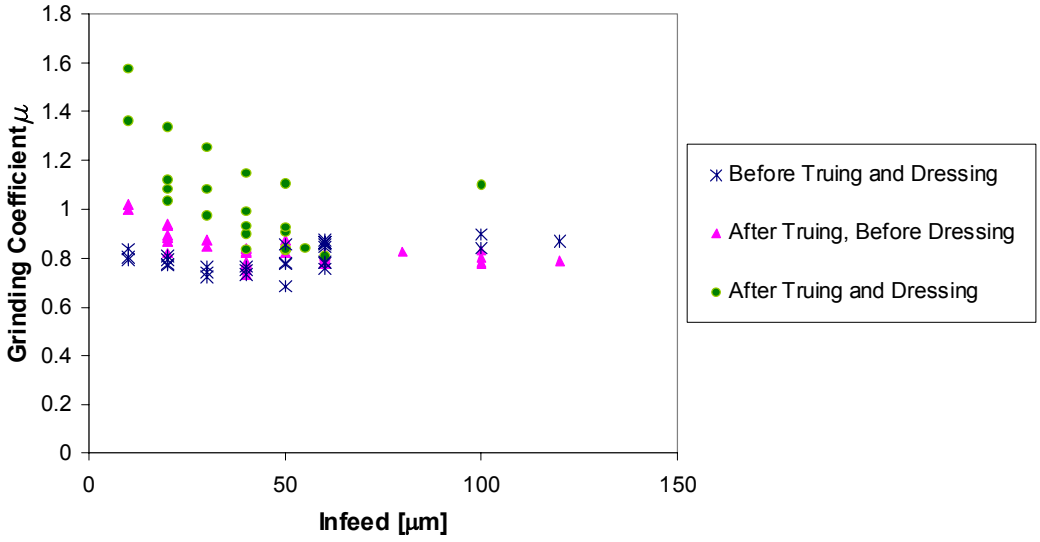

Figure 4.3.3 Ratio of the maximum tangential force to the maximum normal against in-feed, for different grinding wheel conditions

Figure 4.3.3 shows the grinding coefficient μ against in-feed for a grinding wheel with 3 different conditions. A trued and dressed wheel has the highest grinding coefficient. However, all of the 3 series behave similarly. Up to 50 μm , as in-feed increases μ

decreases and for in-feeds above 50 µm it remains almost constant. In fact, up to 50 microns as in-feed increases F_T does not increase as much as F_N does.

When the wheel is sharp, the grinding coefficient is mostly one and greater than one. This indicates that with a sharp wheel F_T produced during grinding is higher than F_N. While in contrast, the normal force generated using a blunt wheel is higher than the cutting force.

Figure 4.3.4 points out the relation between the grinding forces considering wheel sharpness and bluntness. Regardless of how the grinding wheel is prepared, as F_N increases F_T increases as well. Moreover, their relation is almost proportional. Although a sharp wheel produces a smaller range of grinding forces (as shown in Figure 4.4.2) in all of the 3 series the values of F_N and F_T (for each series) are close to each other.

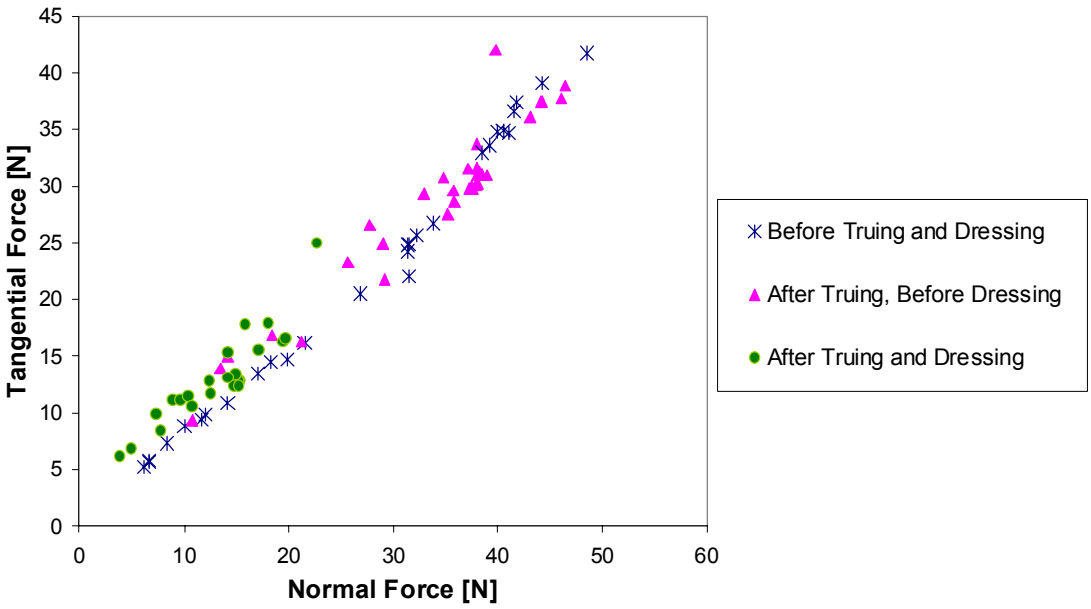

Figure 4.3.4 Maximum tangential against maximum normal force, for different grinding wheel conditions

Now that the dressing importance has been clarified the next section examines the details thoroughly.

4.4. Dressing Time and Sharpness of the Wheel

The aim in these experiments is to achieve an optimal dressing time and to show how sharp a grinding wheel should be. Figure 4.4.1 shows how the normal force fluctuates over time.

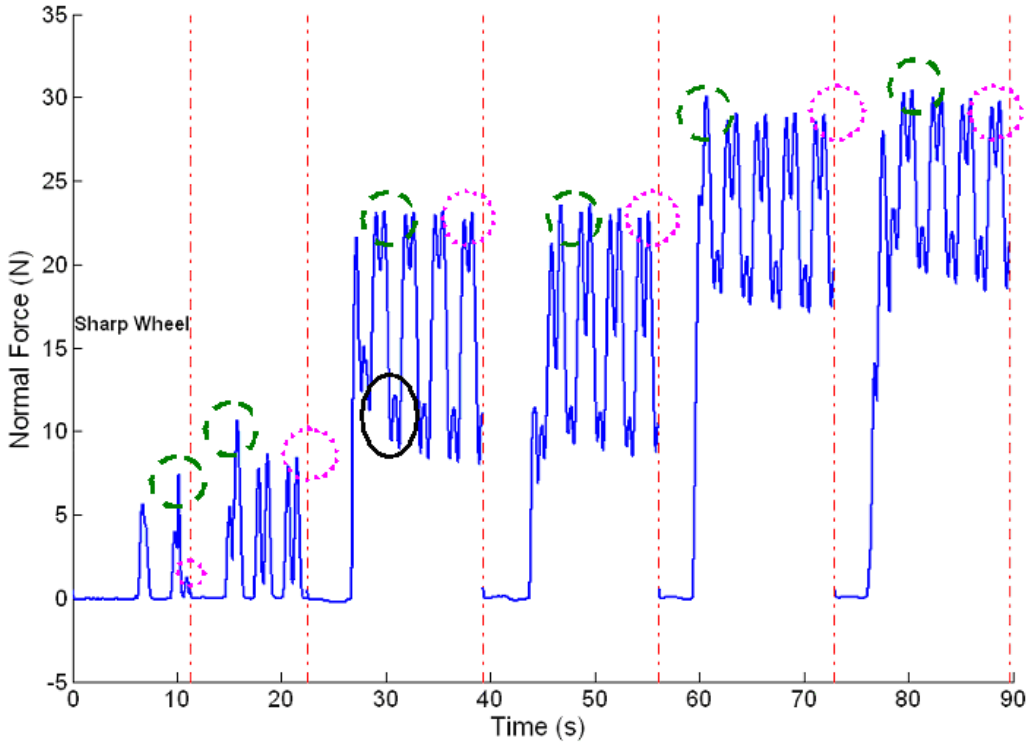

Figure 4.4.1 Normal force vs. time, commencing with a dressed wheel with 20 μm in-feed per section.

Each section of Figure 4.4.1 represents a separate experiment. This set of experiments has started with a trued and dressed wheel contrary to the case in the other sections. Comparing these sections, as the wheel becomes more worn the normal force keeps increasing (using the same settings). For example, for 20 μm constant in-feed F_N can be 5N at the best condition or 30N at the worst. Obviously, when the wheel is sharp (up to a certain degree) the difference between the highest peak (green dashed circles) and the last peak (pink dot circles) is clear. Considering this alteration, as the wheel wears out more, no significant material is removed. Furthermore, looking at the black solid oval drawn in Figure 4.4.1 and comparing it with the valleys of first and second sections or comparing it with V_2 in Figure 3.3.2, it can be realized that instead of one valley, 2 valleys exist. The reason is mainly that some irregularities on the wheel surface

prevent an even contact between the work piece and wheel. Therefore, using an un-trued grinding wheel may damage and reduce the surface uniformity. Eventually, after about 30s grinding the wheel needs to be resharpened.

As discussed in Section 3.5 MRR is one of the most informative parameters in grinding PCD. To achieve similar information it is easy to measure the amount of material removed from the PCD blank using a micrometre other than buying a force sensor. So, even without having information about the grinding forces, MRR determines whether the wheel has become blunt or not.

Figure 4.4.2 shows how the material removal rate varies with the normal force as the grinding wheel becomes blunt. In this case, when the wheel has been sharpened for the optimum time, the MRR is a maximum at the commencement of grinding. As the wheel gets blunt, F_N increases and MRR drops significantly. Material removal stops or decreases to about one fifth of the maximum value or even less.

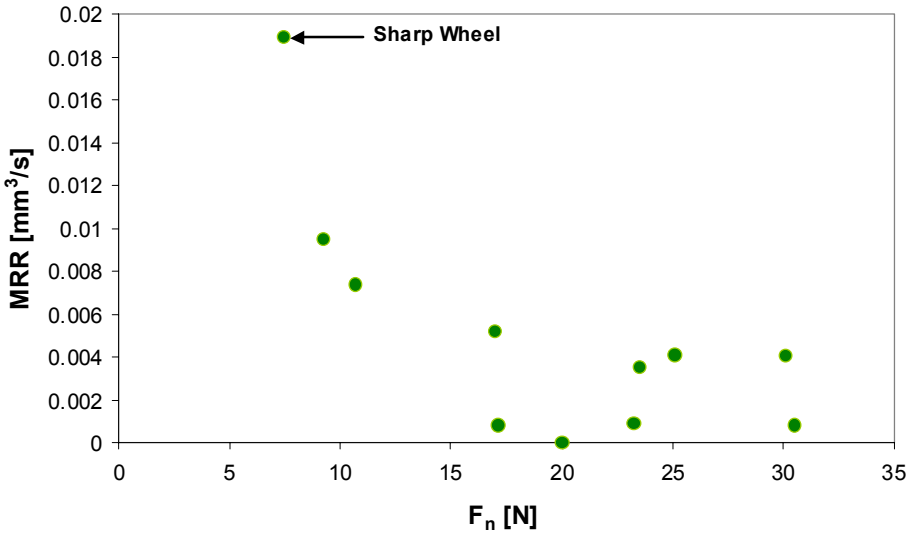

Figure 4.4.2 Material removal rate against normal force, commencing with a dressed wheel with 20 µm in-feed

Figure 4.4.3 shows the normal force vs. time after different dressing periods t_d. A constant in-feed (10 microns) was given per section. According to Figure 4.4.3 a sharper wheel produces higher F_N. The difference between the green dashed circles

and the pink dot circles confirms that material has been removed. The maximum difference between the first and the last peaks in the last section shows that the sharpest wheel has the maximum material removal. One question to be answered is whether the material is removed more from the work piece or the grinding wheel. This question will be answered in Section 5.4.

To select a suitable range of dressing times more information including material removal rate needs to be collected. This information is available in Section 5.4 where Figure 4.4.3 will be studied in detail.

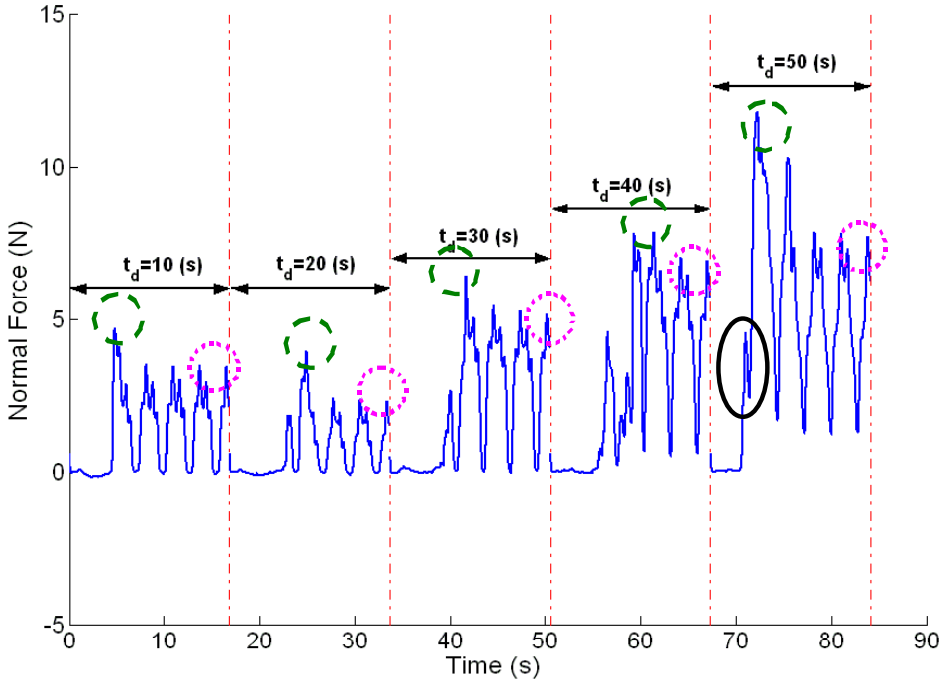

Figure 4.4.3 Normal force vs. time, using a wheel dressed for different dressing times, 10 μm in-feed per section.

Figure 4.4.4 specifications are similar to Figure 4.4.3 except the in-feed is 20 µm instead of 10 µm . No such trend as in Figure 4.4.3 is detected here. The difference between the green dashed circles and the pink dot circles is not as much as it was in Figure 4.4.3. Nonetheless, the clear difference in the last 2 sections of Figure 4.4.4 confirms the same fact that with the sharpest wheel the maximum material is removed.

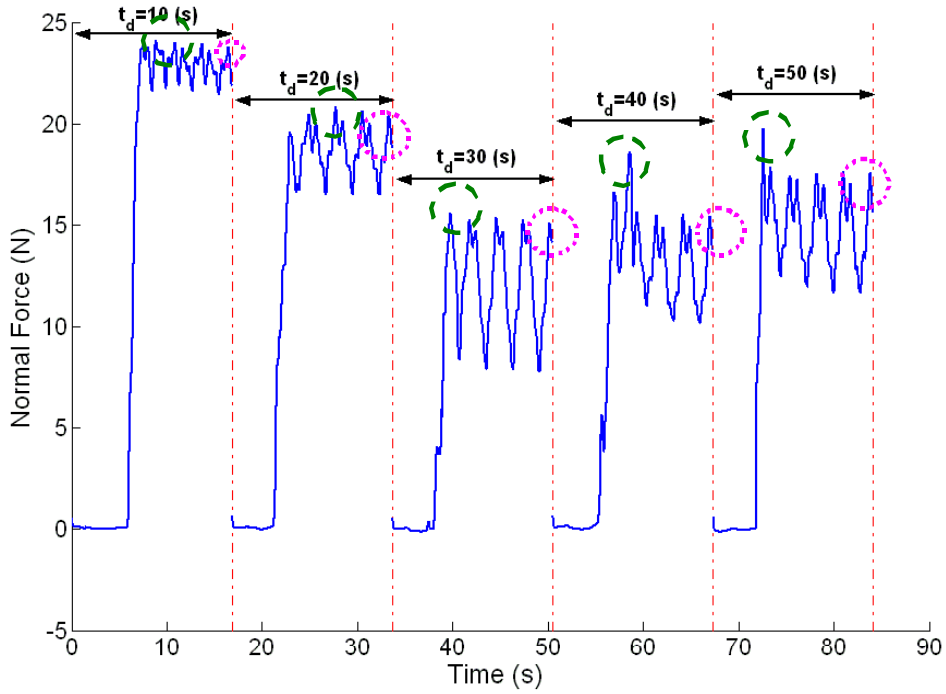

Figure 4.4.4 Normal force vs. time, using a wheel dressed for different dressing times, 20 µm in-feed per section.

To compare the results of the previous 2 figures, the maximum normal forces of each section have been extracted and plotted in Figure 4.4.5. For 10 µm in-feed, up to 20s and for 20 µm in-feed, up to 30s F_N decreases the longer the wheel is dressed while for higher dressing durations F_N increases. For 10 µm in-feed, the maximum t_d has the maximum F_N while for 20 µm in-feed, the minimum t_d has the maximum F_N. Since in general for a certain in-feed a lower F_N gives a better result, the optimum range of t_d for 10 µm in-feed is 10-20s (blue solid oval shown in Figure 4.4.5) and 30-40s for 20 µm in-feed (pink dot oval). Hence, there is an optimum range of dressing time depending on the selected in-feed.

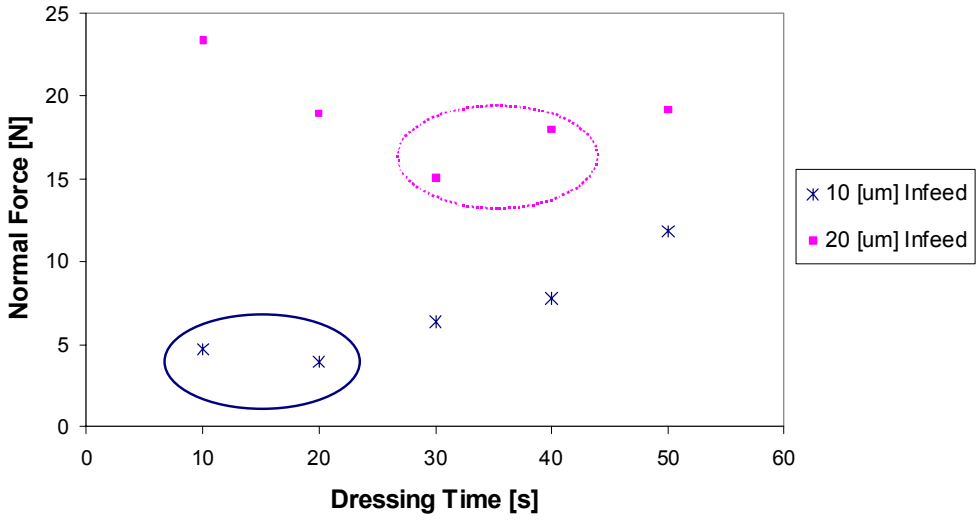

Figure 4.4.5 Maximum normal force against dressing time, for 10 and 20 µm in-feed

Figure 4.4.6 shows the relation between material removal rate and dressing time for 10 and 20 µm in-feed. The maximum material removed from the work piece is after dressing for 20s. The maximum MRR for 10 and 20 µm in-feed is 0.007 and 0.006mm^3/s, respectively. For 10 µm in-feed the least MRR 0.0048mm^3/s corresponds to the shortest dressing time and for 20 µm in-feed the least MRR 0.0021mm^3/s belongs to the sharpest wheel. Based on the highest MRRs the best dressing time range is 20-30s (the solid oval shown in Figure 4.4.6). For 20 µm in-feed the sharpest wheel and the least sharp wheel remove almost the same amount of

material in a certain time. Consequently, there is no need to dress the wheel for too long.

According to Figure 4.4.6, the difference between the maximum and minimum MRR shows that the optimum range of dressing time is more limited for higher in-feeds.

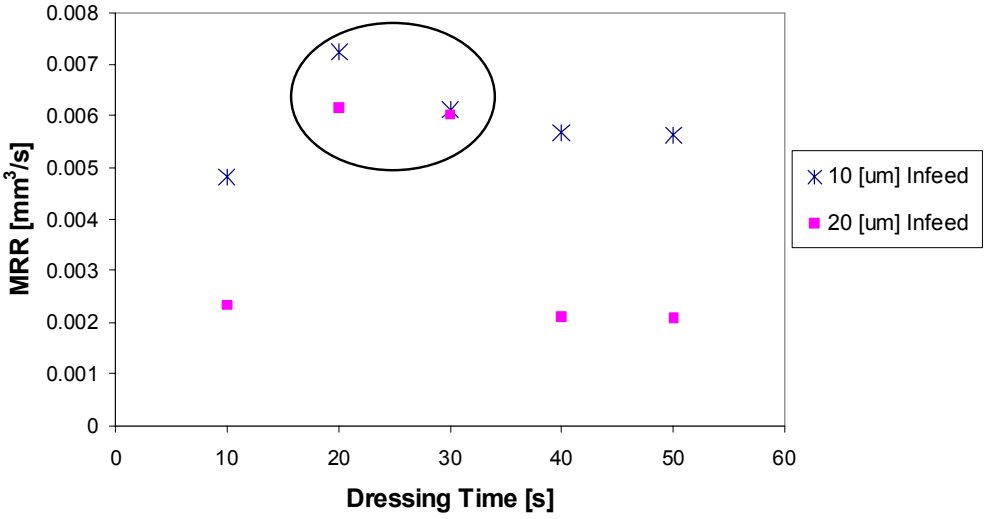

Figure 4.4.6 Material removal rate against dressing time, for 10 and 20 μm in-feed

Even though a sharp wheel would be expected to produce a low force, this is not the case since the sharpest wheel has removed the least material, as shown in Figure 4.4.6. According to Figure 4.4.3 and Figure 4.4.6, the MRR corresponding to the highest F_N is not at its highest value. So, the high F_N is not caused by a too high in-feed. According to the last section of Figure 4.4.3, as the in-feed is applied the material is removed and F_N drops a little (black solid oval) and because the in-feed has not yet finished F_N goes up to its maximum value (green dashed circle) and then falls. In this section due to the high sharpness of the wheel as the in-feed is applied the exposed grains (as discussed in Section 1.4) on the wheel break quickly and a larger area of the wheel becomes in contact with the work piece. Consequently, higher normal force is produced. However, the difference between the green dashed and the pink dotted circles shows that the wheel does not become blunt as soon as the grains break. Furthermore, due to the grains breakage MRR is not as high as previously.

4.5. Conclusions

In this chapter, the effect of dressing on improving the grinding performance has been studied in detail.

It was shown in this chapter that when the grinding wheel is blunt, the ratio of the tangential to normal force is less than one. But, with a sharp wheel this ratio goes over one. So, the grinding coefficient can be used as an indicator of the wheel sharpness.

It was also shown that as the grinding wheel wears out the grinding forces increase and the material removal rate decreases. In other words, for a given in-feed, a sharp wheel produces lower forces. Due to the hardness of PCD the grinding wheel wears so quickly that it needs to be dressed frequently. To find the optimum dressing intervals similar experiments as in Section 4.4 can be carried out. In this research it was found that the wheel needs to be dressed after about 30s grinding, depending upon the working conditions. This value is similar to some other published data [4-6, 22].

Although the grinding coefficient can be used as an indicator of the wheel sharpness it was shown in this chapter that MRR is the most practical indicator in determining when the grinding wheel needs to be dressed and the latter indicator can be used in more PCD grinding experiments.

Interestingly, for a certain in-feed, the sharper wheel does not necessarily remove more material because the exposed grains of a wheel dressed for a long period break more rapidly. So, having a sharper wheel is not necessarily better.

It was also shown that there is an optimum range of dressing time depending on the selected in-feed. The ideal dressing time corresponds to the minimum grinding forces and the maximum MRR. Taking into account all the existing constraints, the best range of dressing time for the available grinding system is approximately 10-30s similar to other published data [5, 6, 8, 15, 16, 44]. It was shown in Chapter 3 that higher in-feeds are not advantageous. However, to find the optimum dressing time for in-feeds higher than the in-feeds used in this research the same experimental procedure is applicable.

It was shown in this chapter how some parameters including material removal rate MRR, grinding forces F_N and F_T and grinding coefficient μ can be used as practical indicators of the roughness of the grinding wheel and also to select the optimum dressing time.

In general it was shown that the dressing procedure must be adapted to the grinding conditions, and this chapter gives several ways in which this can be done.

CHAPTER 5 GRINDING WHEEL WEAR

5.1. Introduction

As discussed in Chapter 4 , for grinding PCD the diamond grinding wheel has to meet special requirements. As the wheel wears out, more of the bonding material in the wheel comes into contact with the PCD blank and the sharp grains are worn and so the wheel must be dressed to open up its surface. Due to the high wear resistance of PCD the material removal ratio of the wheel is usually greater than the material removal ratio of the PCD work piece. Moreover, the material type affects material removal rate and volumetric wheel wear rate in different ways. To avoid high grinding costs it is essential to reduce the rate of volumetric wheel wear by using the correct setup. Hence, the aim of this chapter is to study the effect of wheel wear on grinding parameters and vice versa, and also to show how much the wheel wears by taking into account wheel conditioning, in-feed and work piece material type. Subsequently, the grinding parameters can be optimized to achieve a satisfactory material removal rate and an extended wheel life. Material removal rate (MRR) has been already discussed in Chapter 3 and Chapter 4 . However, some of the results of this chapter need to be discussed in regard to the same MRR graphs of those chapters.

Initially, in Section 5.2 the details of experiments are explained. In Section 5.3 the relation between the material removal rate, volumetric wheel wear rate (after grinding) and in-feed is studied. G-ratio ("a measurement for wheel life" [51]), which is a combination of material removal rate and volumetric wheel wear, is also determined and plotted vs. a range of in-feeds and normal forces. The graphs in this section are against the normal force and in-feed which are two dependent and practically useful variables. The effect of giving in-feed in steps on the wheel wear rate is considered in Section 5.3.1. Some material is removed from the grinding wheel during the process of dressing. The VWW is the volumetric material removed from the grinding wheel during dressing while the VWWR is the rate of material removal during grinding. VWWR and VWW are two distinct terms used in this thesis. The former refers to grinding and the latter refers to dressing. How the sharpness of the wheel influences the wheel wear is discussed in Section 5.4. In Section 5.5 the relationship between the

hardness of the material type and the grinding wheel wear is discussed. Finally, conclusions are drawn in Section 0.

5.2. Description of Experiments

The experimental setup used in this research was described in Chapter 2 . The experiments presented in this chapter are all as in Sections 3.3, 3.4 and 4.4 except that some extra measurements have been included. These extra measurements consist of measuring the amount of material removed from the grinding wheel after grinding and dressing in each single experiment using a micrometer.

5.3. Material Removal Rate (MRR) and Volumetric Wheel Wear Rate (VWWR)

Figure 5.3.1 shows the relation of G-ratio and material removal rate with the normal force as the grinding wheel wears out. Figure 5.3.1 is the result of the experiments as conducted in Figure 4.4.1.

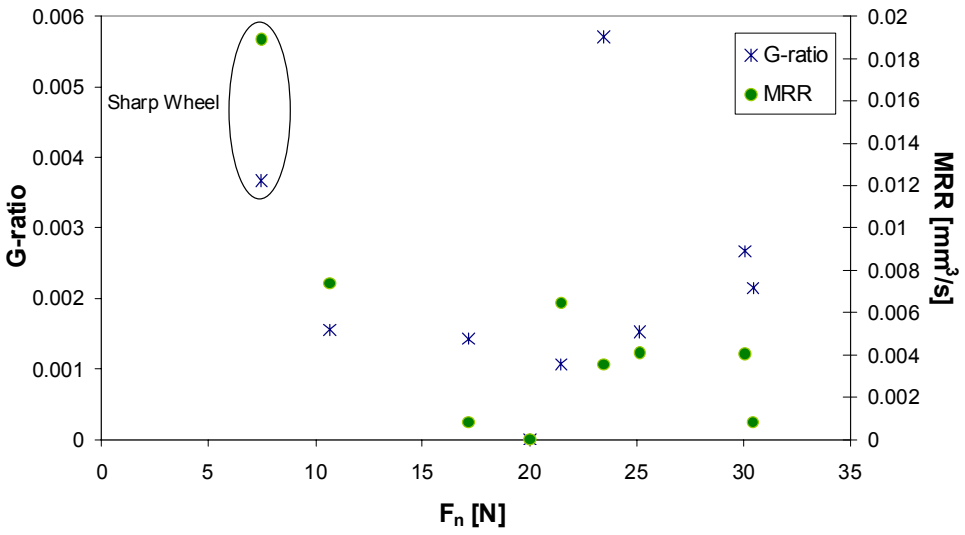

Figure 5.3.1 G-ratio and MRR against normal force, commencing with a dressed wheel with 20 μm in-feed per experiment

It was previously explained that the material removal stops when the grinding wheel becomes blunt. The point is that the amount of material removed from the grinding wheel is as important as the amount of material removed from the work piece. The ideal condition is to have maximum MRR simultaneously with the minimum

volumetric wheel wear rate VWWR. Obviously, it is impossible to reach both of these objectives. However, there is always an optimum range to select.

It was described in Section 1.3.1 that G-ratio is the ratio of volumetric material removed from the wok piece to the volumetric material removed from the grinding wheel for a given grinding time. According to Figure 5.3.1, no consistent trend is detected for G-ratio. Although MRR decreases as the wheel dulls, it is not a dominant factor in determining the trend of G-ratio. Even though in most of the published data [4-9, 11, 13, 14, 22, 41, 51, 61, 62] the authors have referred to G-ratio, in this case the most informative measure is VWWR. So, in this case, the dressing time (as explained in Section 4.4) is determined based on the MRR rather than G-ratio. From Figure 5.3.1 the maximum G-ratio is 0.0057. This means that the material removed from the wheel can be about 170 times more than the material removed from the PCD blank itself. The G-ratio goes to zero when no significant material is removed from the PCD work piece.

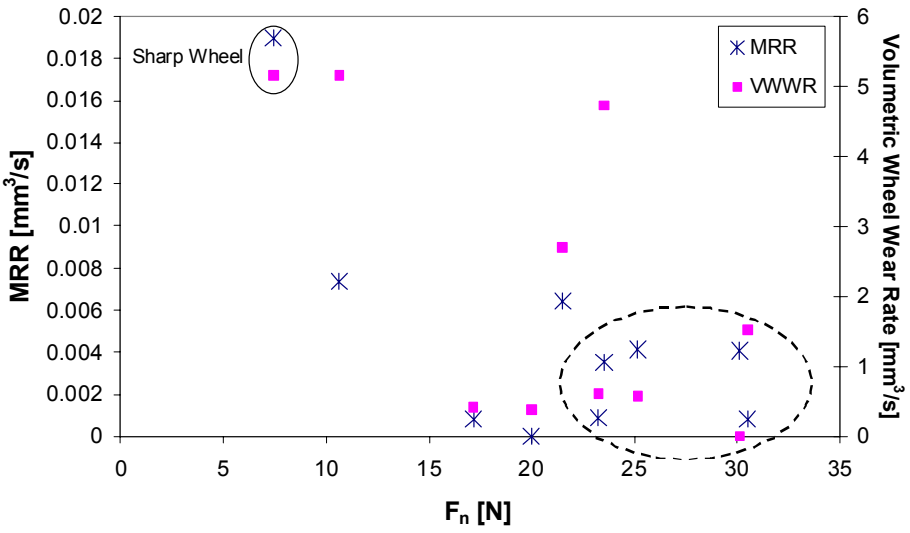

Figure 5.3.2 MRR and VWWR against normal force, commencing with a dressed wheel with 20 µm in-feed per experiment

According to Figure 5.3.2, the sharp wheel not only wears more but also removes the maximum material from the PCD work piece. Figure 5.3.2 is the result of the experiments as conducted in Figure 4.4.1. It is clear how erratic the fluctuations of VWWR are. In fact, the inconsistent trend of VWWR shows that the trend of G-ratio is also erratic. However, the dashed oval in Figure 5.3.2 shows that eventually the material removed from both the work piece and the wheel has decreased. In other words, when the wheel becomes blunt the work piece and the grinding wheel just rub against each other resulting in high grinding forces and negligible MRR. At the maximum point, $5mm^3$ is removed from the wheel each second.

Error! Reference source not found. shows the relation of G-ratio and MRR with in-feed. **Error! Reference source not found.** is the result of tests carried out in Figure 3.3.1. Despite the previous graphs where G-ratio and MRR had different behaviours, in this graph they follow the same trend. Up to $20\,\mu m$, as the in-feed increases (and so does F_N as explained in Section 3.3) G-ratio increases up to 0.0043, as well. But, for higher in-feeds up to $50\,\mu m$, G-ratio keeps decreasing to the lowest value 0.0017. To study the effect of each term in changing the G-ratio curve, VWWR is plotted in Figure 5.3.4.

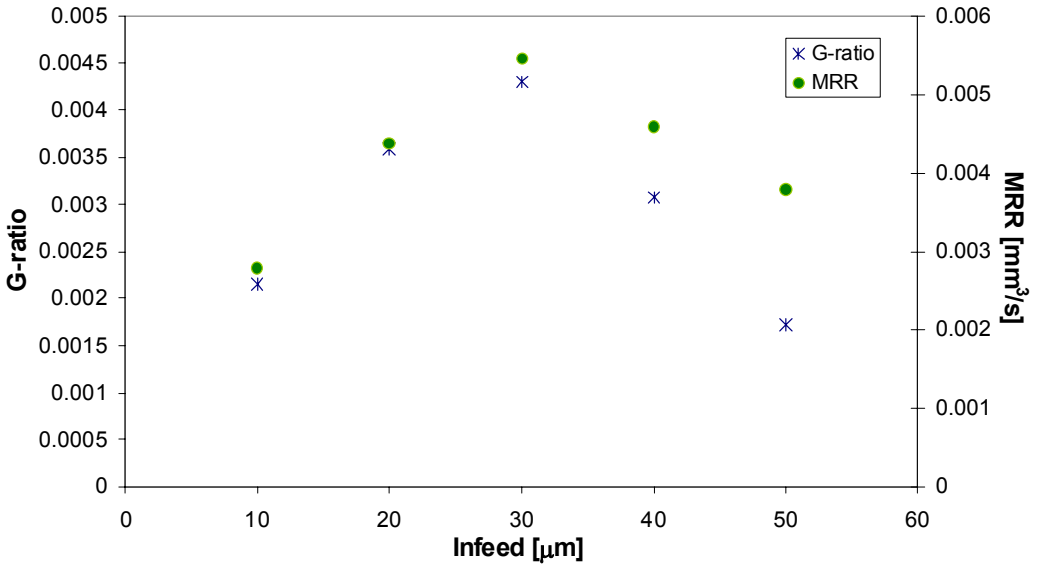

Figure 5.3.3 G-ratio and MRR against in-feed

Figure 5.3.4 shows the relation of MRR and VWWR with in-feed. Figure 5.3.4 is the result of tests done in Figure 3.3.1. As the in-feed increases the grinding wheel wears out more. The range of VWWR is 0.7-2.2mm^3/s. As explained in Section 3.5 this figure also shows that the range of 30-50 μm in-feed is not a suitable and economic range because not only does the wheel become blunter but also MRR drops. Comparing grinding time and in-feed, in-feed is the determining factor in wearing the wheel out.

Comparing **Error! Reference source not found.** and Figure 5.3.4, for up to 30 μm in-feed, MRR is superior to VWWR in determining the trend of G-ratio and between 30 and 50 μm the decreasing MRR and increasing VWWR both influence the G-ratio to fall.

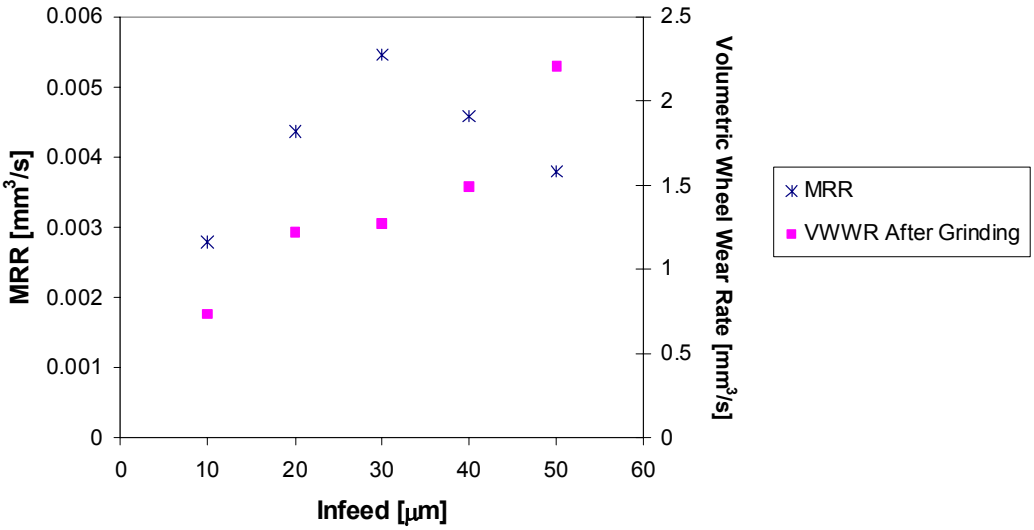

Figure 5.3.4 MRR and volumetric wheel wear rate against in-feed

5.3.1. In-feed in Steps

Figure 5.3.5 shows how giving different in-feeds in steps alters the rate of volumetric wheel wear after grinding. This figure and Figure 3.3.7 result from the same experiment. With a sharp wheel giving a number of single in-feeds during one experiment causes the wheel to wear out less than giving one in-feed equal to the sum of those single in-feeds. So, to avoid high grinding costs, it is suggested to divide the in-feeds over 30 µm into smaller portions. For instance, the VWWR of five 10 µm in-feeds is about one quarter of the VWWR of one single 50 µm in-feed.

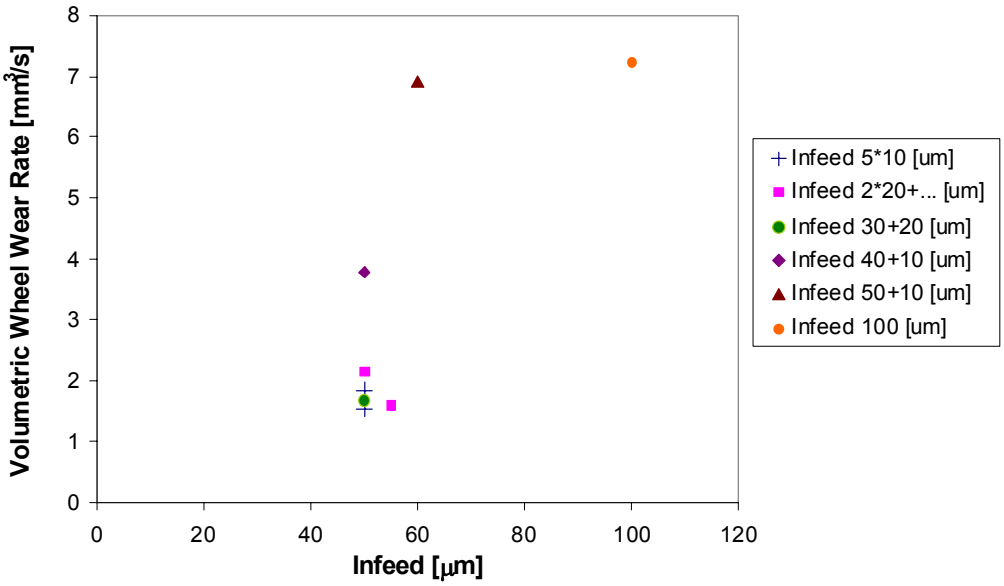

Figure 5.3.5 Volumetric wheel wear rate against in-feed for different in-feed steps

5.4. Dressing Effect on the Wheel Wear

As described in Section 1.4, dressing procedure is a process which opens the abrasive layer of the grinding wheel by removing the bond between the grains and exposing new diamond grains. In this section, the aim is to show how quickly a grinding wheel with different degrees of sharpness wears. The figures of this section are related to Figure 4.4.3 and Figure 4.4.4. Figure 5.4.1 points out the relation of MRR and VWWR with the dressing duration t_d, for 10 µm in-feed. The engagement of grains between the wheel and the work piece is such that as the wheel is dressed for a longer time (up to 30s t_d) VWWR decreases up to the lowest value 0.25mm^3/s. In other words, because of not having enough grains protrusion (as discussed in Section 1.4) the wheel blunts very quickly and cutting performance decreases. The low MRR for a t_d of 10s confirms this fact. Longer dressing times make the wheel too sharp such that the exposed grains (as shown in Figure 1.4.1) break relatively quickly resulting in unreasonably large wheel wear and unsatisfactory material removal rate. In fact, the highest VWWR belongs to the sharpest wheel. The optimum range of t_d is selected by taking into account the satisfactory range of MRR and VWWR. Consequently, the best dressing time range is about 20-30s.

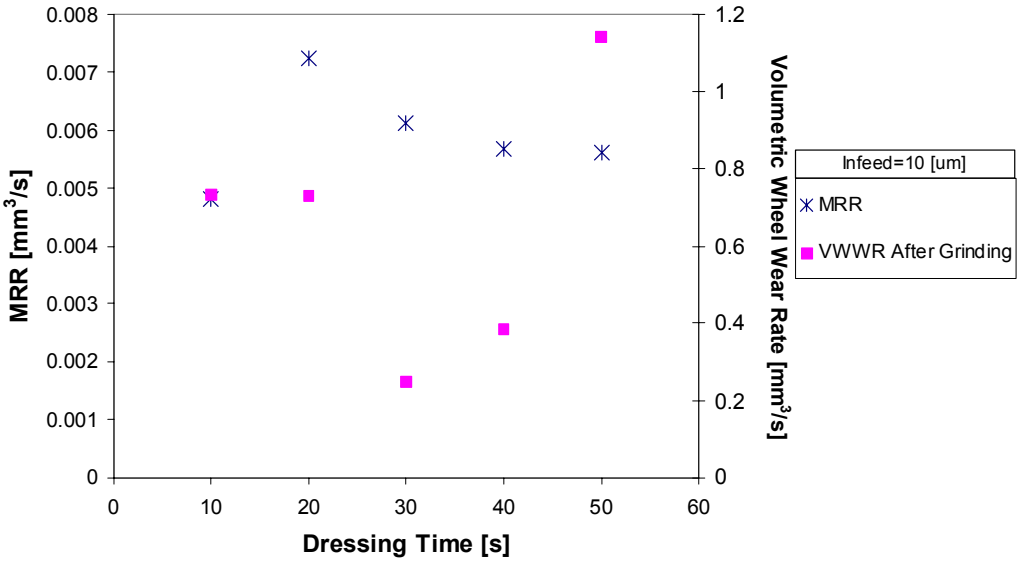

Figure 5.4.1 MRR and volumetric wheel wear rate against dressing time, for 10 μm in-feed

Depending on the dressing procedure and grinding wheel type, the material removed from the wheel during dressing can be a considerable issue. Figure 5.4.2 shows how much material is removed during different dressing times. The difference between Figure 5.4.1 and Figure 5.4.2 is in measuring the volumetric wheel wear after grinding and after dressing operations, respectively. Undoubtedly, dressing for a longer time t_d removes more material from the grinding wheel. Nevertheless the relation between t_d and volumetric wheel wear is not necessarily proportional since the grains protrusion before dressing (generated after each grinding experiment) and other factors including contact pressure (during dressing) can be different. In any case a longer dressing time reduces the wheel life cycle and increases grinding costs. As can be seen from Figure 5.4.2 a reasonable VWW occurs at 10-30s dressing time where the VWW is minimum and MRR is maximum. Note that the VWW is not normalized because the durations of all the experiments were the same.

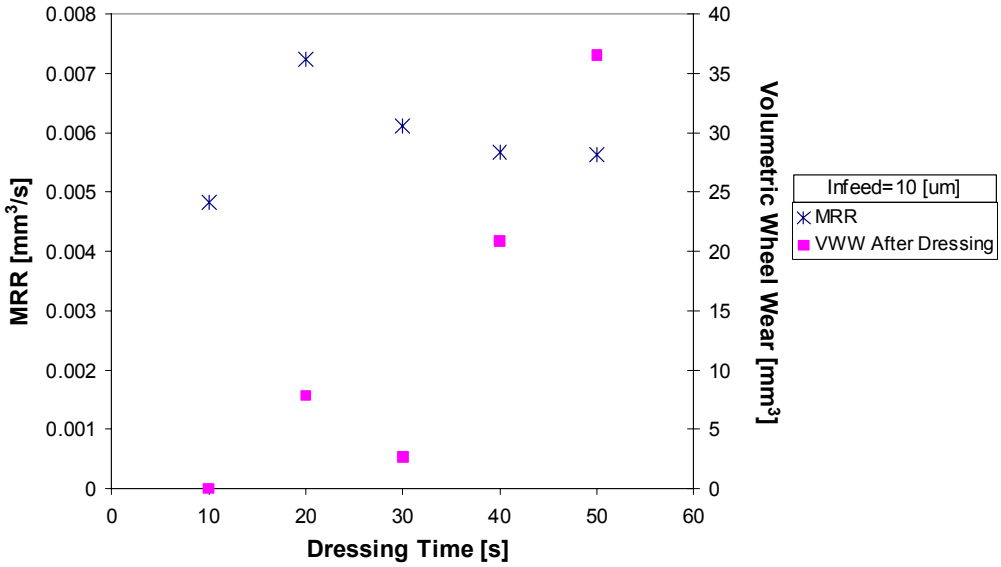

Figure 5.4.2 MRR and volumetric wheel wear after dressing against dressing time, for 10 μm in-feed

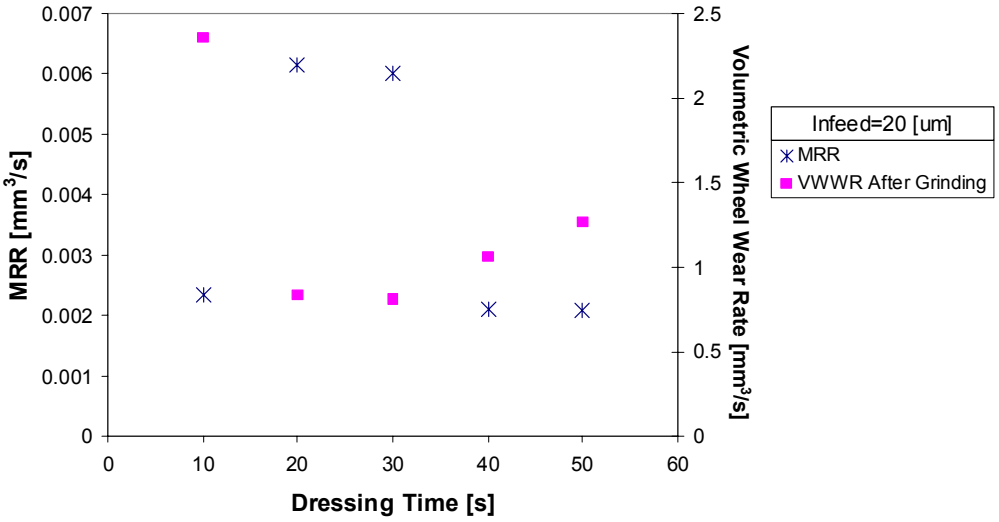

Figure 5.4.3 MRR and volumetric wheel wear rate against dressing time, for 20 μm in-feed

Figure 5.4.3 shows the relation of MRR and VWWR with dressing duration t_d, for 20 μm in-feed. Similar to Figure 5.4.1 as t_d increases up to about 25s the wheel wears less but after 25s VWWR increases gradually. The maximum VWWR is at t_d=10s because of not having enough grains protrusion (shown in Figure 1.4.1). So, before the

desired cutting happens the wheel blunts. The low MRR verifies this explanation. Regarding the VWWR value at t_d=10s it can be said that the least sharp wheel can wear even more than a sharper wheel. Considering the lowest range of VWWR, the optimum dressing time lies in the range of 20-30s, which is also in the range of maximum MRR.

Figure 5.4.4 shows how much material is removed during different dressing times. Below a t_d of 30s no significant material is removed from the wheel during dressing. But, longer dressing time removes some material from the wheel but still not as much as in Figure 5.4.2. Comparing these 2 figures one can notice that the dressing stick (as shown in Figure 2.2.11) used in Figure 5.4.4 is more effective because it has removed less material from the wheel to open the wheel surface. So, the grinding wheel lasts longer. The maximum VWW of 2.5mm^3 in Figure 5.4.4 is considerably lower than the corresponding value of 37 mm^3 in Figure 5.4.2. However, since the maximum MRR and the minimum VWW are both in the same band, the best range of dressing time will be still 20-30s.

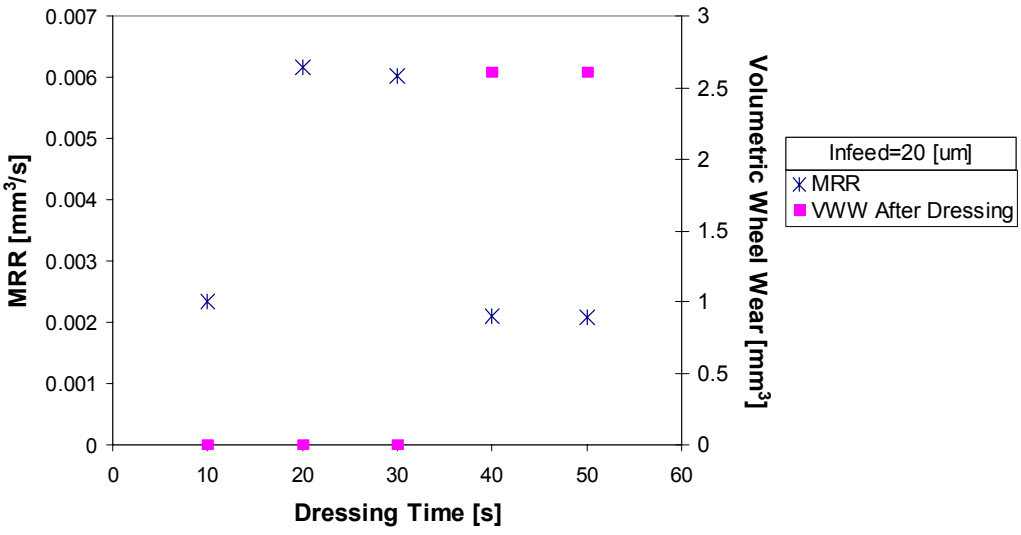

Figure 5.4.4 MRR and volumetric wheel wear after dressing against dressing time, for 20 µm in-feed

The results of VWWs in Figure 5.4.2 and Figure 5.4.4 are distinct due to the use of different dressing sticks and not because of different grinding in-feeds. As the grinding

in-feed does not affect the dressing operation. Depending on the grinding wheel a right choice of dressing stick is important.

Figure 5.4.5 shows the comparison of G-ratio for 10 and 20 µm in-feed against dressing time. Although both curves fluctuate similarly, the curve of 10 µm in-feed is noticeably higher and distinctive compared to the other curve.

It can be seen that up to 30s, as the dressing time increases the G-ratio increases and after that decreases. The MRR of 10 µm in-feed is higher than that of 20 µm in-feed and VWWR (as shown in Figure 5.4.6) is lower for 10 µm. As mentioned in Section 1.3.1 G-ratio is a function of MRR and VWWR. In this case G-ratio can be used as "a measurement for wheel life" [51] because the MRR and VWWR fluctuate oppositely to each other so each of them can be used to determine the trend of G-ratio separately.

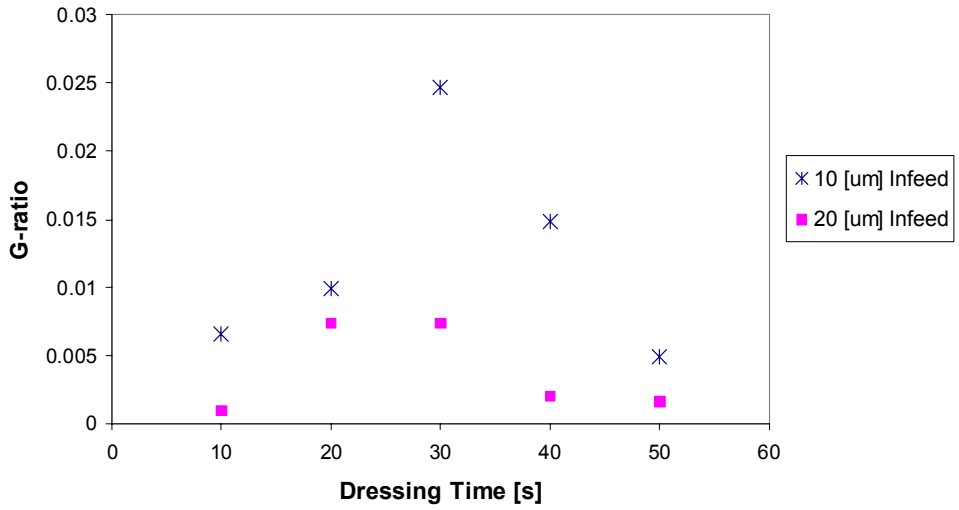

Figure 5.4.5 G-ratio against dressing time, for 10 and 20 µm in-feed

Figure 5.4.6 shows the effect of 2 different in-feeds on wearing of the grinding wheel, which is dressed for a range of different durations. Higher in-feeds make the grinding wheel wear out more (as previously explained in Figure 5.3.4). Both curves have similar behaviour except that for the 20 µm in-feed the rate of decrease in the first stage is considerably higher. The best dressing time range for both curves is 20-40s.

Different depths of cut, or in other words grains engagement, have different effects on wearing the grinding wheel. According to Figure 5.4.6 the sharpest wheel wears more if the in-feed is 10 μm while for 20 μm in-feed the least sharp wheel wears more.

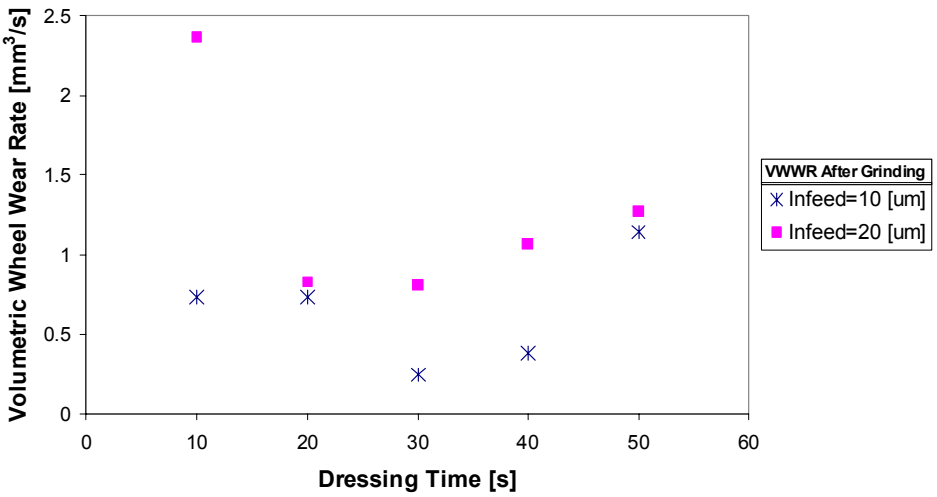

Figure 5.4.6 Volumetric wheel wear rate against dressing time, for 10 and 20 μm in-feed

5.5. Work Piece Hardness and the Wheel Wear

In this section the aim is to show how the extra hardness of PCD wears the grinding wheel in comparison with grinding of cemented carbide. Figure 5.5.1 shows effects of in-feed in grinding of cemented carbide. This figure and Figure 3.4.2 result from similar experiments. In Section 5.3 the relationship of MRR and VWWR was studied for PCD. Obviously, in grinding of cemented carbide not only the desired material is removed but also the grinding wheel does not wear much. In fact, up to a certain value the grinding wheel does not wear significantly at all. Then, when the wheel wears, the maximum value of 1.3mm^3/s is not much compared to the VWWR values in PCD grinding. The difference between the maximum and minimum VWWR in Figure 5.5.1 is because of the shorter grinding time in grinding cemented carbide.

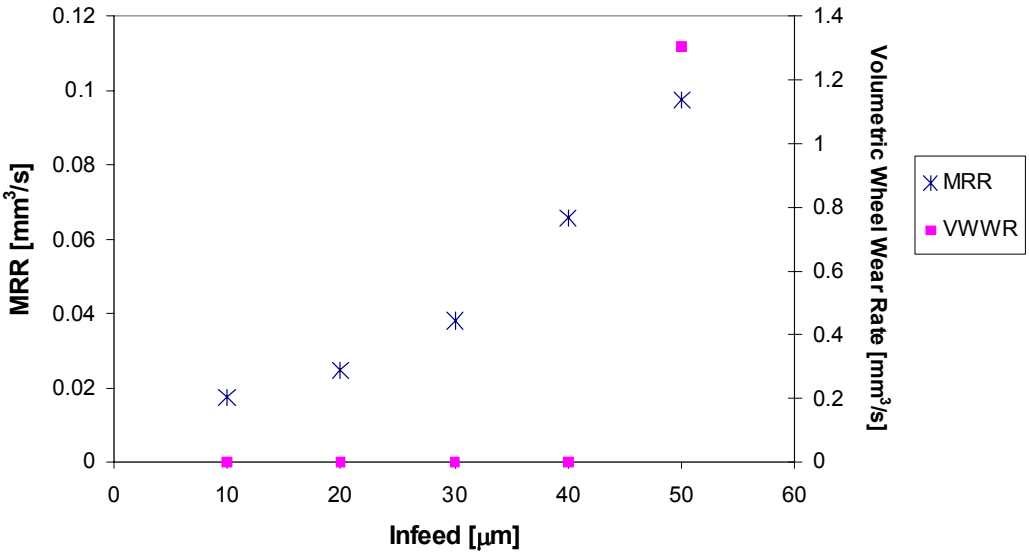

Figure 5.5.1 MRR and volumetric wheel wear rate against in-feed, in grinding cemented carbide

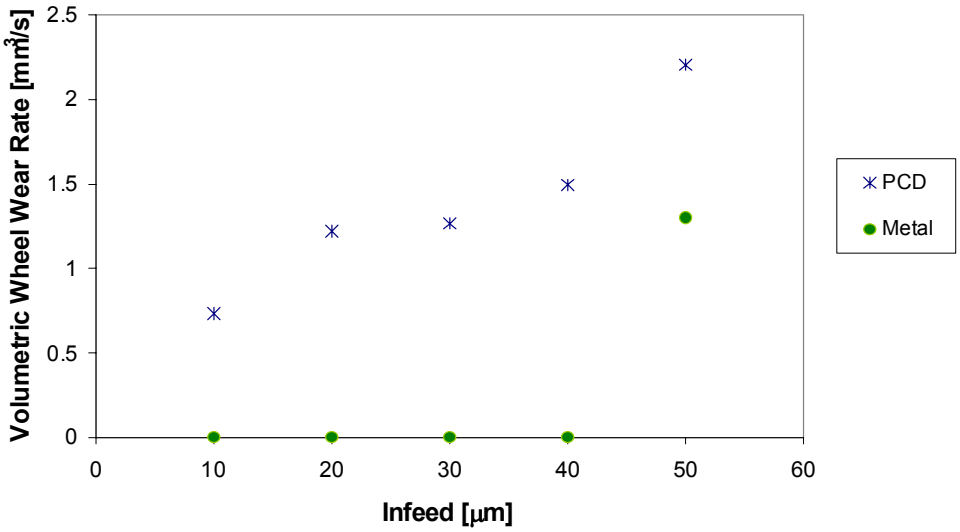

Figure 5.5.2 Comparison of volumetric wheel wear rate against in-feed, for grinding of PCD and cemented carbide

Figure 5.5.2 shows the volumetric wheel wear rate of PCD and cemented carbide against in-feed. Predictably, VWWR of PCD is significantly higher than that of cemented carbide (approx. 2 to tens of times higher). The small range of 0-1.3mm^3/s VWWR shows that in grinding cemented carbide the material removal does not reduce the wheel life cycle as fast as the PCD grinding does. According to this figure and the

dimensions of the diamond grinding wheel described in Section 2.2.1, for 50 μm in-feed the abrasive layer of the wheel decreases 1.8mm per hour in PCD grinding, which is 2 times greater than that in grinding cemented carbide. So, in PCD grinding the grinding costs are higher and the "grinding efficiency" [9] is considerably lower.

5.6. Conclusions

In this chapter, the rate of volumetric wheel wear under different conditions was measured and analysed. From the economic point of view, the rate of wheel wear can be as important as the rate of material removed from the PCD work piece. One of the ideal characteristics of a perfect grinding process is a process with the highest material removal rate and the lowest rate of wheel wear. Of course, it is not realistic to have the maximum MRR and the minimum VWWR at the same time.

It was shown in Section 5.3 that no significant material is removed from the surface of an already blunt wheel.

Relying on the changes in G-ratio is not always an effective way of finding the exact time when the grinding wheel needs to be dressed. In fact, because sometimes the G-ratio fluctuates erratically no consistent trend emerges. In these cases the MRR is a practical indicator of dressing time when G-ratio is not. So, it is suggested that MRR be used instead of G-ratio as an indicator for dressing.

Before using the G-ratio as a measurement of wheel life in any PCD grinding analysis it is suggested that graphs of MRR and VWWR be developed and their trends compared with G-ratio and then the most informative quantity used.

It was also shown in this chapter that instead of using expensive force sensors to measure the grinding forces produced during grinding (studied in Chapter 3) the optimum range of in-feed can be estimated by measuring the amount of material removed from the work piece and the grinding wheel.

In Section 5.3, the effect of in-feed on wearing out the wheel was studied. It was shown that the higher the in-feed the more the grinding wheel dulls. However, it is

shown that an optimum range of in-feed with reasonable high MRRs and low VWWRs exists.

It is also recommended to use small steps of in-feed rather than using one single high in-feed. For example it was shown that the VWWR could be reduced by 3 times or even more using smaller steps of in-feed.

The condition of the grinding wheel surface affects the results of grinding. It was shown how the sharpness of the wheel alters the rate of wear during grinding using 2 different in-feeds. It is not true that a sharper wheel always cuts well. A wheel resharpened for 30s and longer wears more and removes less material from the work piece due to grain breakage. The least sharp wheel also blunts in a shorter time.

During the process of dressing some extra material is removed from the grinding wheel. Depending on the type of dressing method and the grinding wheel the material removed can vary. Sometimes the material removed during dressing can even be greater than the material removed from the grinding wheel during grinding. If the wheel is dressed sufficiently, it can be used for a longer grinding period. It is important to know the optimal time because the material removed from the grinding wheel during a longer dressing time can be 7 times more than the removed material if an optimum range of dressing time was used.

The optimum range of dressing time can be selected by using different dressing methods, measuring the material removed from the wheel after dressing and measuring the material removed from the wheel and the work piece after grinding. According to these experiments (as in Section 5.4) the optimum range of dressing time lies where the maximum MRR, minimum VWWR (rate of volumetric material removed from the grinding wheel after grinding) and minimum VWW (volumetric material removed from the grinding wheel after dressing) are achieved. According to the results of this research and other published data [5, 6, 8, 15, 16, 44] this value is normally 10-30s. In Section 4.5 the same value was obtained based on the minimum grinding forces and maximum MRR.

There are also useful published data about grinding wheel wear and G-ratio [4-6, 8, 9, 11, 13-16, 22, 41, 51] as discussed in the literature. However, due to the different contexts such as different grinding methods, grinding operations using constant feed or constant load, and different grinding parameters including grinding wheel type some results of these published materials could not be compared to a part of the results of this chapter.

CHAPTER 6 GRINDING AND EDGE QUALITY

6.1. Introduction

As discussed in Section 1.8 edge quality of a PCD work piece is very important. Since the PCD is used in tool making to machine other materials, it should have a satisfactory smooth edge with minimal chipping. In previous chapters factors affecting maximum MRR and minimum VWW and the relations between the grinding forces, in-feed, MRR, VWWR, dressing condition and grinding wheel condition were considered. In this chapter the parameters affecting the edge quality and the defects generated during the grinding process are discussed since not only is it important to achieve the maximum MRR and minimum VWWR but also high quality of the ground PCD work piece is required. The quality parameters used in this research consist of chipping, break outs and surface flatness.

Two diamond grinding wheels and two significantly different grinding machines were used in this chapter. The grinding machines were previously specified in Section 2.2. In this chapter the original grinding machine used in the experiments of the previous 2 chapters will be referred to as Machine 1 and the second grinding machine used in the experiments of Section 6.5 will be referred to as Machine 2 (as mentioned in Section 2.2). The aim of grinding with Machine 2 is to study the effect of rigidity of the system and different spindle speeds on the quality.

The details of experiments carried out are described in Section 6.2, where the settings used are defined. In Sections 6.3 and 6.4 PCD compacts are ground using Machine 1. In Section 6.3 the effect of in-feed and MRR on the edge quality is investigated. In the previous chapters the relation of in-feed, MRR and VWWR, as 3 important factors, was studied. The experiments of Section 6.3 comprise these 3 parameters. PCD blanks are ground with different in-feeds and the resultant edge quality analysed. In Section 6.4 a different grinding wheel is used and the results obtained are compared with the results of the previous grinding wheel. It will be shown how changing the grinding parameters can enhance the quality of grinding surface and work piece edge. In Section 6.5 the PCD blanks are ground using Machine 2 (introduced in Section 2.2) to

compare the results of edge quality. Finally, the outcomes of this chapter are discussed and summarised in Section 6.6.

6.2. Description of Experiments

The experiments carried out in this chapter are selected according to the results of the experiments presented in the previous 3 chapters. As shown in Figure 6.2.2, there are 2 different ways to position the PCD work piece and grind it. This difference is because the PCD section is located on the upper surface of the work piece and there is no PCD on the lower surface (as shown in Figure 1.2.1 and Figure 6.2.1). The black triangle shown in the A-A view section of Figure 6.2.2 refers to the PCD area. In part (a) of this figure since the PCD area is on top and the spindle spins clockwise this makes the diamond grains on the PCD break out and cause chipping. To avoid chipping, the work piece is turned to the other side (as shown in part (b) of Figure 6.2.2) so that the PCD area would be underneath and the clockwise spindle will not damage the edge quality. It is also possible to use the right side of the grinding wheel instead of turning the work piece. In other words, it is the peripheral velocity of the wheel that defines where and how to position the PCD work piece.

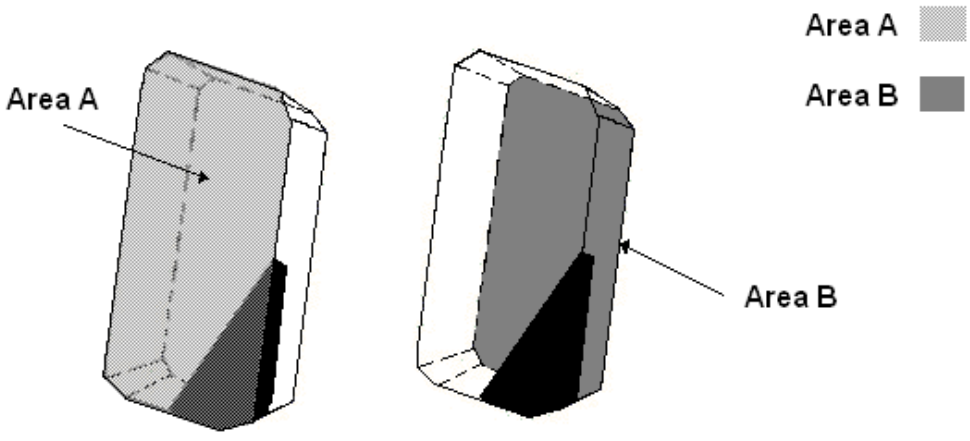

Figure 6.2.1 Upper and lower surfaces of the PCD work piece

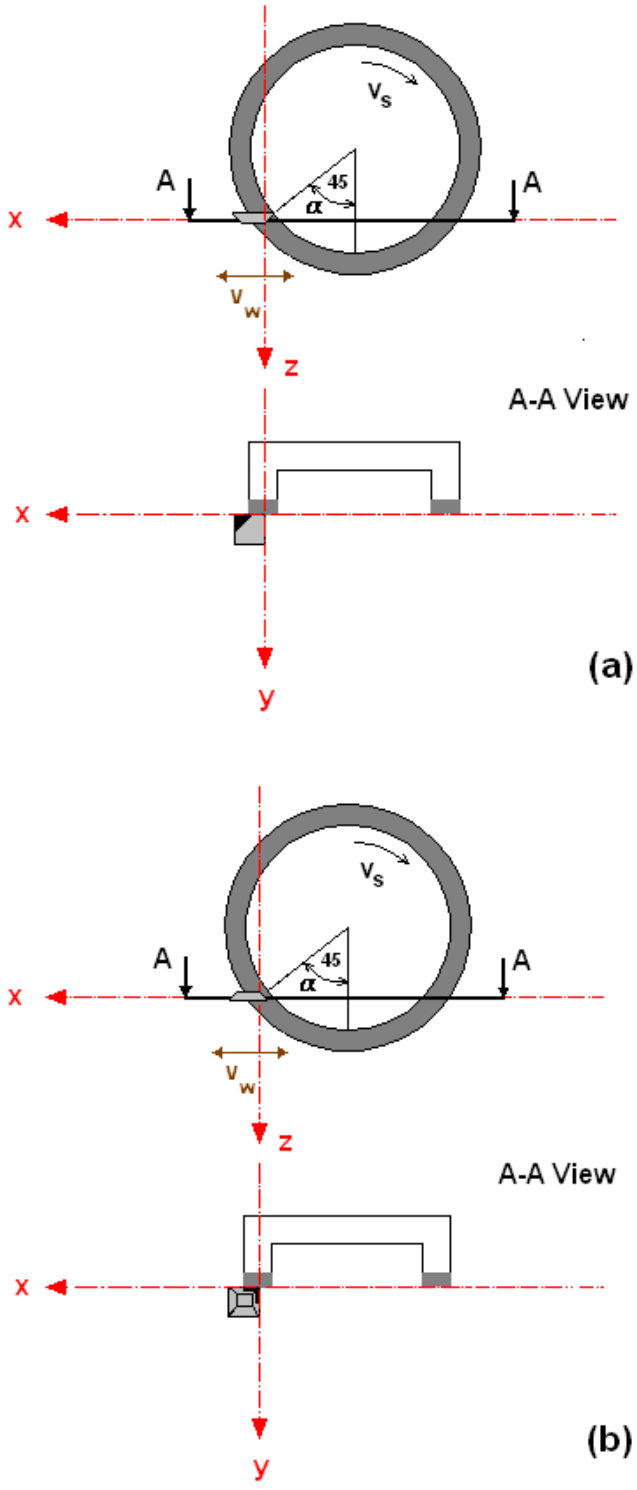

Figure 6.2.2 Two different ways of positioning the work piece (a) Area A upward (b) Area B upward (refer to Figure 6.2.1)

After grinding the PCD work piece, the blanks are ready to be analysed by a microscope. As discussed in Chapter 1 Oderbolz [41] has reported that 20x or 50x magnification is suitable enough to measure the cutting tool wear. However, since PCD is prone to graphitization at temperatures above $600^{\circ}C$, an examination of the edges at high magnifications would have helped to be more certain of the reasons of cracks or fractures during grinding. In this research, the tool wear is examined with an optical microscope with 50x magnification.

Because the chipping happens on the top surface (due to the location of PCD on that surface), it is more reasonable if the top view is captured. In other words, figures of other surfaces (using 20x-50x magnification) of the ground area will not provide useful information.

In Section 6.3 to find the relation between in-feed and material removal rate a combination of experiments of Sections 3.3, 3.5 and 5.3, including using the microscope after each single experiment to detect the edge quality produced after grinding, was used. The procedures used are given below:

1. The grinding wheel was trued once, at the beginning. A truing procedure as given in Section 3.2 was used.

2. The grinding wheel was dressed using a wet dressing stick before each experiment for about 25s.

3. A photo from the edge of the PCD insert was taken using an optical microscope with 50x magnification, prior to grinding.

4. Then, just one $10\,\mu m$ in-feed was given during grinding.

5. The traverse speed was kept constant in each experiment.

6. MRR was measured with a micrometre.

7. VWWR was measured with another micrometer.

8. The edge quality was examined with the optical microscope.

9. Steps 2-8 were repeated but with the in-feed progressively increased 10 μm at a time up to 50 μm .

This set of experiments not only provides the information about the in-feed and quality but also about the MRR, VWWR and quality. Results of these experiments are illustrated in Figure 6.3.2 to Figure 6.3.6.

In Section 6.4, a new coarser grinding wheel with bigger rim (twice the old one as shown in Section 2.2.1) is used. The new wheel has the same diameter (150mm) as the previous one so the relative speeds are the same. However, it has more abrasive area to grind PCD with. The experimental procedure is exactly the same as in Section 6.3.

In Section 6.5, 4 PCD samples were ground using Machine 2 (as described in Section 2.2) with different spindle speeds lower than the spindle speed of Machine 1, as shown in Table 6.1. A diamond grinding wheel similar to the previous ones was used.

Table 6.1 Range of spindle speed used in quality experiments

Sample	Grinding method	Spindle speed (rpm)
1	Machine 2	495
2	Machine 2	666
3	Machine 2	890
4	Machine 2	1195
5	Machine 1	2840

In the experiments carried out in this section the in-feed was given manually without oscillation. Therefore, the in-feed was not necessarily constant in these tests. After each experiment the resulting edge was examined using the optical microscope.

6.3. In-feed, MRR and Edge Quality

The grinding experiments of this section were conducted using Machine 1. Figure 6.3.1 points out that the figures of edge quality refer to the side edge of PCD as shown on the diagram.

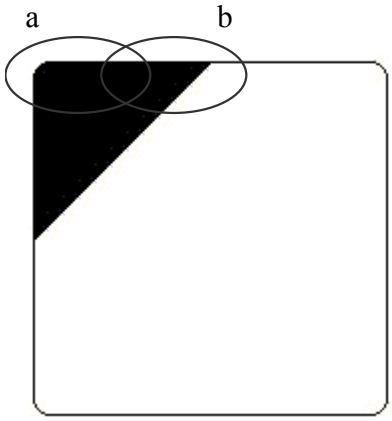

Figure 6.3.1 Typical representation of where the following photos refer to

Figure 6.3.2 to Figure 6.3.6 show the edge quality produced during grinding with different in-feeds. Photos on the left side show the work piece edge before grinding. So, by comparing both right and left pictures it can be easily explained whether the generated edge is affected by the in-feed or not. The black arrow shown in Figure 6.3.2 denotes which side of the PCD work piece was ground. The cavities on the surface of the PCD before grinding can be clearly seen. Consequently, the cracks on the edge after grinding are not necessarily produced during grinding. The black dotted circles in parts (a) and (b) are removed totally during grinding.

In other words, because of the large chipping areas in those sections (black dotted circles shown in Figure 6.3.2) the grains are not supported by the grains next to them so they can be easily detached, no matter what the in-feed is.

Furthermore, the PCD section on the work piece has a sharp corner (black dotted circle in part (b)) at the position where it meets cemented carbide. So, during grinding this sharp edge is under stress and it can be affected and broken during grinding.

The blue dashed circle in part (a) of Figure 6.3.2 shows another sharp edge of PCD on the left side of the PCD work piece. However, the corresponding picture on the right side of part (a) shows that after grinding the corner has not been damaged and in fact, it is still sharp.

These inspections show that small cracks have been removed to some extent and the new edge is not worse than before.

Additional experiments using different samples with different primary surfaces prior to grinding have been conducted. This allows the effect of settings and the capabilities of the system used to be further investigated.

Before grinding

After grinding

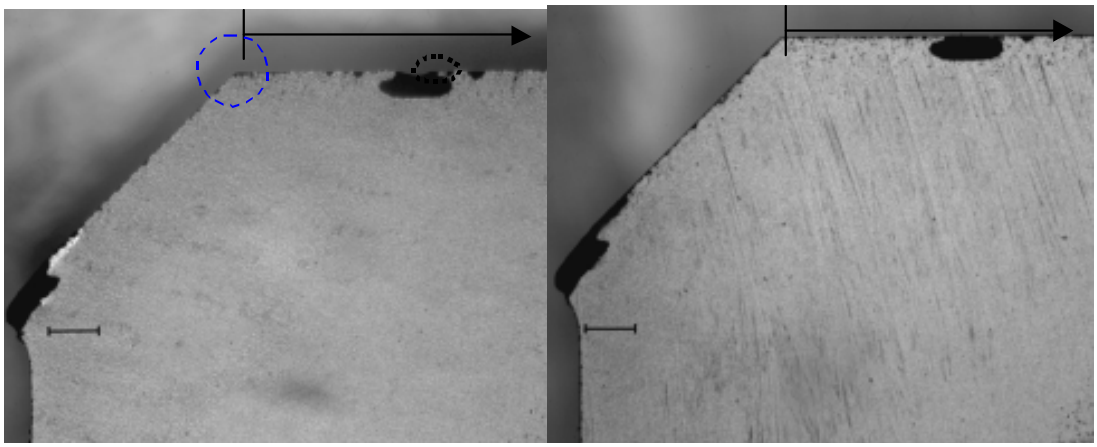

(a) Part (a) as shown in Figure 6.3.1

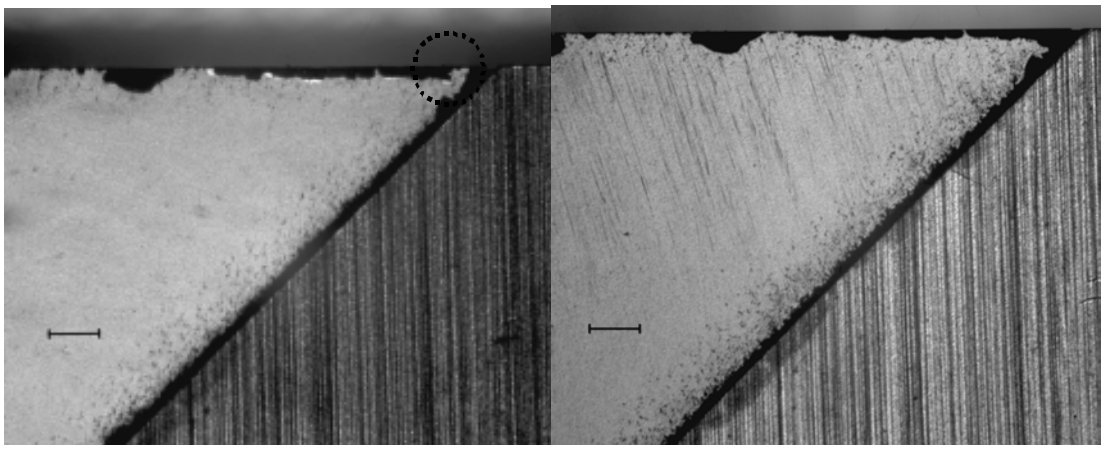

(b) Part (b) as shown in Figure 6.3.1

Figure 6.3.2 10 µm in-feed, scale 380 µm

Figure 6.3.3 shows the result of grinding with 20 µm in-feed. The sample used in the related experiment had lots of cracks and fractures on its edge. To remove the uneven surface of PCD, several grinding experiments need to be done. Since the surface of the work piece was already damaged no further fractures would have been generated as a result of grinding. However, by comparing the results, before and after grinding, it can be seen that the material was removed because the depth of cracks has decreased.

As Tso and Liu [24] stated with lower in-feed a finer PCD surface can be obtained. But, considering Figure 6.3.4 to Figure 6.3.6, where 30, 40 and 50 μm in-feed were given respectively, it can be concluded that all the in-feeds used have not caused any damage to the surface and so higher in-feeds do not necessarily have an adverse effect on the ground edge. In other words, from the quality point of view the range of 10-50 μm in-feed can be used without restrictions. However, according to the results of Section 3.5 and 5.3 the desired setting can be selected with respect to the optimum range of MRR and reasonable range of VWWR.

Note that the unusual surface of PCD before grinding (shown in Figure 6.3.6) is because of minor surface oily residues on the work piece.

Before grinding

After grinding

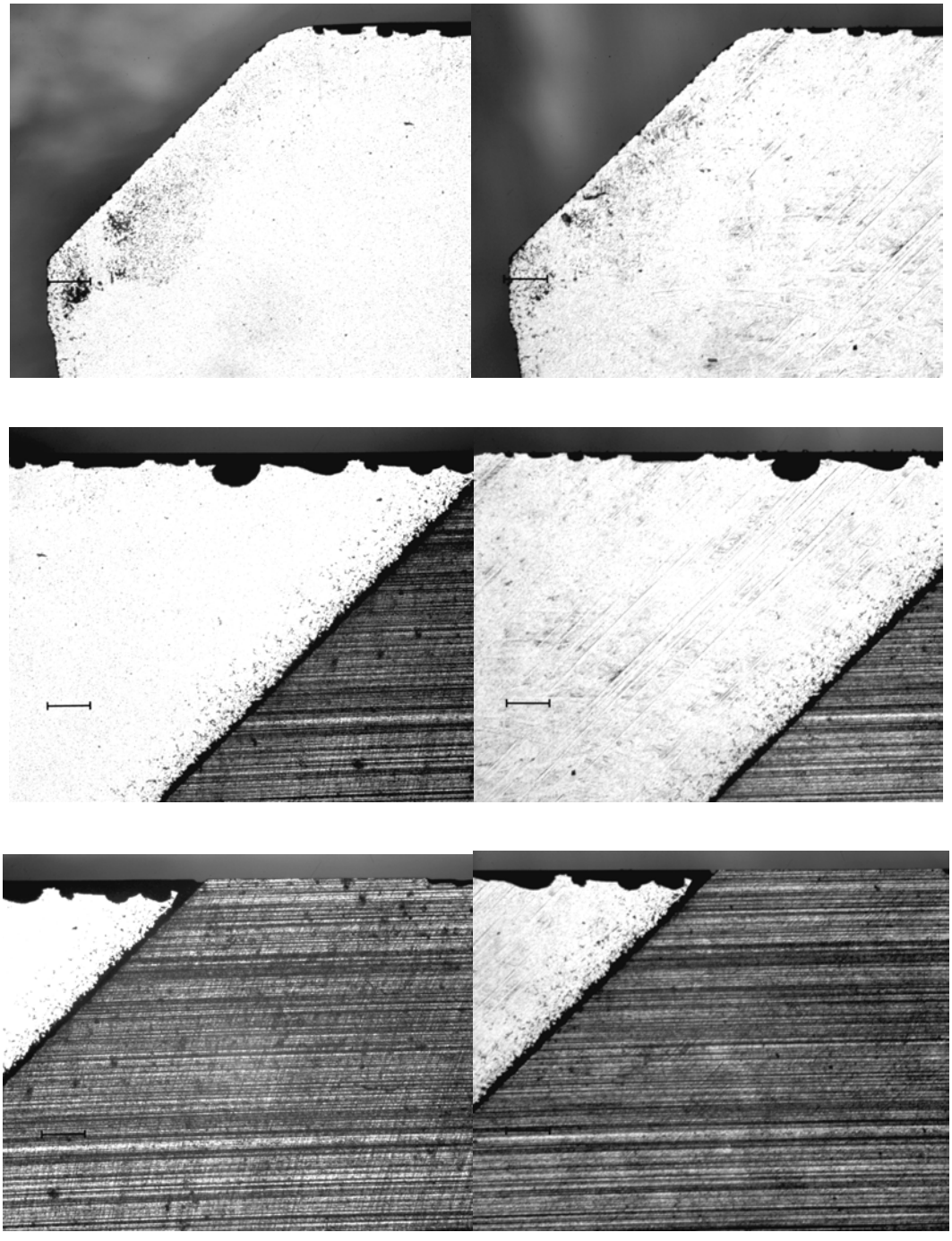

Figure 6.3.3 20 μm in-feed, scale 380 μm

Before grinding

After grinding

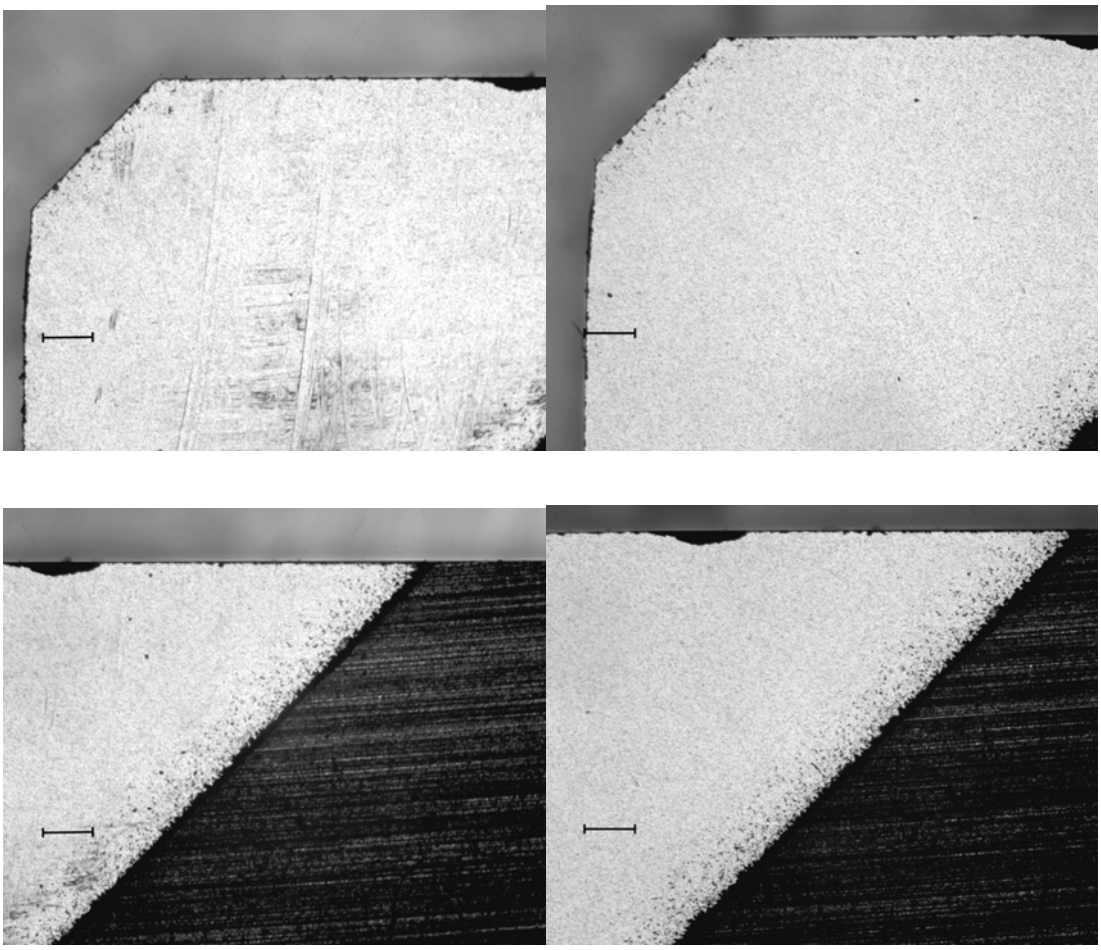

Figure 6.3.4 30 µm in-feed, scale 380 µm

Before grinding

After grinding

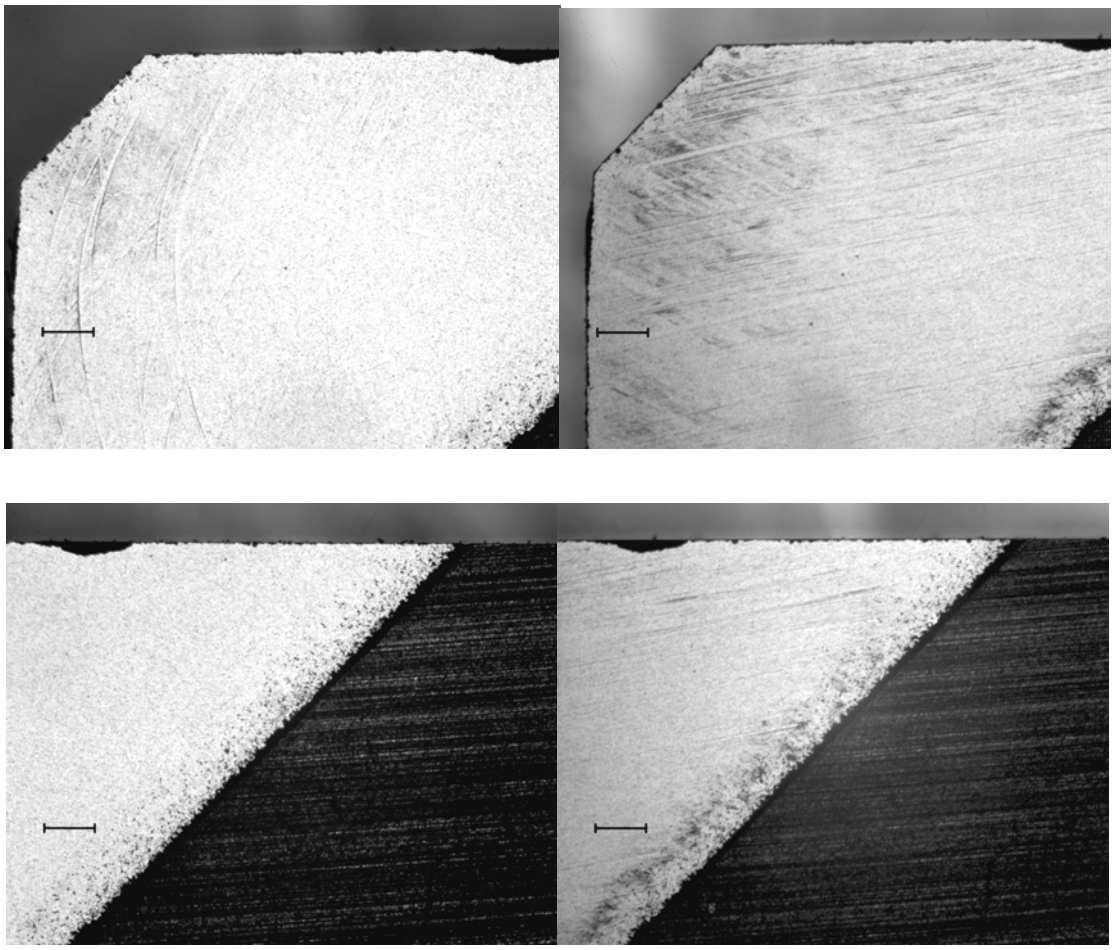

Figure 6.3.5 40 µm in-feed, scale 380 µm

Before grinding

After grinding

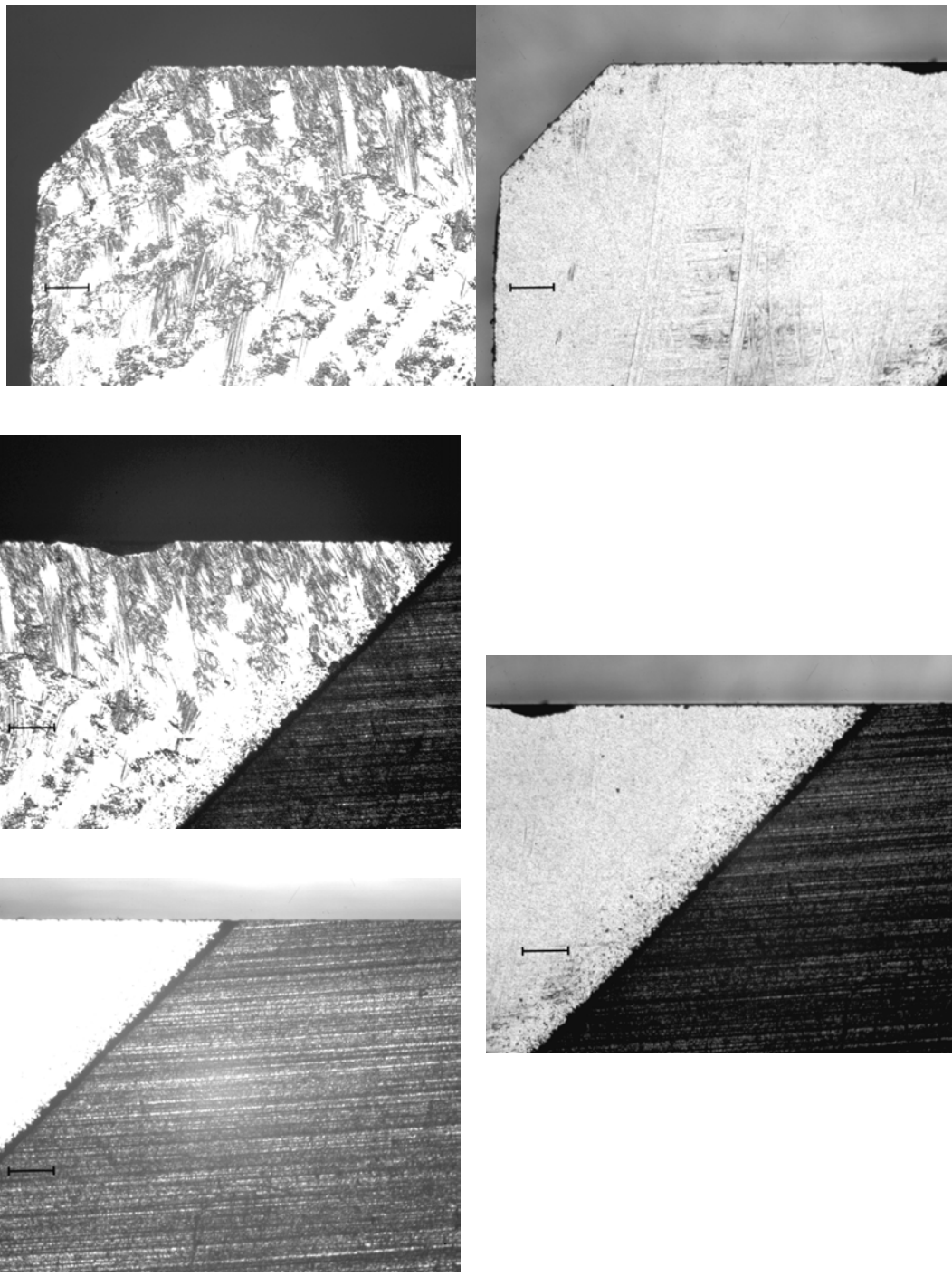

Figure 6.3.6 50 µm in-feed, scale 380 µm

6.4. Grinding Wheel Type and Quality

Figure 6.4.1 to Figure 6.4.5 show the edge quality of PCD work piece ground with a new diamond grinding wheel. Black dotted ovals drawn in these figures refer to the fractures before and after grinding. It can be seen that the cracks have been removed to a large extent and no significant chipping has occurred on the other ground areas. The sharp corners have remained sharp and the material has been removed successfully, no matter what in-feed was used. Although the grinding wheel used in this section is a coarser grinding wheel the quality of the ground edge is completely satisfactory. One of the reasons can be due to the small range of in-feed used in these experiments.

Before grinding After grinding

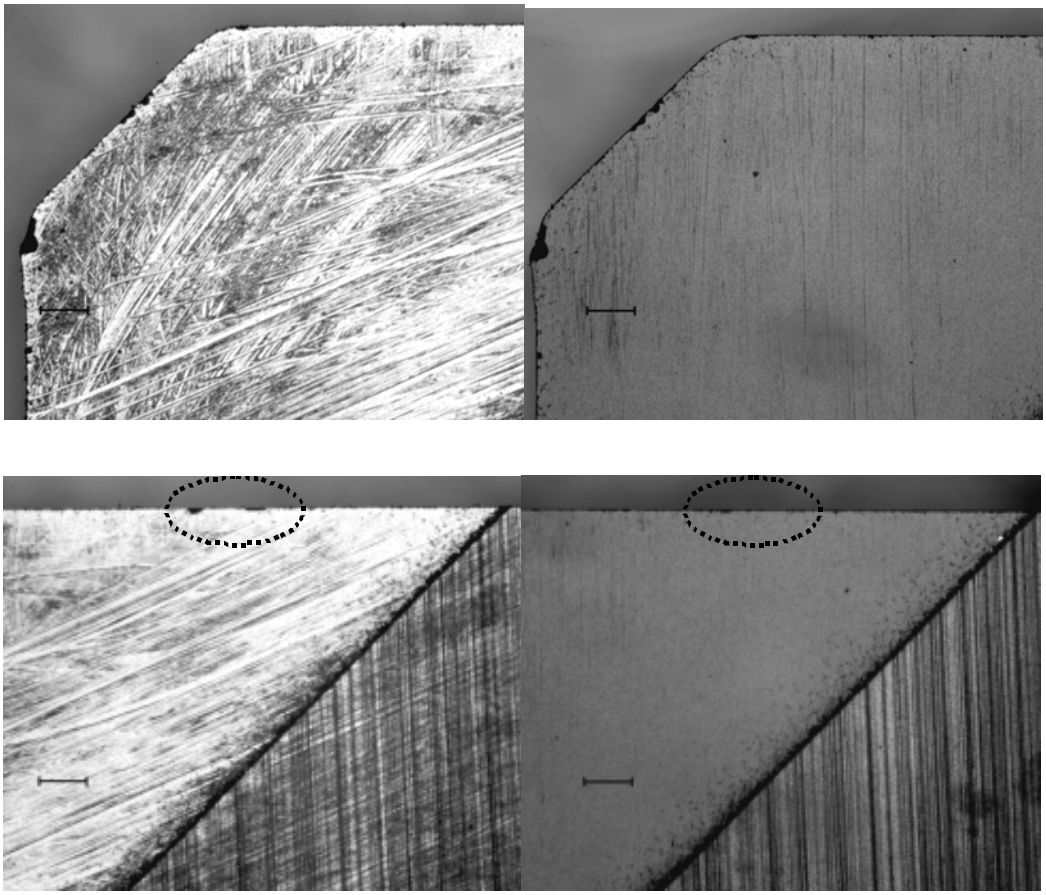

Figure 6.4.1 10 µm in-feed, scale 380 µm

Before grinding

After grinding

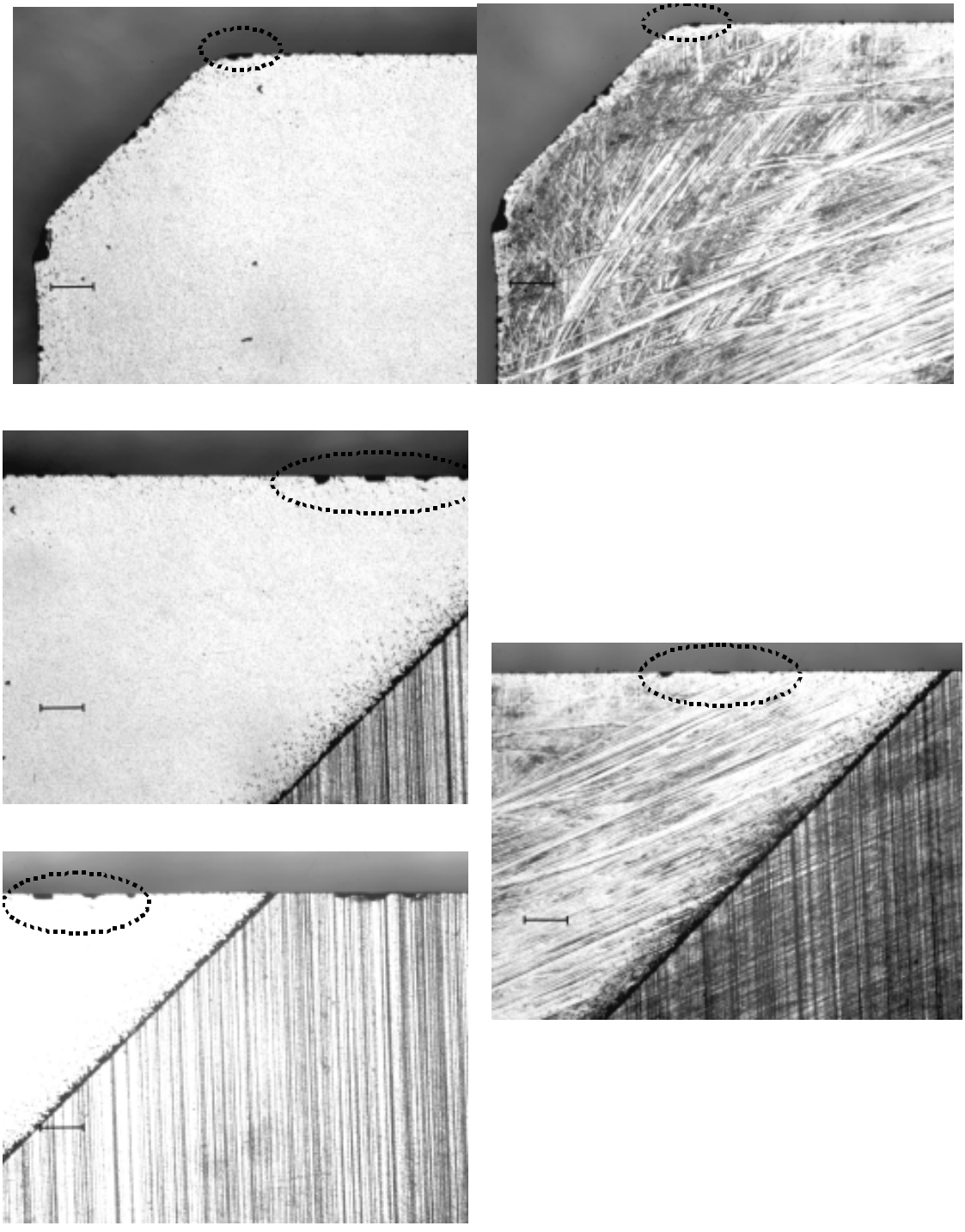

Figure 6.4.2 20 µm in-feed, scale 380 µm

Before grinding

After grinding

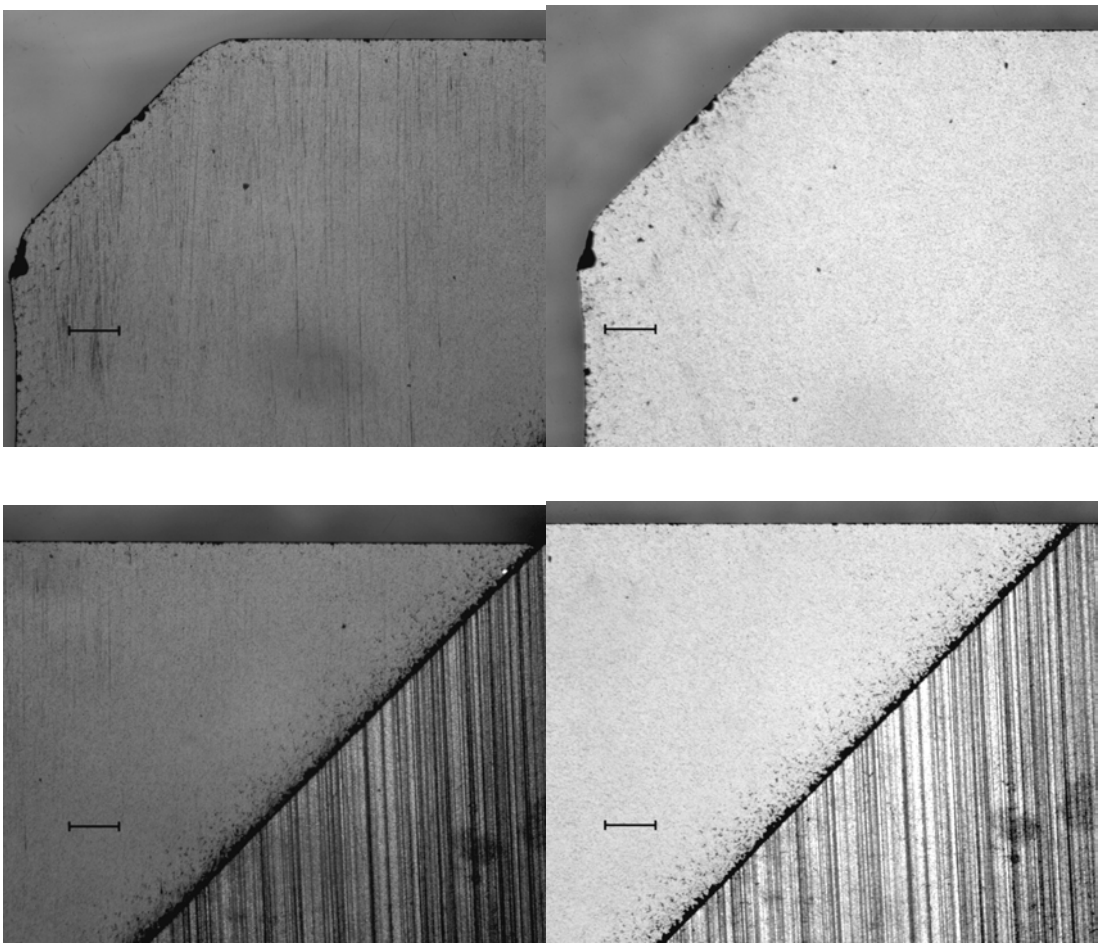

Figure 6.4.3 30 μm in-feed, scale 380 μm

Before grinding

After grinding

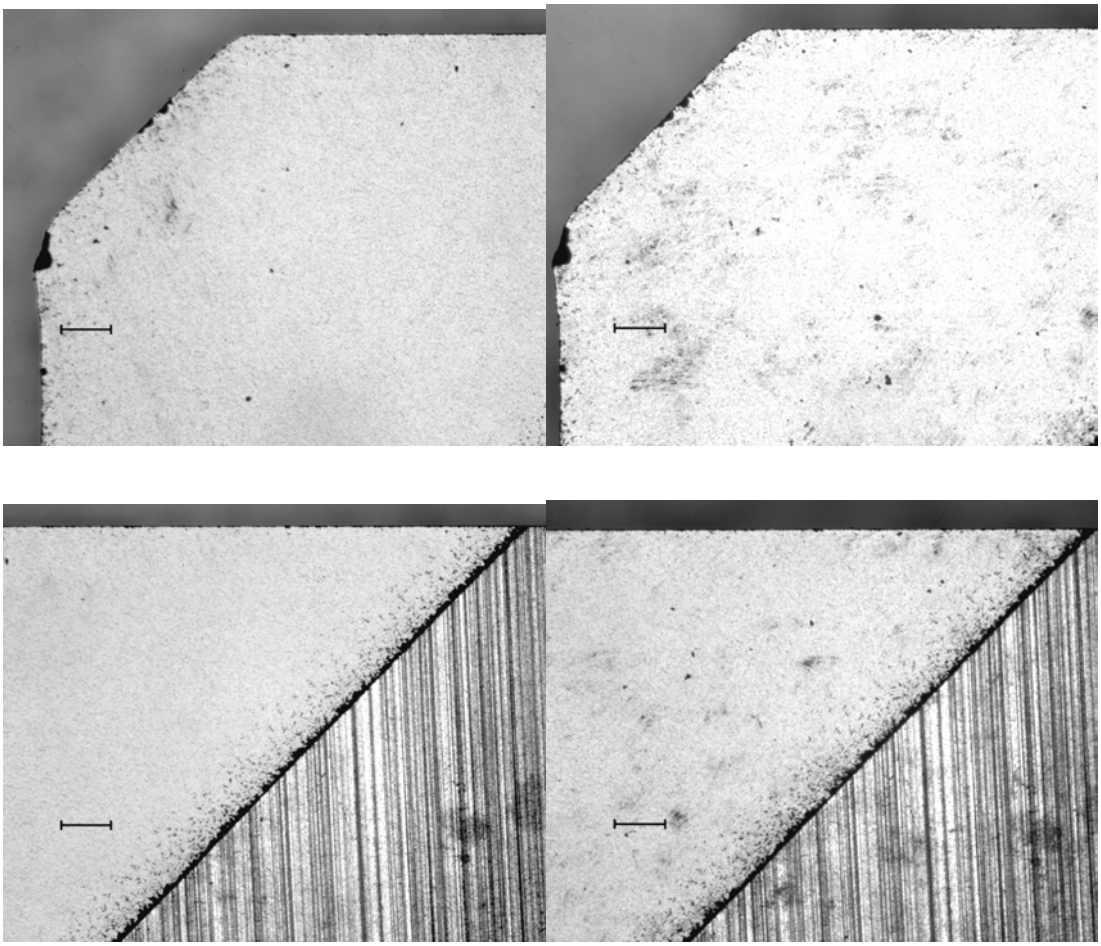

Figure 6.4.4 40 μm in-feed, scale 380 μm

Before grinding

After grinding

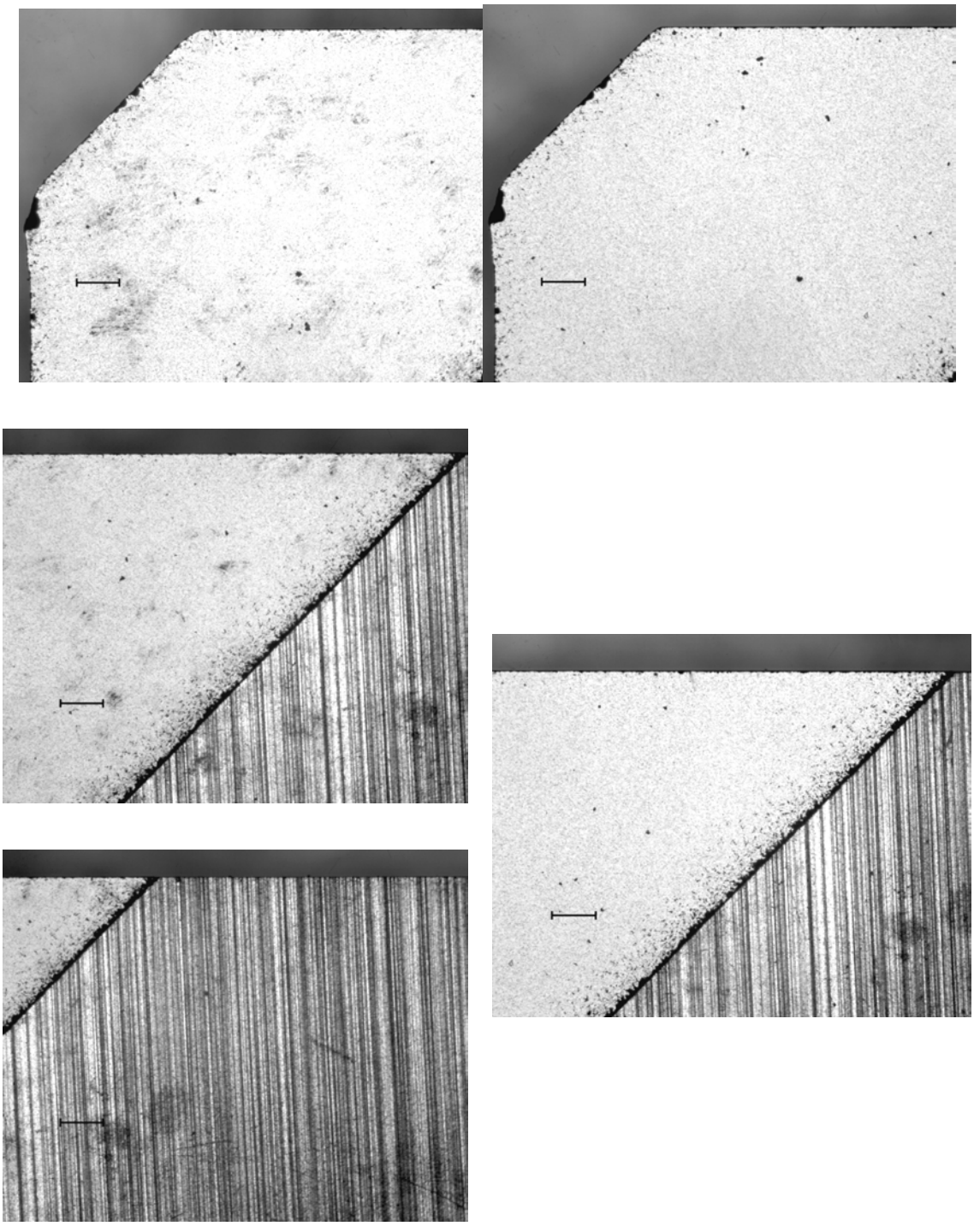

Figure 6.4.5 50 μm in-feed, scale 380 μm

Many authors [8, 9, 11, 13, 19, 24] state that finer diamond wheels produce a better PCD surface and that is why they are mostly used for finishing purposes. To confirm

this a higher microscope magnification can be used. Furthermore, it is clear that "the machining operation for which the tool will be used determines which grinding wheel will be the most economical" [11, 13].

6.5. Grinding Using Machine 1 and Machine 2

Figure 6.5.1 shows edge quality of 4 PCD blanks ground using Machine 2 (described in Sections 2.2 and 6.1). Both figures in each row correspond to the same state of grinding. In other words, both figures present the PCD work piece after grinding.

The in-feeds used in these experiments are significantly higher than the in-feeds given in Machine 1, because Machine 2 is much more rigid. The distinct depth of cut near the dashed vertical line shows this. The vertical distance between the un-ground edge and ground edge is the given in-feed. An example is shown in part (b) of Figure 6.5.1.

As described in Sections 2.2 and 6.2 the spindle speeds used are considerably lower than the speed of Machine 1. Nevertheless, no significant relation between the spindle and edge quality emerges from these figures. A similar conclusion was drawn from the experiments done by Herzig [13] for a range of 8-65m/s wheel speeds, where only small differences were ascertained though according to his research the best results were achieved at 22-28m/s. On the other hand, according to Tso et al [24], with lower wheel velocity a finer PCD surface can be obtained. In this research the spindle speeds used in Machine 1 and Machine 2 ranged from 495rpm to 2840rpm corresponding to 4-22m/s wheel speed. So, according to Herzig [13] Machine 1 generates a better edge quality because its 22m/s wheel speed lies in the optimum range.

The black dotted ovals (shown in Figure 6.5.1) indicate the cracks produced as a result of grinding. Since the given in-feeds have been high, these cracks are definitely generated during grinding. But the cavities on the surface of Sample #3 existed prior to grinding (as shown in part (c) of Figure 6.5.1).

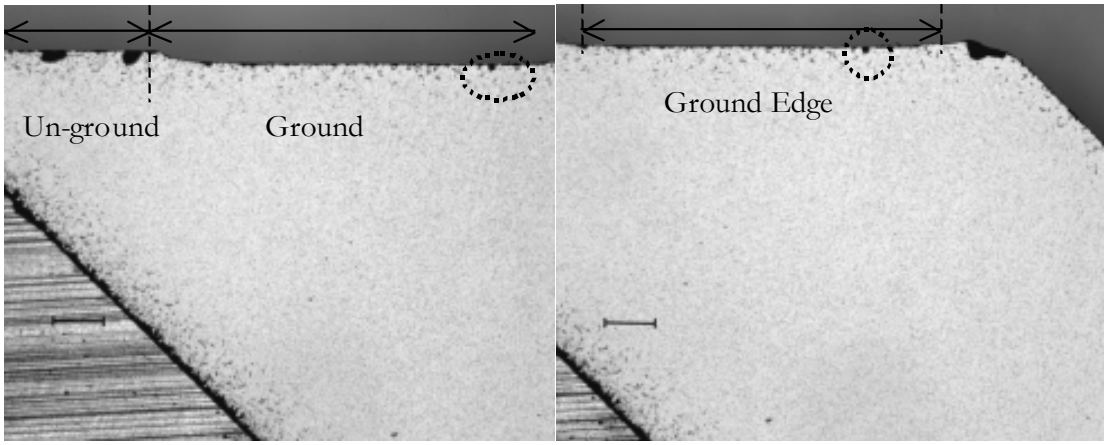

a) Sample #1 ground at 495rpm

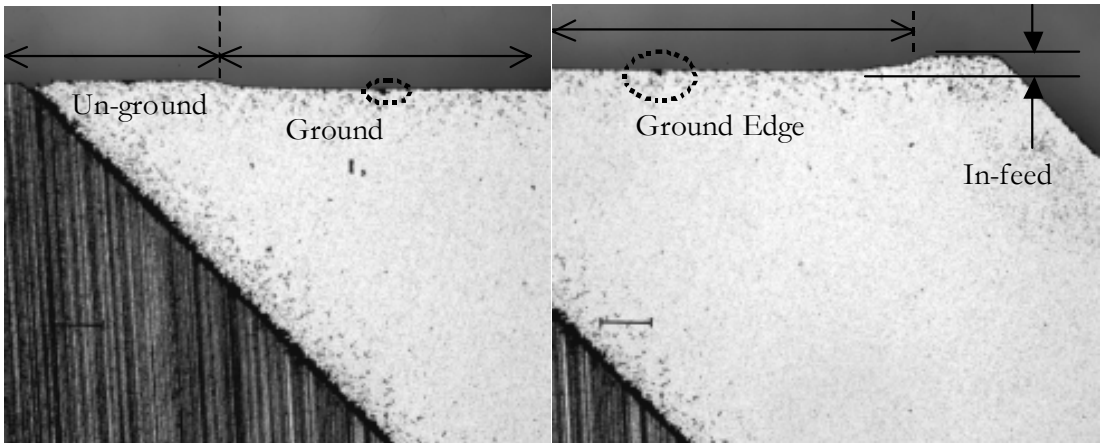

b) Sample #2 ground at 666rpm

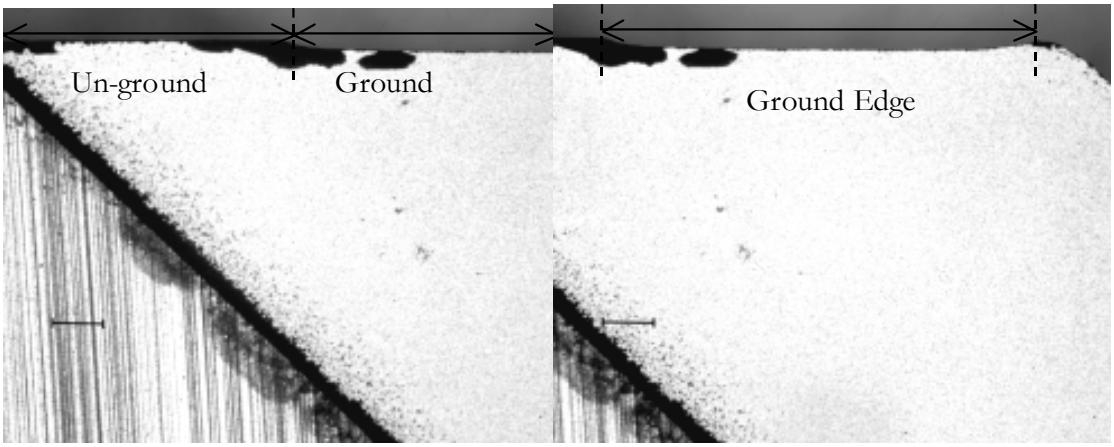

c) Sample #3 ground at 890rpm

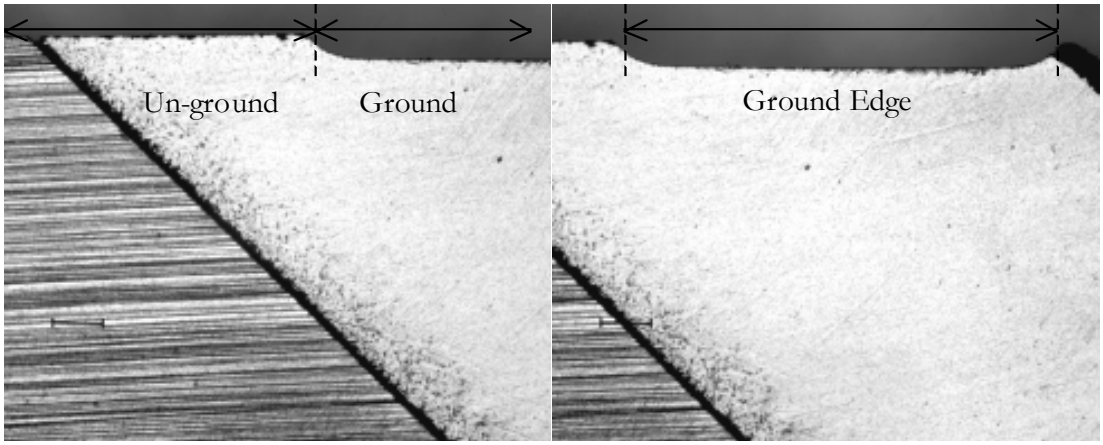

d) Sample #4 ground at 1195rpm

Figure 6.5.1 Photo of edge quality using Machine 2, scale 380 μm

Comparing the results of Section 6.5 with Sections 6.3 and 6.4 it can be seen that Machine 1, though not designed for PCD grinding, is sufficiently rigid to grind PCD successfully.

6.6. Conclusions

In this chapter factors affecting edge quality were analysed. Several experiments were carried out with varying grinding parameters: in-feed (including MRR), grinding wheel, grinding method and spindle speed. The aim is to reduce the irregularities at the edges of PCD inserts and improve the edge uniformity on the work piece. The cracks on the tool edge not only shorten the insert life but also influence the chip flow, which will lower the cutting quality.

The ground edges were studied using an optical microscope with 50x magnification. A range of 10-50 μm in-feed was used. The selected range was based on the results obtained in the previous chapters, which defined the limitations of the available system. It had been concluded that there is no need to use higher in-feeds. However, in order to have enough grain engagement it is important to use the correct in-feed. Otherwise, the grinding may result in chipping of the PCD and an unsatisfactory edge.

It was observed that during grinding unsupported parts of PCD grains could be easily broken and removed. In fact the initial surface of PCD affects the edge quality produced after grinding.

It was also shown that within the range of 10-50 μm in-feed the Conventional Grinding Machine 1, designed for non PCD uses, is stable enough dynamically to attain the optimal material removal rate.

A different grinding wheel was also used in order to study and compare the edge quality generated during grinding with a different wheel. The same range of in-feed was used with the new wheel. The edge and surface integrity remained almost free of defects during grinding, even when using the new coarser grinding wheel.

The PCD work piece was also ground on a different machine referred to as Machine 2 using different wheel speeds: 495, 666, 890 and 1195rpm equivalent to 4, 5, 7 and 9m/s peripheral speeds, respectively. One of the aims of this experiment was to compare the results of PCD grinding with two machines of different stability and rigidity. The other aim was to study the effect of wheel speed on the edge quality. No significant relation between the spindle speed and edge quality emerged from the related experiments, which covered the wheel speeds of 4-9m/s.

It was shown that the machine built for grinding of cemented carbide could achieve satisfactory quality with acceptable feed rates.

To achieve a chip-free edge and satisfy other requirements it is suggested that only a small range of in-feeds be used. If this is done, a conventional grinding machine, with about 3000rpm spindle speed, is capable of grinding PCD producing a high standard edge. However, it is stressed that the process quality also depends to some extent on the operator's experience.

CHAPTER 7 CONCLUSIONS AND RECOMMENDATIONS FOR FUTURE RESEARCH

7.1. Conclusions

This thesis has studied the grinding of polycrystalline diamond using two grinding machines with different specifications and different diamond grinding wheels. The grinding experiments were carried out using constant feed. Both metal and vitrified bond diamond grinding wheels were used in the research presented in this thesis. The results of this thesis and the experimental procedures can be extended to other research in PCD grinding area.

In Chapter 1 a literature review on several aspects of PCD grinding was carried out, the importance and need for this research was established, and an outline of the thesis was given.

In Chapter 2 the grinding systems and the other experimental equipment used in this thesis were described. The normal and tangential grinding forces produced during grinding were shown and calculated based on the force data obtained using the force sensors thus allowing the grinding forces to be mathematically analysed.

In Chapter 3 the relation between the grinding forces and in-feed was studied. It was shown that the trends of normal and tangential forces were the same. The forces were analysed and it was found that the maximum grinding forces vary with the in-feed, contact zone, material removal rate and the oscillation rate. The behaviour of the normal force was shown as the grinding wheel wears out. The relation between the in-feed and the material removal rate was extracted. Then, the range of in-feed was optimized with respect to the lower range of normal force and higher range of material removal rate. To find the grinding coefficient and its relationship with in-feed the relation between the normal and tangential forces was studied. There was a comparison between cemented carbide and PCD grinding. Furthermore, different ways of giving in-feed were investigated and it was found that smaller steps of in-feed produce lower grinding forces than the forces produced by applying the whole in-feed at once. The tested range of oscillation rate showed that those oscillations do not

significantly affect the grinding forces. The experiments and findings from Chapter 3 were used in Chapter 4 , Chapter 5 and Chapter 6 .

In Chapter 4 the condition of the grinding wheel surface before grinding and how it affects the grinding process were studied. The grinding wheel in this thesis was dressed based on the findings of this chapter. It was shown that material removal rate MRR, grinding forces F_N and F_T and grinding coefficient μ can be used as a practical indicator of the roughness of the grinding wheel and also to select the optimum dressing time. In Section 4.3 it was shown that after truing and dressing the grinding forces drop considerably. No significant change in the grinding forces was observed for high in-feeds. The grinding wheel condition has no effect on the ratio of tangential and normal forces. It was also shown how the grinding coefficient can be used as a control parameter of the wheel sharpness. It was found in most of the experiments that when the grinding wheel is sharp the tangential force, or in other words the cutting force, is greater than the normal force. So, more material is removed in a shorter time.

According to the published data [4-6, 22] and the results of this chapter, it was concluded that in most of the PCD grinding experiments the grinding wheel needs to be dressed after every 30s of grinding. It was explained in Section 4.4 that as the wheel wears out the material removal rate decreases and the grinding forces increase.

In Chapter 4 the grinding wheel was dressed for different durations. Depending on the given in-feed, the optimum duration was selected based on the maximum MRR and the minimum grinding forces achieved. It was found that for a certain in-feed, the sharper wheel does not necessarily remove more material. Grinding breaks the exposed grains of a wheel dressed for a long time more quickly.

In Chapter 5 the effect of grinding parameters on the wheel wear and vice versa was studied. These grinding parameters include the condition of the grinding wheel surface, in-feed and the work piece material type. The aim of this chapter was to increase the wheel life and the material removal rate by optimizing these parameters. In this chapter the results of G-ratio were presented for the first time. The rate of volumetric wheel wear in different settings was measured and analysed. It was concluded that the G-ratio, MRR and VWWR should all be considered and not be taken in isolation from

each other. The optimum range of in-feed can also be estimated based on the results of material removed from the work piece and wheel other than the results of the expensive force sensor obtained in Chapter 3 . It was found that if the given in-feed is divided into small steps the rate of material removed from the wheel during grinding is noticeably lower.

According to Section 4.4 when the diamond grinding wheel wears out, material removal from the work piece stops. It was found in Section 5.3 that no significant material is removed from the surface of an already blunt wheel. In other words, when the wheel gets blunt the material is neither removed from the work piece nor from the wheel but will result in high grinding forces.

Because of the erratic fluctuations of the G-ratio ("measurement for wheel life" [51]) relying on the changes in G-ratio is not always an effective way of finding the exact time when the grinding wheel needs to be dressed. In these cases it is suggested that MRR be used as a practical indicator of dressing time as found in Section 4.4. Based on the results of Chapter 5 and the published data [5, 6, 8, 44] normally the grinding wheel needs to be dressed for 10-30s.

It was also discovered that the sharpness of the wheel alters the rate of wear during grinding. Depending on the grain protrusion of the wheel, dressed wheels cut differently. In Section 5.4 it was shown that during the dressing process some material is removed from the wheel. So, it is essential to choose a dressing method adapted to the PCD grinding application. Combining the results of Chapter 4 and Chapter 5 the optimum dressing duration is selected depending on the material removal rate, grinding forces, dressing method, material removed from the wheel after dressing and the rate of material removed from the wheel after grinding.

Chapter 6 is dedicated to studying the edge quality of the PCD work piece. Two different grinding wheels and two different grinding machines with different stiffness, power ratings, degrees of freedom, work piece holder systems and spindle speeds were used. The relations between the edge quality and the grinding parameters in-feed (including MRR), grinding wheel, grinding method and spindle speeds were

established. It was found that a conventional grinding machine, designed for non-PCD uses, could be dynamically stable enough to attain the optimal material removal rate.

Although many authors [8, 9, 11, 13, 19, 24] have found that a finer diamond grinding wheel produces a better PCD surface, in this research the edge quality of the PCD compact ground using two different wheels did not show such a difference. It was found that no significant relation between the edge quality and spindle speed exists. However, Herzig [13] has stated that with 22m/s wheel speed (2840rpm) a better edge quality is generated. It was also suggested to use a small range of in-feeds to achieve a chip-free edge. In addition to all these parameters the quality also depends to some extent on the operator's experience. The results of the conducted experiments showed that inadequate grinding parameters can reduce the life cycle of the grinding wheel and downgrade the edge quality.

Detailed analysis of cost is beyond the scope of this thesis. However, many of the topics in this investigation will also provide useful information to users wishing to make cost tradeoffs.

7.2. Future Work

There are various areas of work related to this thesis that could further improve the PCD grinding process developed in this research. These include:

The edge quality of the work piece can be more accurately evaluated by measuring the ground face roughness. The edge roughness can be measured using different methods such as with a profilometer. A profilometer can measure surface roughness, image topography in 3D non-destructively (non-contact) as well as do statistical computation of surface data. To increase the PCD tool life the cutting edge of the PCD work piece has to have a satisfactory quality. In order to achieve less chippings and break outs the experimental investigations of PCD grinding need to be done more precisely including using more accurate equipments and higher magnifications to provide detailed information on PCD cutting edge.

In this thesis two diamond cup wheels were used. This study could be extended to include different types of grinding wheel to grind various PCD compacts in a different

way. It would also be useful to the Industry for the PCD grinding methods and techniques used in this thesis to be extended to different PCD grits applications.

The truing procedure can be studied more extensively. The truing process in this thesis was based on existing industrial practices. More experiments can be carried out using different truing and grinding settings to further explore the truing parameters affecting the PCD grinding process.

The measured forces were all the forces produced during grinding. To find more information about the truing process the truing forces can also be measured using the force sensor. Then, more tests can be done to measure "the truing/dressing intensity" [63] and the effect of truing and dressing on the grinding performance of the wheel can be more comprehensively examined. The truing/dressing intensity is defined as the resultant force acting on an individual grain. Truing/dressing intensity is considered a good measure to evaluate the truing/dressing efficiency [63].

The force estimation techniques and force control procedures presented by Simpson [35] can be applied to this research to assist in monitoring the rate of wheel wear. This would assist in the development of a grinding model, which accounts for wheel wear. This would also allow the expensive force sensor to be replaced, in a production machine, by force estimation techniques. With force control schemes PCD blanks can be ground with constant normal force as recommended by many authors [4-14] instead of at constant feed rate. The truing forces could also potentially be estimated using similar grinding force estimation procedures and also based on the motor power and spindle speeds of both the grinding wheel and the truing wheel.

Since a scanning electron microscope (SEM) provides more detailed and precise information the wear mechanism and edge quality can be further analysed using a SEM in addition to the optical microscope.

All the results found in this thesis are only valid for the range of settings used in the experiments. Using other grinding methods a wider range of settings could be used to extend the application of the conclusions drawn here. Research can also be carried out to apply many of the techniques used here to constant force grinding.

Detailed analysis of cost was beyond the scope of this thesis. Research can be done to evaluate cost tradeoffs including costs in cycle time, wheel costs, costs of the PCD compacts, truing costs, dressing costs, etc.

In this research one axis of the grinding wheel was moved at a time. Extending the research to cover multiple axis grinding would provide a more comprehensive coverage of the characteristics of PCD grinding.

BIBLIOGRAPHY

[1] Tonshoff, H. K., Peters, J., Inasaki, I., and Paul, T., "Modelling and simulation of grinding processes," *Cirp Annals*, vol. 41, pp. 677-688, 1992.

[2] Fernandes, M., "Intelligent automated drilling and reaming of carbon composites," Thesis in School of Electrical, Computer and Telecommunications Engineering at University of Wollongong, 2005.

[3] Prasad, K. V. S., "Real Time Control of Polycrystalline Diamond Grinding," Thesis in Faculty of Engineering at University of Wollongong, 2004.

[4] Werner, P. G. and Kenter, I. M., "Work material removal and wheel wear mechanisms in grinding of polycrystalline diamond compacts," presented at *Intersociety Symposium on Machining of Advanced Ceramic Materials and Components*, Westerville, Ohio, 1987.

[5] Werner, P. G. and Kenter, I. M., "Grinding of Polycrystalline Diamond: Influence of PCD Type and Contact Forces," presented at *Intersociety Symposium on Machining of Advanced Ceramic Materials and Components*, Illinoise, 1988.

[6] Werner, P. G. and Kenter, M., "Grindability of PCD," *Industrial Diamond Review*, vol. 49, pp. 15-19, 1989.

[7] Fernandes, M., "PCD Grinding," Report at Engineering Faculty of University of Wollongong, February, 2004.

[8] Kenter, M., "Effect of process parameters when grinding PCD-3," *Industrial Diamond Review*, vol. 53, pp. 313-318, 1992.

[9] Liu, Y. and Tso, P., "The optimal diamond wheels for grinding diamond tools," *International Journal of Advanced Manufacturing*, vol. 22, pp. 396-400, 2003.

[10] Cook, M. W., "Wear-resisting properties and application examples of PCD," *Industrial Diamond Review*, vol. 56, pp. 107-111, 1996.

[11] Anonymous, "Advancing the art of PCD tool grinding," *Manufacturing Engineering*, vol. 104, pp. 41-42, 1990.

[12] Wyss, R. and Pollak, E., "Machining concept for PCD tools," *Industrial Diamond Review*, vol. 51, pp. 280-283, 1991.

[13] Herzig, P., "Grinding polycrystalline diamond tools," *Industrial Diamond Review*, vol. 42, pp. 41-42, 1982.

[14] Wälchli, H., "A new machine for grinding polycrystalline diamond tools," *Industrial Diamond Review*, vol. 40, pp. 170-172, 1980.

[15] Kenter, I. M., "Effect of process parameters on material removal when grinding PCD-1," *Industrial Diamond Review*, vol. 52, pp. 29-33, 1992.

[16] Kenter, I. M., "Effect of process parameters on material removal when grinding PCD-2," *Industrial Diamond Review*, vol. 52, pp. 75-80, 1992.

[17] Savington, D., "Maximizing the grinding process," *Technical Paper - Society of Manufacturing Engineers*, pp. 1-14, 2002.

[18] Fath, J. and Wagner, K.-W., "All-round machine for EDM and grinding," *Industrial Diamond Review*, vol. 63, pp. 42-43, 2003.

[19] Cassidy, R., Marinescu, I. D., and Coman, R., "Production grinding of PCD," *Abrasives*, pp. 13-15, 2001.

[20] Cassidy, R., "PCD grinding optimization," presented at *6th InterAmerican Conference on Engineering and Technology Education (INTERTECH)*, Cincinnati, OH, 2000.

[21] Halprin, C., "Grinding PCD and CBN tools," *Tooling & Production*, vol. 64, pp. 53-54, 1998.

[22] Shimaoka, H., Tomimori, H., and Tawakita, T., "A new machine and wheel system for grinding sintered diamond tools," *Industrial Diamond Review*, vol. 42, pp. 155-160, 1982.

[23] Bex, P. A. and Shafto, G. R., "The influence of temperature and heating time on PCD," *Industrial Diamond Review*, vol. 44, pp. 128-132, 1984.

[24] Tso, P. and Liu, Y. G., "Study on PCD machining," *International Journal of Machine Tools & Manufacture*, vol. 42, pp. 331-334, 2002.

[25] Silveri, P., "Shaping PCD tools by rotary EDM," *Industrial Diamond Review*, vol. 46, pp. 108-109, 1986.

[26] Anonymous, "Two-in-one machine erodes PCD tools as well as grinds carbide and HSS tooling," *Aircraft Engineering and Aerospace Technology*, vol. 74, pp. 277-296, 2002.

[27] Bai, Q., Yao, Y., and Chen, S., "Research and development of polycrystalline diamond woodworking tools," *International Journal of Refractory Metal & Hard Materials*, vol. 20, pp. 395-400, 2002.

[28] Miller, S. F., Shih, A. J., and Qu, J., "Investigation of the spark cycle on material removal rate in wire electrical discharge machining of advanced materials," *International Journal of Machine Tools and Manufacture*, vol. 44, pp. 391-400, 2004.

[29] Spur, G., Puttrus, M., and Wunsch, U. W., "Wire EDM of PCD," *Industrial Diamond Review*, vol. 48, pp. 264-266, 1988.

[30] Wang, S. Z., Rajurkar, K. P., and Kozak, J., "Effect of grain size on wire electrical discharge machining of polycrystalline diamond," presented at *International Conference on Machining of Advanced Materials*, Gaithersburg, USA, 1993.

[31] Peak, R. C., "EDG: non-abrasive grinding," *Carbide and Tool Journal*, pp. 7-10, 1982.

[32] Anonymous, "Top-quality syndite PCD edges with EDG," *Industrial Diamond Review*, vol. 54, pp. 80-83, 1994.

[33] Jennings, M., "New laser dicing machine for PCD fabrication," *Industrial Diamond Review*, vol. 63, pp. 38-39, 2003.

[34] Harrison, P. M., Henry, M., and Brownell, M., "Laser processing of diamond, tungsten, carbide and related hard materials," *Journal of Laser Applications*.

[35] Simpson, J. W. L., "Force and low speed control in mechatronic systems with friction," Thesis in Electrical, Computer & Telecommunications Engineering at University of Wollongong, 2003.

[36] Clark, I. E. and Sen, P. K., "Advances in the development of ultrahard cutting tool materials," *Industrial Diamond Review*, vol. 2, pp. 40-44, 1998.

[37] Heath, P. J., "Developments in applications of PCD tooling," *Journal of Materials Processing Technology*, vol. 116, pp. 31-38, 2001.

[38] D'Evelyn, M. P., "Industrial Diamond," Report at GE Research & Development Center, 2001/03, 2001.

[39] Pasuleti, A. K., "Polycrystalline Diamond Grinding," Thesis in Faculty of Engineering at University of Wollongong, 2004.

[40] Xu, Z. and Gu, C., "Dressing of corundum wheel with polycrystalline diamond," *Journal of China Textile University, English Edition*, vol. 8, pp. 35-40, 1991.

[41] Oderbolz, B., "A new approach to PCD grinding," *Metalworking*, vol. 14, pp. 30,32, 1999.

[42] Shaw, M. C., *Principles of abrasive processing*, Oxford : New York, Clarendon Press ; Oxford University Press, 1996.

[43] Pfluger, J. A., "Automatic grinding of PCD/PCBN blanks," *Industrial Diamond Review*, vol. 46, pp. 128-130, 1986.

[44] Kramer, D., "ECD grinding - a quantum leap in the machining of modern cutting tool materials," *Industrial Diamond Review*, vol. 62, pp. 183-193, 2002.

[45] Colvin, F. H. and Stanley, F. A., *Grinding practice*, New York, McGraw-Hill, 1943.

[46] Konig, W. and von Arciszewski, A., "Continuous Dressing--Dressing Conditions Determine Material Removal Rates and Workpiece Quality," *CIRP Annals*, vol. 37, pp. 303-307, 1988.

[47] Fathima, K., Kumar, A. S., Rahman, M., and Lim, H. S. L., "A study on wear mechanism and wear reduction strategies in grinding wheels used for ELID grinding," *Wear*, pp. 1247-1255, 2003.

[48] Chen, X., Rowe, W. B., Mills, B., and Allanson, D. R., "Analysis and simulation of the grinding process. Part IV: Effects of wheel wear," *International Journal of Machine Tools and Manufacture*, vol. 38, pp. 41-49, 1998.

[49] Mueller, J. A., "Proper truing and dressing means better toolroom grinding," *Metalworking production*, vol. 100, pp. 1775-1780, 1956.

[50] Syoji, K., Zhou, L., and Matsui, S., "Studies on Truing and Dressing of Diamond Wheels (1st report). The Measurement of Protrusion Height of Abrasive Grains by Using a Stereo Pair and the Influence of Protrusion Height on Grinding Performance," *Bulletin of the Japan Society of Precision Engineering*, vol. 24, pp. 124-129, 1990.

[51] Jakobuss, M., "The Dynamics of Diamond Retention in Grinding Wheel Systems," *Finer Points*, pp. 54-58, 2002.

[52] Chen, X., "The sharpness of grinding wheels: An important measure of grinding behaviour," *Proceedings of the Institution of Mechanical Engineers*, vol. 216, pp. 829-832, 2002.

[53] TYROLIT, "*Innovation on the edge*," (brochure).

[54] Wang, X., Ying, B., and Liu, W., "EDM dressing of fine grain super abrasive grinding wheel," *Journal of Material Processing Technology*, vol. 62, pp. 299-302, 1996.

[55] Rhoney, B. K., Shih, A. J., Scattergood, R. O., Ott, R., and McSpadden, S. B., "Wear mechanism of metal bond diamond wheels trued by wire electrical discharge machining," *Wear*, vol. 252, pp. 644-653, 2002.

[56] Schopf, M., Beltrami, I., Boccadoro, M., and Kramer, D., "ECDM (electro chemical discharge machining), a new method for truing and dressing of metal-bonded diamond grinding tools," *Annals of the CIRP*, vol. 50, pp. 125-128, 2001.

[57] Kramer, D. and Rehsteiner, F., "ECD (electrochemical in-process controlled dressing), a new method for grinding of modern high-performance cutting materials of highest quality," *CIRP Annals*, vol. 48, pp. 265-268, 1999.

[58] Tonshoff, H. K. and Friemuth, T., "In-process dressing of fine diamond wheels for tool grinding," *Precision Engineering*, vol. 24, pp. 58-61, 2000.

[59] Davim, J. P. and Baptista, A. M., "Relationship between cutting force and PCD cutting tool wear in machining silicon carbide reinforced aluminium," *Journal of Material Processing Technology*, vol. 103, pp. 417-423, 2000.

[60] Texas Instruments, "TMS320 Floating Point DSP Optimising C Compiler," Texas Instruments, Houston, 1991.

[61] Malkin, S., *Grinding technology*, Chichester, Ellis Horwood, 1989.

[62] Simons, E. N., *The grinding of steel: a comprehensive treatment of modern methods and machines suitable for use in engineering workshops*, London, Odhams, Odhams Press Limited, 1954.

[63] Huang, H., "Effects of truing/dressing intensity on truing/dressing efficiency and grinding performance of vitrified diamond wheels," *Journal of Materials Processing Technology*, vol. 117, pp. 9-14, 2001.